EXPERIMENTS ON WIND ENVIRONMENT AROUND ISOLATED TALL BUILDINGS

Waman Parshionikar

A Thesis

in

The Centre for Building Studies

Faculty of Engineering

Presented in Partial Fulfillment of the Requirements
for the degree of Master of Engineering (Building) at
Concordia University
Montréal, Québec, Canada

November 1983

ABSTRACT

EXPERIMENTS ON WIND ENVIRONMENT AROUND ISOLATED TALL BUILDINGS

Waman Parshionikar

Tall buildings in urban settings almost always produce an unpleasant wind environment at the plaza level. This is a result of complex interaction between wind and buildings. Different building configurations may create zones of overspeeds and vortices at plaza level. Consequently, an acceptable wind environment is a major design consideration for new and existing buildings.

An approach to look into the problem of adverse wind conditions is presented. Experiments conducted on different building configurations in the Building Aerodynamics Laboratory of the Centre for Building Studies, Concordia University, Montreal are described. Experiments have included square and chamfered tall buildings of different heights in an open environment. General trends of plaza level wind environment observed from a number of model studies are discussed. Experiments conducted on tall chamfered buildings have shown a significant reduction in adverse wind region at pedestrian level. Wind tunnel test results highlighting wind environment around square and chamfered building configurations are presented. The application of results to provide statistical predictions of the plaza level wind environment by combining wind tunnel data superimposed with the statistics of local wind climate is described.

ACKNOWLEDGEMENTS

I wish to express my deepest gratitude and sincere appreciation to Dr. Theodore Stathopoulos, my supervisor, for having provided the topic of this thesis and for his perceptive guidance, valuable advice and encouragement throughout my study. I greatly appreciated his effort and time reviewing this thesis and giving suggestions to improve the content.

Special thanks go to Joseph Zilkha and Hans Obermeir for their valuable contribution in providing technical assistance to the work.

I would also like to thank my professors, friends and colleagues for their help and encouragements, as well as my parents for their patience and understanding, and G. Miller for the typing of the manuscript.

Financial support for this thesis was provided by Ministry of Home Affairs, Government of India through the award of a National Overseas Scholarship.

TABLE OF CONTENTS

LIST OF TABLES

LIST OF FIGURES

CHAPTER 1

INTRODUCTION

In the last three decades, configurations of grouped buildings of more or less uniform height have been replaced by tall buildings through changes in style and construction techniques. A random spread of tall buildings rising out of a matrix of smaller buildings is not new in many modern cities. These tall buildings have been erected for both prestige and intensive site exploitation. In fact, in many cases the presence of tall buildings has created inhospitable and even dangerous ground level wind conditions. In some cases these conditions have proven detrimental to the creative and financial success of the new buildings.

The wind environment at ground level around buildings is a result of complex interaction between wind and building. With certain combinations of shape, height and open space configuration, tall buildings may create zones of overspeeds and vortices in the plaza areas. Adverse changes in plaza level winds can make pedestrian activities uncomfortable, difficult and even dangerous. As a result an acceptable wind environment in these areas has become a major design consideration for new building complexes and a concern for existing areas which have been found undesirable by public opinion.

Recognizing the possible environmental impact, many cities now require some sort of pedestrian level wind evaluation. The seriousness of the matter is demonstrated by proposed guidelines for the development

of the city core area which include pedestrian level wind considerations (16). An assessment of prospective environmental wind conditions at the pedestrian level is carried out to safeguard from further deterioration for virtually all major building development in Australia (25). It is also necessary to demonstrate the wind environment around any new tall building as defined by local building by-laws to acquire a building permit in a number of cities around the world including Boston, Calgary, London and Tokyo (13, 17).

Wind environment as a design criterion in plaza areas around building requires the following information:

1. Prediction of magnitude and frequency of ground level wind speeds likely to be encountered; and
2. Evaluation of the acceptability of particular wind conditions based both on physical danger as well as on user comfort.

Such information comes mainly from wind tunnel tests on models, with measured wind speed in the vicinity of a building being expressed in terms of the free wind speed on an open unobstructed site. The frequency of occurrence of free wind speeds can be found from local meteorological data, so that the frequency of high wind speeds around buildings can be estimated. It is much easier to evaluate the acceptability of an environment from values derived through experimentation than from questioning people in the field.

With no general theory available for predicting the flow field around buildings the wind environment has to be studied in a wind tunnel. However, with the growing experience in the field, general guidelines are beginning to emerge. Some conclusions of general value may be drawn from case studies of which fairly large number have been reported in the literature. Theoretical model studies have defined the aerodynamic effect for various building configurations. Very few studies have emphasized reducing strong vertical flow and promoting lateral flow on the windward face to improve adverse wind conditions around a building of fixed dimensions. The suggested configurations of building parameters through the studies carried out in the wind tunnel may not be directly applicable to new designs in urban areas because they are specific and precise in character.

The objective of the present work is to study the problem of adverse wind conditions at the pedestrian level by experimenting on building models of fixed cross-sectional dimensions. The work attempts to provide design guidelines to reduce the possible existence of zones in which high ground wind speeds would cause unacceptable discomfort to users. The suggested design guidelines may be applied directly in new design in urban areas without major modification in cross-sectional configurations of the building geometry.

Tests were carried out on building models in a boundary layer wind tunnel to investigate the effect of chamfered building corners on adverse wind conditions at the pedestrian level. The experimental work

was carried out in the Building Aerodynamics laboratory of CBS. In the experiments parameters such as the height of the building, the wind attack angle and the height of measurement above ground were examined. The general application of test results is described and an example case is illustrated for a particular location (Montreal).

In Chapter 2, the literature is reviewed briefly and the scope of the test experiments is described in detail. Chapter 3 deals with the general description of wind effects on people. A comparison of comfort criteria for various pedestrian activities is also presented. Chapter 4 describes the experimental set-up and the test programme. Chapter 5 presents and discusses the test results and their application. Chapter 6 demonstrates the application of the results for a particular location (Montreal). Finally, Chapter 7 summarizes the experimental work and recommends the study to be carried out in the future.

CHAPTER 2

LITERATURE REVIEW

2.1 GENERAL

Adverse ground level wind conditions are most frequently associated with buildings significantly taller than their surroundings (2, 16,22,26,36,37). Some examples include isolated tall buildings or groups of tall buildings surrounded by open plazas in an urban environment or even modest height buildings located in an open environment.

The general flow pattern around tall buildings and the main regions at their bases where accelerated wind flow is likely to be found are of primary interest. It is also important to know the mechanism which induces windy conditions at the base of tall buildings.

2.2 GROUND LEVEL WIND CONDITIONS AT THE BASE OF TALL BUILDINGS

There are two types of air flows which cause adverse wind conditions at the base of a building. These flow fields also generate turbulence depending on the building geometry and surrounding conditions.

The first type of flow is caused by the pressure distribution on the windward face of a building. The pressure distribution is directly related to the local wind dynamic pressure which increases with height. The resulting pressure gradient induces flow down the face below the stagnation point (2). The stagnation point is found at about 70 to 80

per cent of the building height. The faster moving air from higher levels is drawn downward. The downward flow increases the speed of the accelerated flow around the sides near the base of the building. This effect is found to be stronger with higher buildings. The downward flow rolls up into a standing vortex system at the base of the building as shown in Figure 2.1, causing high wind velocities in arcade and around corners.

Curved or cylindrical buildings promote lateral flow and do not produce strong vertical flows. Conversely, rectangular and concave buildings do produce strong vertical flows with consequent high wind conditions in the standing vortex system. The flow separation for sharp-edged building forms normally occurs at the upstream edges. Ground level flow may be further accentuated in constricted areas such as narrow passageways between adjacent buildings, through openings, or in open spaces if the building is elevated on columns. Buildings surrounded by open plazas and buildings of different forms in an open environment are illustrated in Figure 2.2. Also shown in the figure are different flow fields around buildings.

The second type of flow which creates adverse wind conditions is caused by the pressure differences between low pressure wake regions (leeward face) and relatively high pressure regions at the base of the windward face. Flow directed between these two regions through arcades or around corners can cause very high local wind velocities. The low wake pressure tends to be dependent on the velocity along the free-stream velocity at the top of the buildings. The taller the building,

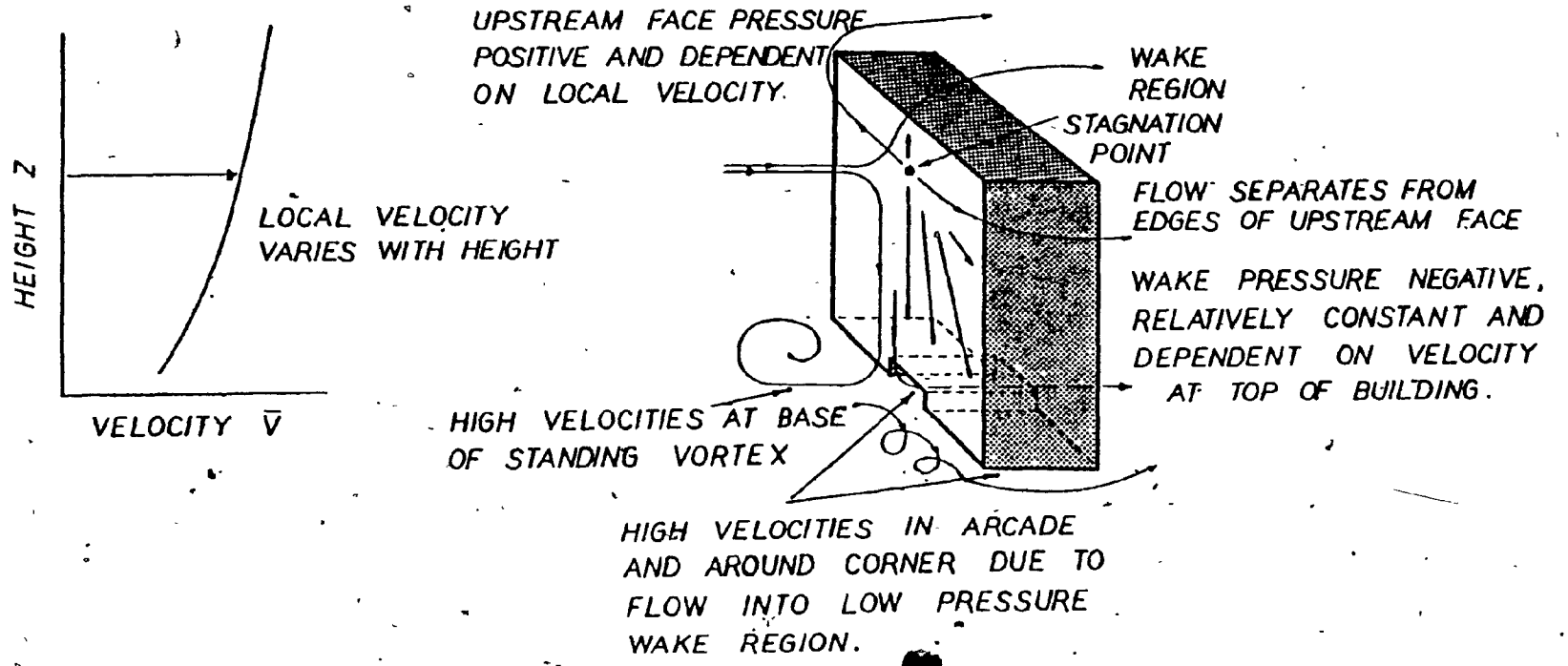

FIGURE 2.1 FLOW FIELD AROUND A LARGE BUILDING (26).

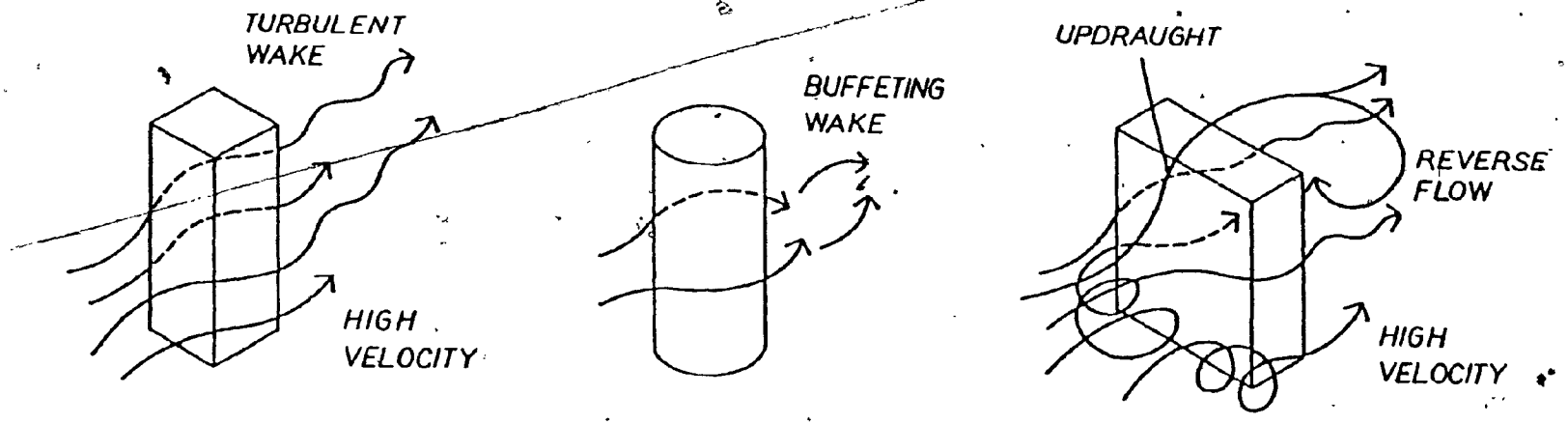

FLOW FIELD AROUND BUILDINGS OF DIFFERENT FORMS IN AN OPEN ENVIRONMENT

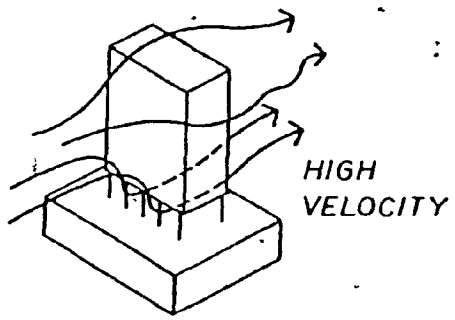

BUILDING RAISED ON STILTS ABOVE PODIUM

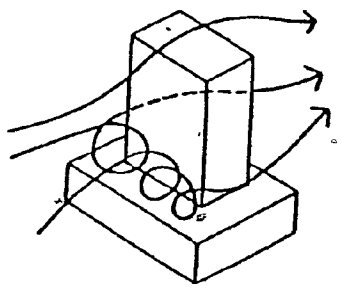

BUILDING RAISED ON PODIUM OF ONE OR TWO-STORIES

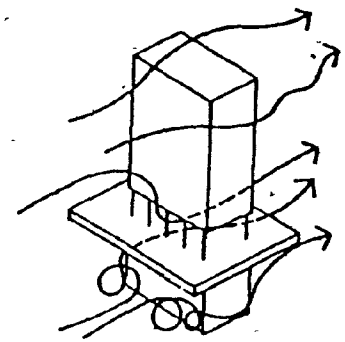

BUILDING RAISED ON STILTS ABOVE PROJECTING CANOPY

FIGURE 2.2 FLOW FIELD AROUND BUILDINGS SURROUNDED BY PLAZAS (32)

the lower the wake pressure and higher the velocities induced through arcades and around corners for a given aspect ratio. In general this phenomenon is hard to control because wake pressure cannot easily be modified.

The juxtaposition of buildings may form deflectors for the wind and also channel the air through narrow zones. Different types of flow can be combined while, at the same time, they depend on the characteristics of the oncoming wind. This gives a particularly complex resultant which makes wind tunnel study necessary for calculation of overspeed for various building shapes or groups of buildings. The solution of the aerodynamic problem, namely the definition of local speed amplification, is principally based on wind tunnel simulations. A wind tunnel study is necessary to quantify the flow around a building in a complex urban environment or even in an open environment.

Wind tunnel model studies offer the principal means of providing quantitative predictions of wind speed environment around buildings. Results of wind tunnel studies can be used to predict the relative increase and decrease of wind velocities in terms of a dimensionless ratio. This ratio can be calculated for any azimuth by measuring wind velocities as affected by the presence of the building and dividing them by velocities measured at the same point in absence of the building. Similar ratios can be established for turbulence.

2.3 BRIEF DESCRIPTION OF PREVIOUS STUDIES

Only a small amount of research on wind conditions around tall buildings at plaza level has been done in the last few years. Since full-scale studies are expensive and time consuming, and cannot be done for new buildings, wind tunnel model studies are essentially the only means for the estimation of wind environment around buildings. Earlier studies were mostly carried out in an aeronautical wind tunnel without the appropriate simulation of the wind profile. More recently, studies have been carried out in boundary layer wind tunnels. The most significant of these studies are briefly reviewed in this section.

One of the first studies in this area was carried out in the sixties by Wise, Sexton and Lillywhite (37) who tested a rectangular building and low rise buildings of different configurations in a low turbulence wind tunnel. They used a model scale of 1/120 which did not adequately simulate the natural wind characteristics. This study found that at the base of the windward face of a rectangular building, the wind speed exceeds two to three times the value of the free wind at the same height between low rise buildings. It was reported that at the sides of a rectangular building wind speeds were remarkably high. However, in the area downstream of a rectangular building the wind speeds were comparatively lower than at the sides.

A few years later Wise (36) carried out tests in a boundary layer wind tunnel to investigate the wind environment around a group of buildings. Buildings of up to 100 m in height were modelled to a scale of

1/120 simulating natural wind characteristics for suburban exposure. Wise reported that the group of buildings influences the development of a steady vortex in front of a taller building for width/height around one and less. The mean wind velocities may increase up to three or four times the plaza level velocity around the sides of the tall building. Figure 2.3 shows the effect of rectangular building on wind velocities in front and around corners. An increase in wind speed (measured as the ratio, r, of the velocity at a particular point to the mean wind velocity at the top of the building) of up to 1.6 could be found near the corner of the building. Wise also found that the velocity ratio r reaches up to 2.1 in passages and 1.9 in other areas around the group of tall buildings. In a similar test, on a square tower 50 m high, Lawson (21) reports that r at the sides of the buildings may reach as high as 1.3 at about one metre above the ground.

Assessment of flow conditions induced by full scale building situations from wind tunnel tests by Melbourne and Joubert (26) pointed out that the pressure on the wake depends on the velocity at the top of the building and that pressure differential increases with building height. This was based on experiments with tall rectangular and octagonal building models carried out in a boundary layer wind tunnel. This study also suggested that a rectangular building facing the prevailing wind should be avoided. An octagonal cross section is more desirable than a rectangular building because it promotes lateral flows and, thus, it reduces vertical flow downwards.

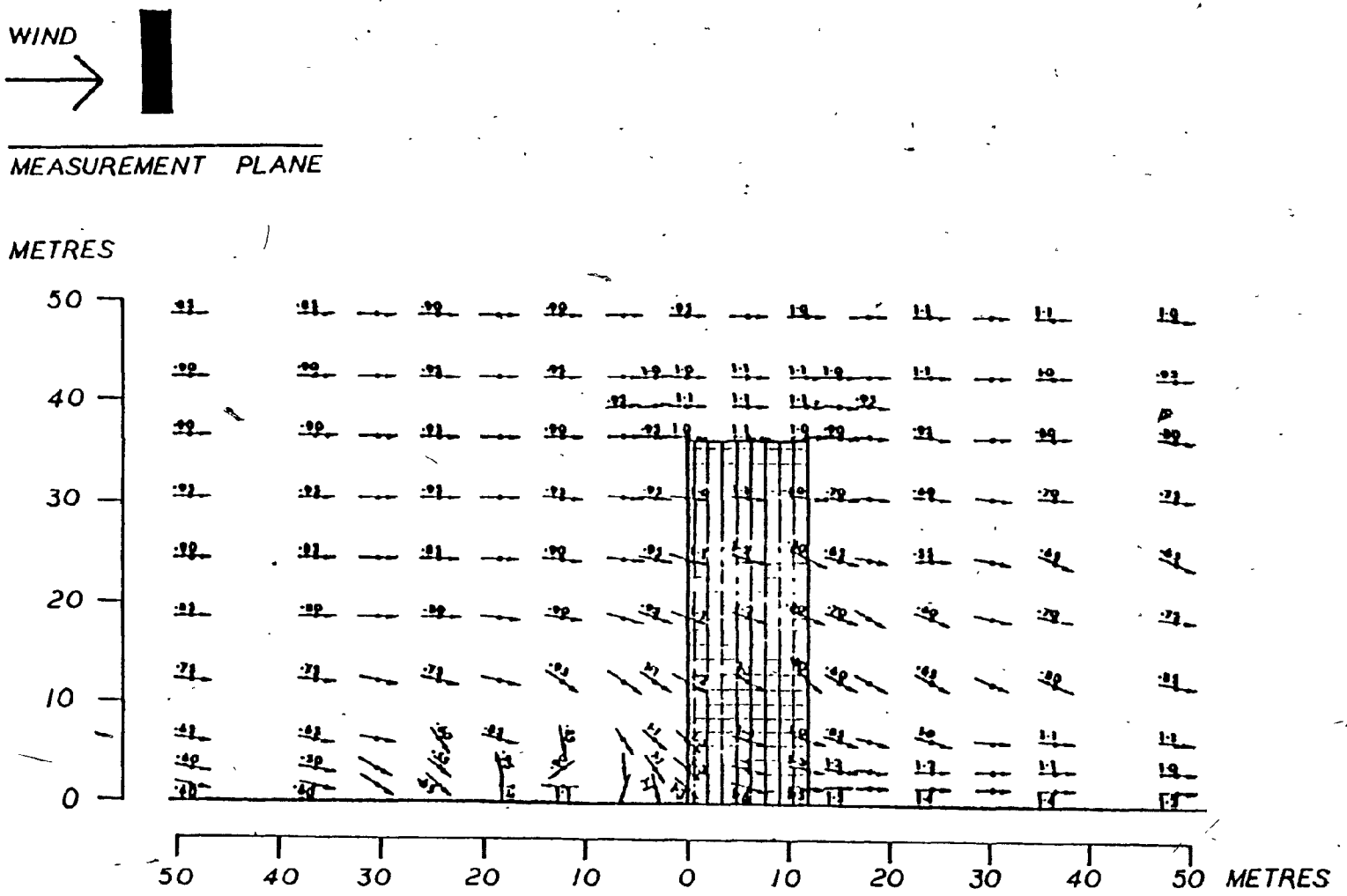

FIGURE 2.3 AMPLIFICATION OF WIND SPEED IN FRONT AND AROUND CORNERS OF A BUILDING (36)

The growing awareness of the problem of adverse wind conditions at the base of existing tall building complexes nas raised numbers of enquiries by users and designers for comfort and safety reasons. This has initiated the study by Penwarden (30) on a group of buildings suggests that the wind speed amplification ratio, ($\bar{V}_hP/\bar{V}_hA$, measured as the wind speed at pedestrian height with the buildings to the mean wind speed at pedestrian height on open site) in the front and around the sides of tall buildings at least four times higher than their surroundings may be 1.5 and 2.0 respectively. Amplification ratios as high as 3.0 have been observed under buildings elevated on columns or in narrow passageways. It has also been found that the wind amplification ratios do not exceed one for buildings of heights less than twice that of the surroundings.

Isyumov and Davenport (16) carried out wind environment tests on some existing tall buildings at plaza level in a boundary layer wind tunnel. The mean wind speeds were measured at 2.75 m above ground level around a tower of 240 m high. Results show that wind speeds may be exceeded by up to 40 to 50 percent of free mean wind speed for varying azimuths. They have also reported wind speed exceeding 65 percent of free mean wind speed around two very tall towers 409 m high at pedesterian level.

The studies of specific building configurations cannot adequately answer the needs of every individual or group of building configurations in view of their aerodynamic properties. Gandemer (10) attempted to

define and quantify the various aerodynamic effects in the built context. He tested models of existing and proposed buildings in a boundary layer wind tunnel for an open country exposure. The measurements were taken at an equivalent height of 2 to 3 m above ground level. Results were expressed in terms of a dimensionless velocity ratio, described as the comfort parameter (ψ), which included a term to allow for local turbulence intensity. For an open exposure, approximately 2 to 3 m above ground, the mean level of comfort and discomfort, ψ, may be equivalent to 0.6 and 2.0 respectively. Results show that the maximum value of the comfort parameter (ψ) generally occurs with buildings higher than 30 or 40 m and ranges between 1.5 to 2.0 or more depending on the shape, size and general arrangement of the buildings. Especially, in an enclosure type of courtyard, as shown in Figure 2.4, if the length of the opening is less than 25 percent of the perimeter of courtyard, ψ reaches up to 1.1 for a windward opening or up to an angle of 45°. A typical example of the venturi effect is also presented in Figure 2.4 for buildings of different configurations for which ψ reaches up to 1.6 for buildings 50 m high (H) having very narrow spacings.

A study of wind environment at the base of rectangular tall buildings by Lawson and Penwarden (22) reported that maximum wind speeds around the building corners are not sensitive to a wide range of wind directions. The maximum wind speeds around corners were varied very little with wind angle (typical $\pm$ 15% during a rotation through 360 degrees) although the position at which the maximum occurs does change. This has also been observed by Penwarden and Wise (31), who tested wind

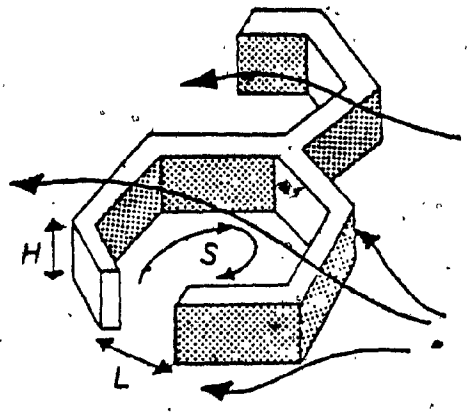

L ≤ 25 % OF THE PERIMETER
S : AREA

MESH EFFECT

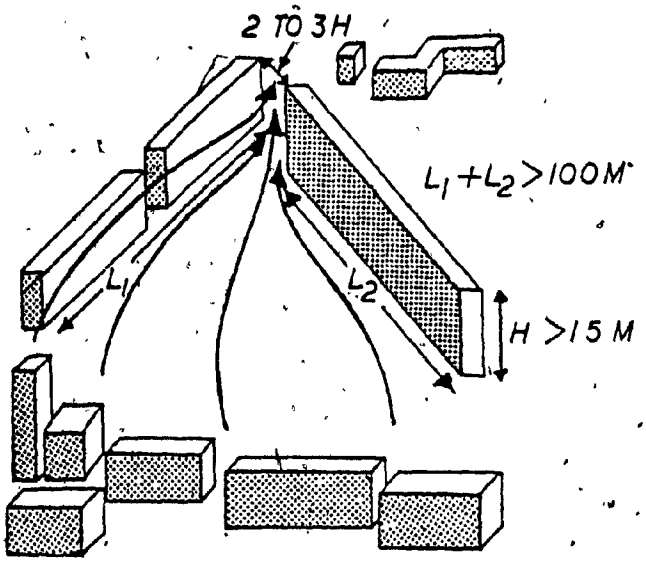

VENTURI EFFECT

FIGURE 2.4 AERODYNAMIC EFFECTS (10)

conditions around an 80 m tall building modelled in a boundary layer wind tunnel. The mean wind speed ratio at a point equivalent to 10 m from the ground to the top of the building was 0.56. The maximum speed ratio around the corners of the building was between 0.85 and 0.9.

Most of the studies previously refered to have examined specific building configurations. In contrast, very few studies have dealt with the effects of building geometry on the intensity and the extent of the adverse wind region at pedestrian level. Kamei and Maruta (17) carried out tests on isolated tall building models in a boundary layer wind tunnel to define and quantify this adverse wind region. The effects of building height and wind direction on wind environment at the base were tested on a model measured at a full scale equivalent of 10 m above ground level. Additional tests were conducted on 1/1000 scale models for evaluating wind environment around building in wind tunnel. The tests include the variation of parameters such as measurement height above ground level, the size of the building and different wind velocity profiles. Results have been presented as contours of the velocity velocity amplification ratio $(\bar{V}_hP/\bar{V}_hA)$ where $\bar{V}_hP$ is the mean wind speed measured at a point in presence of the building and $\bar{V}_hA$ is the mean wind speed at the same point in absence of the building. Figure 2.5(a), shows typical velocity amplification ratios at different measurement heights. For the investigation of wind conditions at the pedestrian level the standard 10 m meteorological height was used. The results also show that the wind velocity and the area of the strong wind

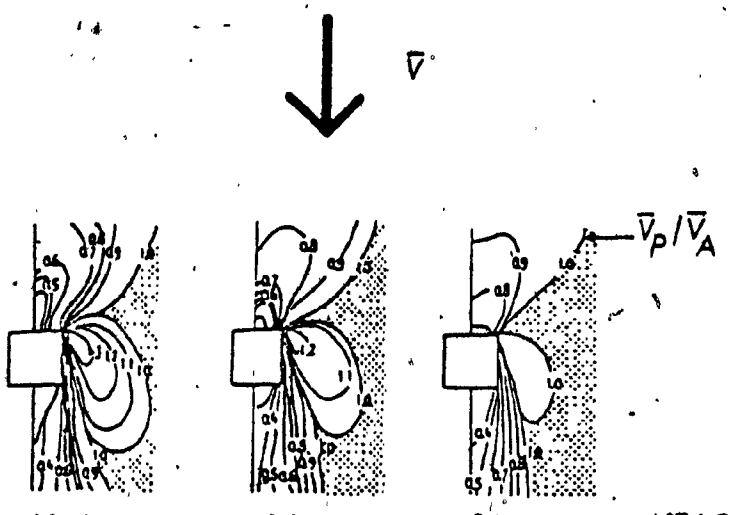

(a) AIR FLOW AROUND BUILDING AT DIFFERENT MEASUREMENT HEIGHTS. (H=200 M, D = W=60M)

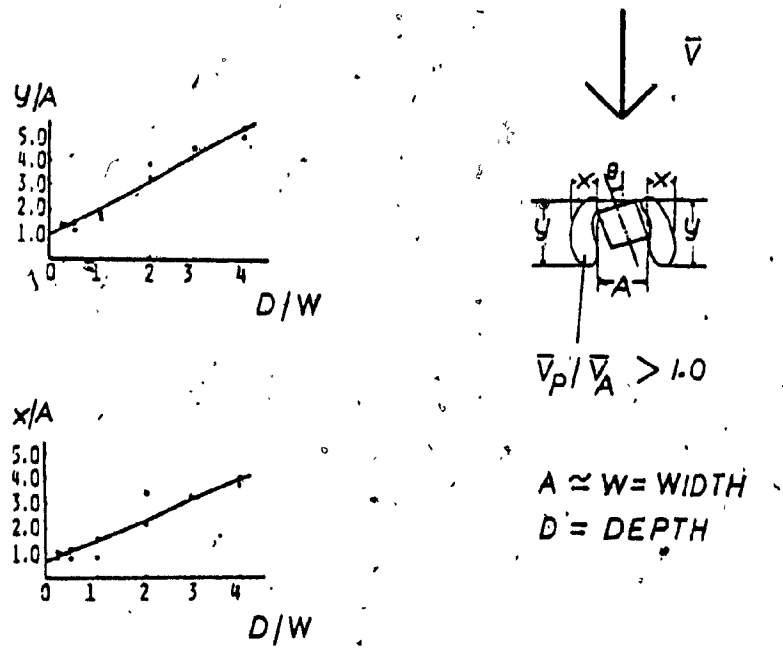

FIGURE 2.5 (b) VARIATION OF THE STRONG WIND REGION FOR RECTANGULAR BUILDING CONFIGURATIONS (17)

region around corners of the tall building increase at plaza level with increasing building height. For a 200 m tall building the maximum value of the wind velocity ratio measured was 1.3. The results presented in Figure 2.5(b), show the variation of the size of the strong wind region for various rectangular building geometries. Note that the width of a building has great influence on the air flow around that building. Additional test results show that the mean wind profile does not affect the amplification of wind velocity significantly.

Murakami, Uehara and Komine (27) tested a square tall building surrounded by low buildings in a boundary layer wind tunnel. The objective of the experiments was to measure the influence of a tall building on wind speed amplification at a full scale equivalent height of 5 m above ground level in a built up area. The parameters studied included the height of the tall building, the heights of the surrounding low buildings, different building shapes, the width of the street and the wind direction. Results show that the maximum value of the velocity amplification ratio is 2.5 at the base of the tall building surrounded by low buildings. The size of the strong wind area increases at the base when the tall building is six times higher than the surrounding low buildings. For wedge-type tall buildings the amplification ratio, r, increases at the downstream corner, as indicated in Figure 2.6. The figure shows the wedge type of a building 100 m high surrounded by 25 m high square low buildings. The effect of building shapes on the amplification of wind speeds is comparatively low for polygonal buildings.

Sand erosion and flow visulization techniques, as presented in

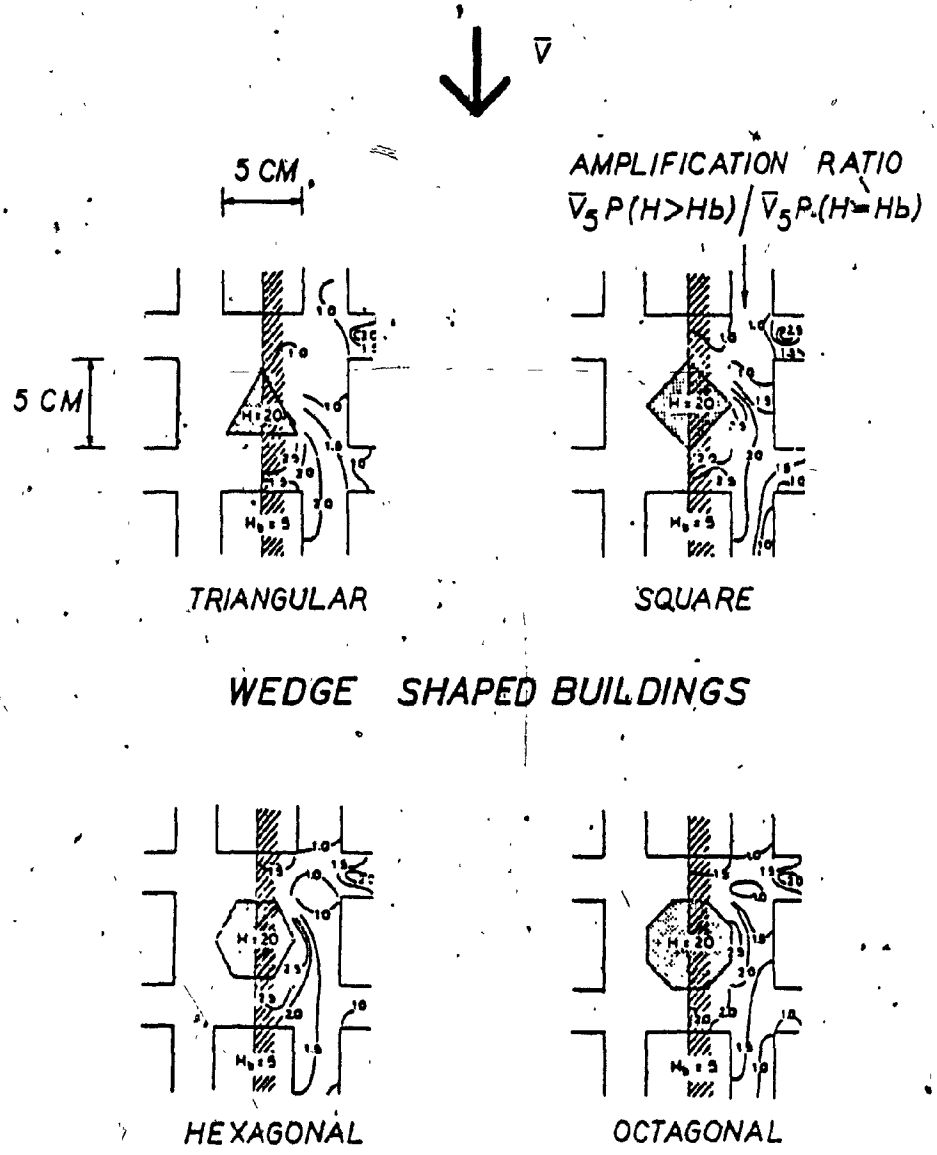

FIGURE 2.6 AMPLIFICATION OF WIND SPEED AROUND BUILDINGS OF DIFFERENT SHAPES. (Hb = HEIGHT OF LOW BUILDINGS, POWER LAW $\alpha = 0.14$, MODEL SCALE = 1:500 AND MEASUREMENT HEIGHT = 5 M IN FULL SCALE) (27)

Figure 2.7 have been used to determine the wind environment around buildings. Beranek's and VanKoten's (5) results give a pictorial impression of the wind speeds around building complexes as they are presented in the form of an amplification factor defined as gust wind speed with building divided by gust speed of free wind. The wind speed at the base of the tall buildings increases with height, particularly near the building corners.

Dye (9) carried out wind tunnel tests without correct simulation of atmospheric turbulence. An isolated tower type building 69.5 m high was made to a scale of 1/250. Results show that at the pedestrian level (1.59 m, full scale) the wind speed may be up to 2.5 times higher than the speed without the building.

A brief review of some of the techniques and their limitations while estimating pedestrian level winds around a building has been provided by Durgin and Chock (8). They have tested 16 and 24 storey buildings surrounded by low rise structures modelled in a boundary layer wind tunnel simulating suburban terrain. Their results show that wind speeds around the corners of a building at the base increased up to 40 to 60 percent of free wind speed.

The review of these building configuration studies in boundary layer wind tunnels gives a good picture of the wind environment around tall buildings at the plaza level. While defining the aerodynamic effects for various general model configurations the descrepancies have been noted in the numerical values associated with the amplification of

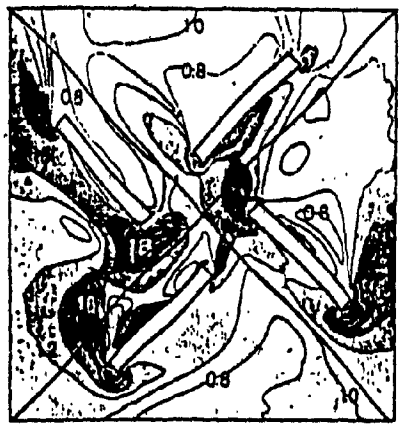

SAND EROSION TESTS GIVE CONTOUR LINES FOR AMPLIFICATION OF WIND VELOCITIES

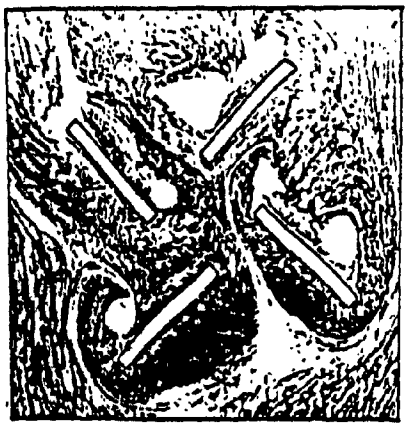

SURFACE FLOW VISUALIZATION GIVES AVERAGE WIND DIRECTION

FIGURE 2.7 WIND TUNNEL MEASURING TECHNIQUES(5).

mean wind speed at the base of a tall building and the model scales simulating natural wind characteristics.

In urban areas, the geometry of the building is mainly governed by the site boundaries and local building by-laws. The suggested configurations of building parameters through these studies may not be directly applicable to new designs because they are specific and precise in character. They may, however, be easily adopted for flexible site conditions. In this respect a renovation of ratio of gross building area to site area is expected in Australia (11). It will help in reducing adverse wind conditions, as higher velocities are induced due to lower wake pressure which is directly dependent on the height of the building.

Very few studies (26,27) have emphasized the reduction of strong vertical flow by promoting lateral flow on the windward face to improve excessive wind speeds around a building of fixed dimensions. Measurement height above ground level becomes very controversial since it has been pointed out that strong wind region increases in intensity and area at lower heights of measurement. The exact location and number of measurement points have not been mentioned in detail in some previous studies and interpolation or extrapolation may not be accurate.

In existing plaza building model studies, emphasis has been placed on only a few points of problematic areas. In fact, generalised aerodynamic effects occur in every building configuration which generates its own flow field. Suggested remedial measures are very much localised (specific) in nature. The findings of such studies (16,31) are certainly good but they are inadequate for application to new designs.

Studies have not shown the turbulent character of wind flow in detail which is an important constraint in determining comfort conditions for pedestrians. Very few studies have given a detailed picture of the extent of strong wind regions and their exact locations from building faces. These regions however, are considered to be one of the major criteria for the physical planning of activities at the pedestrian level in a high-rise built up urban environment.

The knowledge of the phenomena around isolated tall buildings of simple shapes provide significant understanding of the behaviour of the flow field around buildings. The results of those isolated building model studies (5,9,17,21,27) may be useful for application in real buildings. In one of those studies (9) wind tunnel model results have been compared with full scale data for a suburban type of terrain. A reasonably good agreement has been found. The results of such isolated building studies however, are expected to be different if proximity of other buildings affect the flow conditions significantly (26).

CHAPTER 3

WIND EFFECTS ON PEOPLE

3.1 GENERAL

The wind environment at ground level around a building results from a complex interaction between wind and buildings. Different settings of buildings of different geometry may create zones of overspeed and vortices which result in an unacceptable wind environment at the plaza level. The wind environment at plaza level becomes a major design consideration for new buildings and a concern for existing areas which have been found undesirable by public opinion.

The most serious direct effect the wind can have upon man is to blow him over. This can cause injury and sometimes death. Reports of accidents due to adverse wind conditions at the base of tall buildings can be found in the literature and the press. Typical examples include the following cases:

Two elderly ladies died in Great Britain as a result of skull accidents received when blown over by wind around tall buildings. The gust speed in one of these cases was estimated at 25 m/s (90 km/h) (31). In Australia, people were having great difficulties with balance at wind speeds gusting up to 20 m/s (72 km/h) around an exposed rectangular building. People were also blown over around the same building at a gust speed of 23 m/s (82 km/h) (26). A report from the United States mentioned people being blown over by wind around skyscrapers (23). In

Japan, display stands, bicycles and motor bikes are being blown down by strong winds and difficulties are often encountered with opening doors at plaza level (17).

Wind can create annoyances such as turning umbrellas inside out or the flapping of clothes. It can also make activities such as strolling, shopping, entering a building, or sitting, uncomfortable, difficult and even dangerous. North American plazas have been found hazardous during winter when icing further reduces balance (16). Criteria for losing one's balance and even toppling can be based on purely mechanical and aerodynamic considerations. The wind force required to topple a person varies with surface area, weight, physical fitness, body position and wind direction.

Additional effects caused by strong ground level wind and having indirect influence on people include increased convective heat transfer, greater rain penetration through the building skin, increased noise level and increased snow drifting. Problems such as malfunctioning of fountains, damage to traffic and flying debries are also caused by the strong wind. These effects are also important for total design.

Acceptable wind speed levels in plaza areas for pedestrian comfort should therefore be an important consideration. It is difficult to evaluate the exact wind speed influence below the physical danger threshold since it deals with the subjective consideration of human comfort. In general, comfort or discomfort for particular wind conditions depends on the type of activity and dress, climatic differences, the season and

specific weather conditions, and the physical, physiological and psychological state of the individual (29).

3.2 COMFORT CRITERIA

Wind-induced discomfort at the plaza level may be expected to occur with certain frequencies which depend on the degree of discomfort, the building geometry and the wind climate at the location. Statements specifying the maximum acceptable mean frequencies of occurrence for various degrees of discomfort are known as comfort criteria. Comfort criteria should in principle be based on the knowledge of the degree to which pedestrians are prepared to accept discomfort associated with excessive wind speeds at the base of the tall buildings. Attempts have been made to gain such knowledge by questioning in the field (11).

Existing criteria for acceptable wind conditions in outdoor areas are largely based on physical and thermal comfort considerations (7,29). In 1805 Admiral Sir Francis Beaufort encountered the problem of determining wind speed at sea with some degree of accuracy. He defined wind speed ranges numbered from 0 (calm) to 12 (hurricane). A detailed description of the effects of winds of various intensities as defined by the Beaufort scale of wind force with factors relating to human comfort, is presented in Table 3.1. Recognition features relating to wind effects on people have been added to the Beaufort scale by Davenport (7) and Penwarden (29).

Based on the Beaufort scale for an average mean wind speed $\bar{V}$ measured at approximately 2 m above ground, wind effects on people suggest

Description of wind	Beaufort number	Speed (m/s)	Effects of Land	At Sea
Calm, light air	0,1	0-1.5	Calm, no noticeable wind	Sea is mirror-smooth; Small wavelets like scales, but not foam crests
Light breeze	2	1.6-3.3	Wind felt on face leaves rustle	Waves are short and more pronounced
Gentle breeze	3	3.4-5.4	Wind extends light flag Hair is disturbed Clothing flaps Leaves and twigs in motion	Crests begin to break: foam has glassy appearance, not as yet white
Moderate breeze	4	5.5-7.9	Raises dust, dry soil and loose paper Hair disarranged moves small branches	Waves are longer: many white horses
Fresh breeze	5	8.0-10.7	Force of wind felt on body Drifting snow becomes airborne Limit of agreeable wind on land Small trees in leaf begin to sway	Waves are more pronounced: white foam crests seen everywhere
Strong breeze	6	10.8-13.8	Umbrellas used with difficulty Hair blown straight Difficult to walk steadily Wind noise on ears unpleasant Windborne snow above head height (Blizzard) Large branches begin to move: telephone wires whistle	Larger waves form: foam crests more extensive
Near gale	7	13.9-17.1	Inconvenience felt when walking Whole trees in motion	Sea heaps up: foam begins to blow in streaks
Gale	8	17.2-20.7	Generally impedes progress Great difficulty with balance in gusts Twigs break off: progress generally impeded Slight structural damage occurs: chimney pots removed	Waves increase visibly: foam is blown in dense
Strong gale	9	20.8-24.4	People blown over by gusts	
Strong gale	10	24.35-28.40	Trees uprooted: considerable structural damage	High waves with long overhanging crests: great foam patches
Storm	11	28.40-32.40	Damage is widespread: seldom experienced in England	Waves so high that ships within sight are hidden in the troughs: sea covered with streaky foam:
Hurricane	12	> 32.40	Countryside is devastated: winds of this force are encountered only in tropical revolving storms	Air filled with spray

WIND SPEED AT REFERENCE HEIGHT OF 10 M

TABLE 3.1 - WIND EFFECTS ON PEOPLE BASED ON THE BEAUFORT SCALE (1)

that the following degrees of discomfort are induced by various speeds (33):

$\bar{V}$ = 5 m/sec onset of discomfort

$\bar{V}$ = 10 m/sec definitely unpleasant

$\bar{V}$ = 20 m/sec dangerous

In the Beaufort scale, the descriptive specifications do reflect the influence of associated atmospheric turbulence (16) but difficulties are always encountered when using it in an urban environment due to the local increase in turbulence intensity.

An approach to evaluating acceptable pedestrian level wind speeds based on the comparison of values of publicly acceptable wind environment at a location with values of wind speed considered acceptable for new buildings is used in the wind tunnel. Another wind tunnel approach is to evaluate the impact of a new building on the wind environment by comparing the surrounding wind speeds with and without buildings. Particular values of the threshold of danger, annoyance and/or comfort level have been suggested by various investigators (10, 12,16, 29). The use of absolute threshold levels, without acceptable frequencies of occurrences are difficult for practical evaluation unless only used as relative indices.

Criteria which state both the wind speed and its acceptable probability of exceedance have been suggested by many researchers (7, 13, 18, 26). In all cases some attempt is made to differentiate between the criteria for danger and comfort. Comfort criteria proposed by Davenport

(7) are presented in Table 3.2, which shows the frequencies of wind speeds for a range of activities or utilization of outdoor areas. Although comfort levels vary with activity type, the danger threshold which depends only on wind force consideration is invariant for all activities.

3.3 COMPARISON OF COMFORT CRITERIA

It has been discussed and pointed out in several studies (10, 13, 16, 22, 25, 27, 29, 33) that to estimate the real effect of wind in the building environment, the consideration of gust with mean wind speed is important. Comparison of various comfort criteria based on wind speeds is complicated by the use of both mean and gust speed. Difficulties are always encountered when using mean velocities characterizing the Beaufort scale for increased turbulence level in an urban environment. To overcome this difficulty an effective wind speed, V^e, which results in much higher values than the mean wind speed (14, 27) is defined as follows:

$$V^e = \bar{V} \left[1 + K \frac{V_{rms}}{\bar{V}}\right]^{(33)} \quad \text{.....} \quad [3.1]$$

where, $\bar{V}$ is the mean speed, V_{rms} is the rms of the longitudinal velocity fluctuations, and K is a constant reflecting the degree to which the effects of the fluctuation are significant.

ACTIVITY	AREAS APPLICABLE	RELATIVE COMFORT			
		PERCEPTIBLE	TOLERABLE	UNPLEASANT	DANGEROUS
1. Walking fast	Sidewalks	5	6(43%)	7(50%)	8(53%)
2. Strolling, skating	Parks, entrances, skating rinks	4	5(23%)	6(34%)	8(53%)
3. Standing, sitting - short exposure	Parks, plaza areas	3	4(6%)	5(15%)	8(53%)
4. Standing, sitting - long exposure	Outdoor restaurants, band-stands, theatres	2	3(0.1%)	4(3%)	8(53%)
Representative criteria for acceptability			< 1 occasion/ week	< 1 occasion/ month	< 1 occasion/ year

Units: Beaufort number; values in parentheses are frequencies with which wind speeds above 5 m/s occur, calculated as described in reference (31).

Temperature: >10°C; at lower temperatures relative comfort level might be expected to be reduced by one Beaufort number for every 20°C reduction in temperature.

TABLE 3.2 - DAVENPORT'S COMFORT CRITERIA (16)

The value of the K varies from 0 to 4 in the literature. A zero value is suggested by Penwarden (22), 1 by Gandemer (10), 1.5 by Isyumov and Davenport (16) and 2 by Feis (20) to 3 and 4 by Hunt et al. (13, 20). The subjective nature of the value accounts for the variation. Some efforts have been made, however, to arrive at values of K by experimenting in the wind tunnel. A value of 3.0 was derived from wind tunnel results (13) by evaluating reaction of people to steady and gusting winds by means of both questioning and measurements. Based on these results various degrees of discomfort and their corresponding V^e (with K approximately equal to 3.0) are suggested as follows:

V^e = 6 m/sec onset of discomfort

V^e = 9 m/sec performance of simple tasks affected

V^e = 15 m/sec control of walking affected

V^e = 20 m/sec dangerous

A summary of values of threshold of danger, annoyance and/or comfort level in probabilistic terms inclusive of turbulence level is presented in Figure 3.1. The figure shows four solid lines representing Melbourne's criteria (24). The criteria range from the maximum threshold of acceptability above which all pedestrian activities are dangerous to the threshold below which activities entailing long exposures are acceptable. The various other symbols are those of other investigators (7, 13, 18, 31) with their respective probabilities for the wind speed exceeding 5 m/s for a given frequency of occurrence. Davenport's (7) criteria relating activities to frequencies of occurrence in terms of

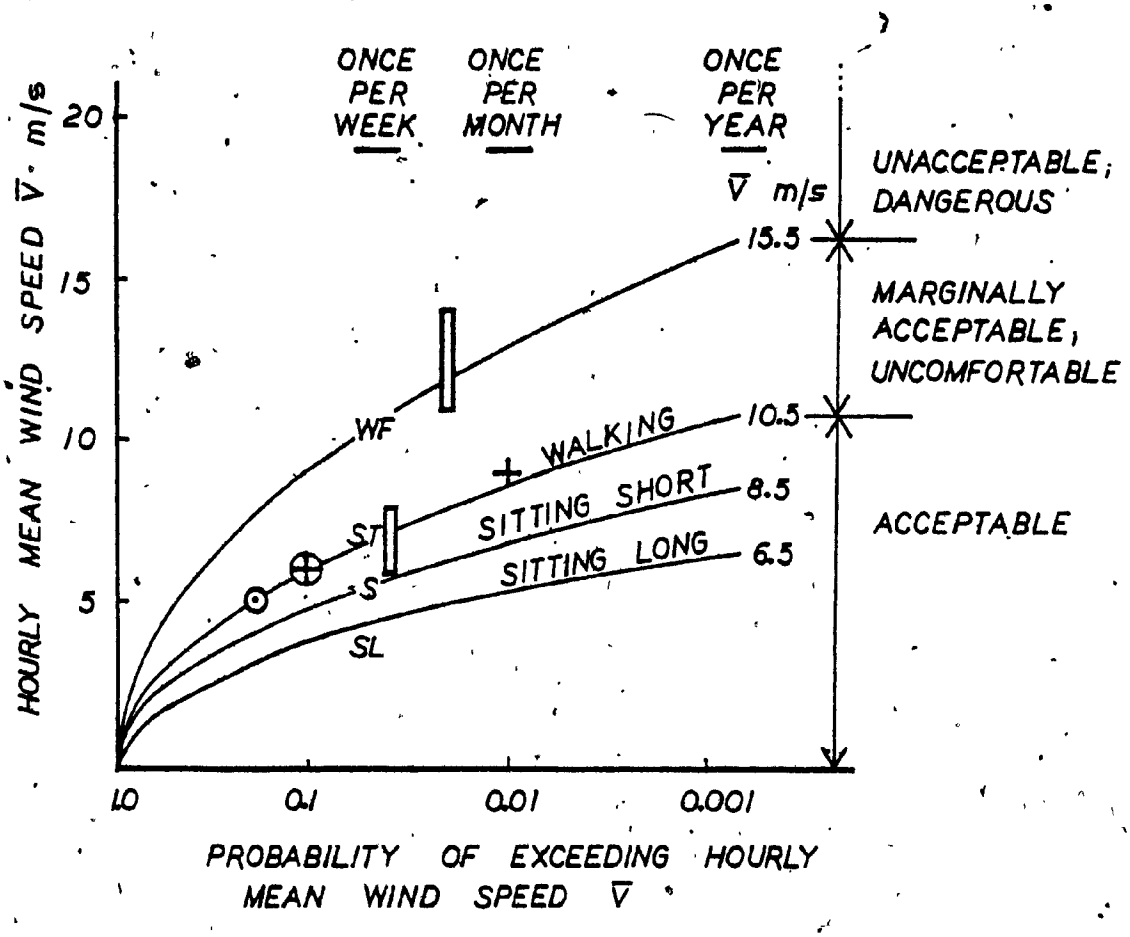

CRITERIA	SYMBOL
MELBOURNE (24)	——
DAVENPORT (7)	
WALKING FAST	WF
STROLLING	ST
SITTING	S
SITTING LONG EXPOSURE	SL
PENWARDEN AND WISE (31)	⊙
LAWSON (18)	
WALKING FAST	▬
WALKING AND SITTING	═══
HUNT, POULTON AND MUMFORD (13)	
STROLLING	⊕
WALKING	+

FIGURE 3.1 COMPARISON OF COMFORT CRITERIA (24)

the mean wind speed shown in figure are interpreted as follows:

Walking fast	if $P(\bar{V} > 10) \leq 0.05$
Strolling, skating	if $P(\bar{V} \geq 7.5) \leq 0.05$
Standing, sitting, short exposure	if $P(\bar{V} \geq 6.5) \leq 0.05$
Standing, sitting, long exposure	if $P(\bar{V} \geq 3.5) \leq 0.05$

The wind effect on people at pedestrian level for various activities based on probabilities of mean wind speed would be incomplete without turbulence level. The information on mean wind speed and turbulence in the presence of the building could be derived from wind tunnel model tests. Chapter 5 gives such information derived from a series of building model tests carried out in a boundary layer wind tunnel. The description of building model tests is given in the next chapter.

CHAPTER 4

EXPERIMENTAL WORK

4.1 EXPERIMENTAL ENVIRONMENT

The experimental measurements for studing the problem of adverse wind conditions at the pedestrian level around tall buildings and also experimenting on wind environment around buildings of square and chamfered configurations of fixed cross-section dimensions to reduce adverse wind conditions were carried out on building models. The tests were done at the boundary layer wind tunnel of the Building Aerodynamics laboratory of the Centre for Building Studies.

The wind tunnel has a test section 12.20 m long, 1.80 m wide with a suspended roof allowing for an adjustable height ranging between 1.40 and 1.80 m. The tunnel is built in sections of wood supported by steel frames placed on casters for ease of removal. Plexiglass windows are set on one side of each section and both sides of the most downstream section. The test area is equipped with a turntable 1.21 m in diameter. The turntable can be operated either manually or electrically. Figure 4.1 shows the plan view and the elevation of the boundary layer wind tunnel.

A Mark-Hot double inlet centrifugal blower with a capacity of about 40 m^3/s at a static pressure of 4 cm of water is capable of producing a maximum wind velocity of 14 m/s. A speed control system operating manually can produce a variable speed to a minimum of about 3 m/s through outlet volume control.

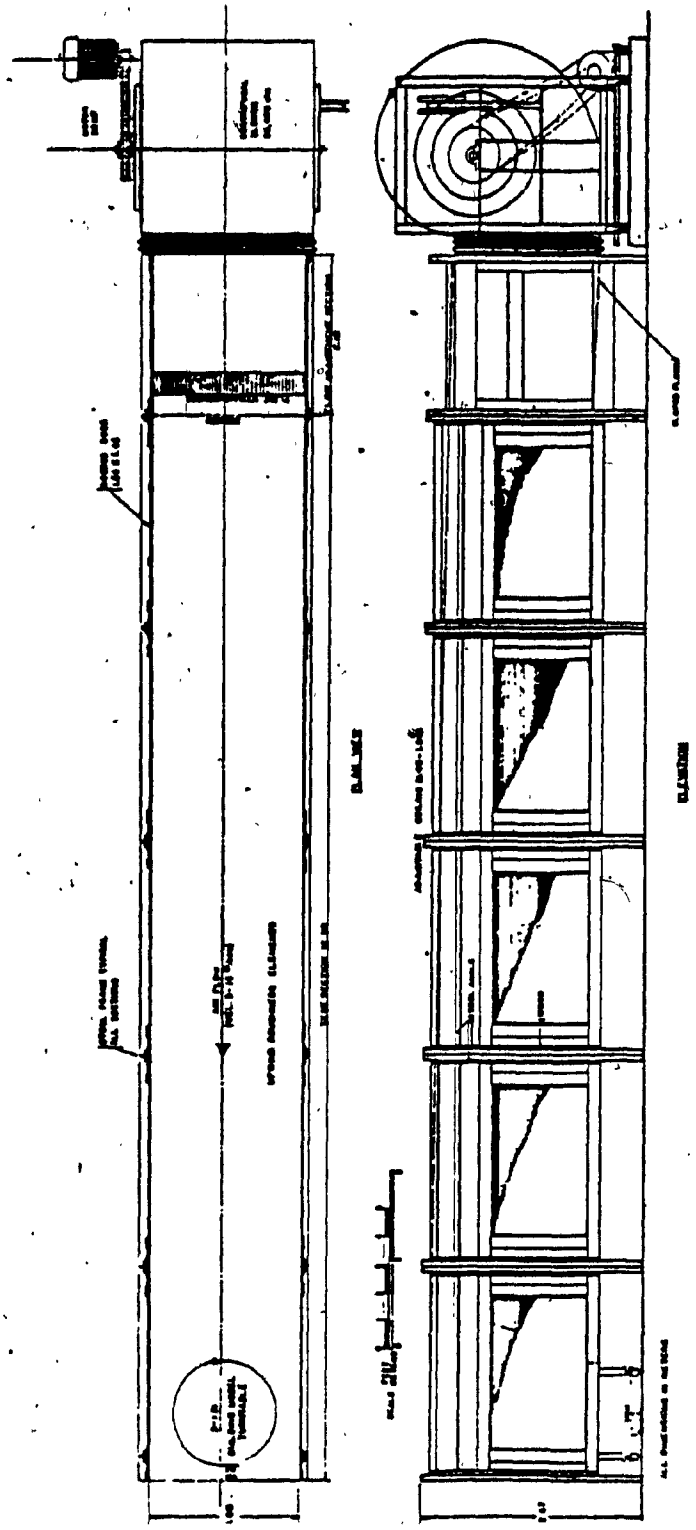

FIGURE 4.1 BOUNDARY LAYER WIND TUNNEL (34)

Figure 4.2(a) shows a picture of the inside view of the tunnel with one of the building models on the turntable while Figure 4.2(b) presents an outside view. The carpet on the floor of the tunnel is used for the simulation of the terrain roughness of an open country exposure. More details about the wind tunnel facility are given in reference 34.

4.2 ATMOSPHERIC BOUNDARY LAYER SIMULATION

The objective of the wind flow simulation is to reproduce in the wind tunnel the natural wind characteristics. For flow simulation purposes, the mean velocity profile, and the intensity, scale and spectrum of the longitudinal turbulence component are of primary importance.

In the present study, a smooth (open country) exposure was simulated in the wind tunnel by using the carpet shown in Figure 4.2(a). Figure 4.3 shows mean velocity and longitudinal turbulence intensity profiles taken above the centre of the turntable. An exponential law

$$\bar{V}/V_g = (Z/Zg)^{\alpha}, \qquad \text{[4.1]}$$

in which $\bar{V}$ is the mean velocity at height Z and α is an experimentally determined constant, agrees well with the measured values. An alternative expression for the velocity profile near the surface is the logarithmic law

$$\bar{V}/Vg = (1/k)\ Cg\ \ln\ (Z/Zo) \qquad \text{[4.2]}$$

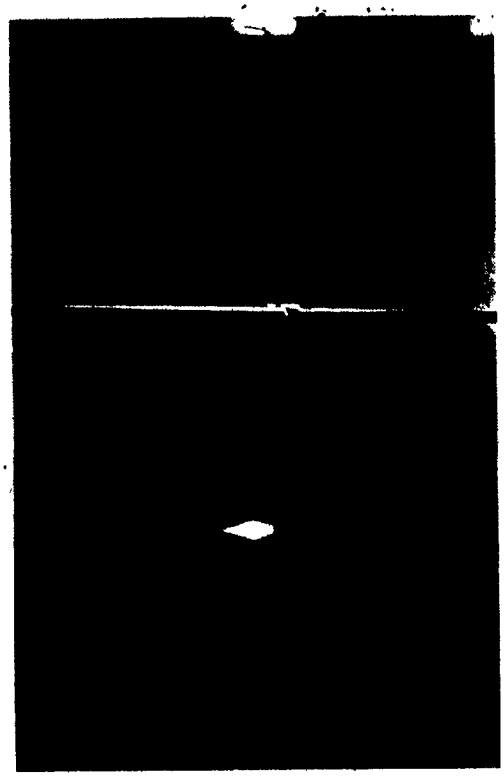

(a) INSIDE VIEW OF THE WIND TUNNEL

FIGURE 4.2 (b) OUTSIDE VIEW OF THE WIND TUNNEL

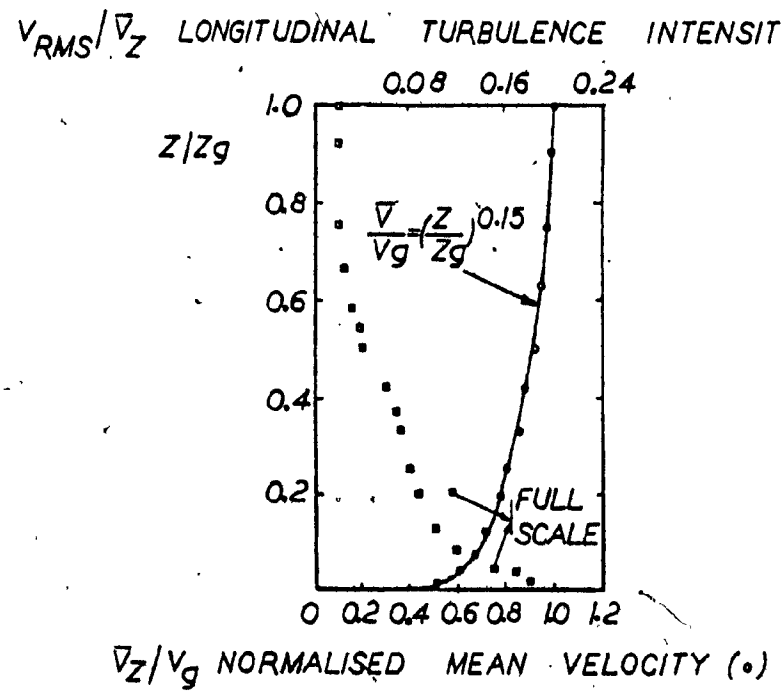

FIGURE 4.3 MEAN SPEED AND TURBULENCE INTENSITY PROFILES FOR OPEN COUNTRY SIMULATED TERRAIN EXPOSURE (34)

where, k is the Von Karman's constant equal to 0.4, Cg is a surface drag coefficient defined in terms of the surface shear stress τ_o as $Cg^2 = \tau_o / \rho V_g^2$; and Zo is the roughness length, i.e. a quantity which characterizes the surface roughness. Typical values of these parameters measured in the wind tunnel and in full scale for two basic exposures are given in Table 4.1. These data together with the spectra of the longitudinal turbulence component presented in Figure 4.4 suggest a geometric scale of about 1/400 for the simulation of the natural wind in the wind tunnel.

4.3 INSTRUMENTATION FOR WIND ENVIRONMENT AT GROUND LEVEL

Wind speed measuring instruments are called anemometers. The techniques and instruments which are generally used for wind tunnel measurements of air speeds are as follows:

1. Point by Point Measurement Techniques

Instruments used for point by point measurements of wind speed include a pitot-static tube (26), a hot-wire or hot-film anemometer (10, 14, 17, 36) measuring only wind speed, with flags or silk thread mounted on it and a black styrofoam ball on a string (16) for measurements of wind direction. The instruments such as optical dynamometer (5), which consists of a cylinder on top of a spring measuring both the wind speed and direction and pulsed hot-wire (3), which consists of two parallel sensor wires and a pulsed-wire equispaced between them giving a measure

	FULL SCALE		WIND TUNNEL	
Exposure	Open Country	Urban	Open Country	Urban
Z_g (m)	270	515	0.60	0.81
Z_o (cm)	1-10	100-500	0.01	1.20
α	0.16	0.40	0.15	0.38
C_g	0.042	0.046	0.042	0.046

TABLE 4.1 - PARAMETERS FOR FULL SCALE AND SIMULATED TERRAINS (34)

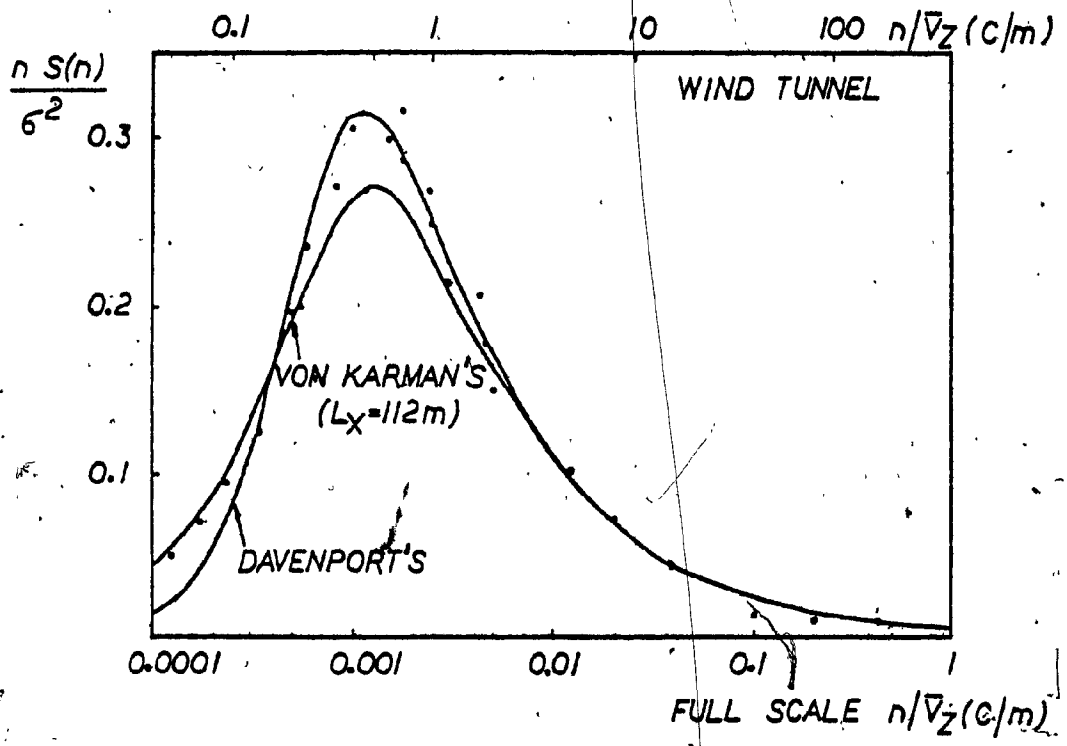

FIGURE 4.4 SPECTRA OF TURBULENCE COMPONENT AT $Z/Z_G = 1/6$ (OPEN COUNTRY EXPOSURE)

of wind speed only are also used for measurements. In addition, thermister anemometers (14, 16, 27) with single ended cylindrical hot-film sensors which cannot measure wind direction have also been used for point by point measurements of wind speed.

2. Continuous Measurement Techniques

Surface flow visualization and sand erosion (5) techniques are based on interpreting erosion patterns, which are formed by the saltation of fine grain patterns spread uniformly on a smooth ground plate. Other measuring methodologies such as the surface pigment techniques (21) have also been used in wind tunnels. The friction of the air blowing on the painted surface with pigment in paraffin leaves contours of pigments of air-flow direction after evaporation of paraffin.

3. Semi-continuous techniques which include smoke (31), smoke wire recording (28) and soap bubbles (5) have been rarely used for recording wind environment around buildings.

Point by point measurement techniques are most commonly used for wind tunnel measurements. Continuous and semi-continuous techniques give only a quantitative description of the wind effects but they are not sufficient for any numerical evaluation of the wind environment in three dimensional flows, especially those around buildings. Accessibility for photographing becomes difficult and particles in the flow may prove dangerous to the delicate instruments around.

In the present work, based on the previous comments and the availability of instruments at the time of the tests, a pitot static tube and a hot-film anemometer were used for wind speed and turbulence measurements. Data were obtained as mean and rms values of the wind speed at different points in the building environment.

4.4 TEST INSTRUMENTS

The instruments used in the present study were a pitot-static tube, a dual channel TSI 1056 linearised anemometer and a TSI 1076 digital voltmeter. These instruments are shown in Figure 4.5 (a and b).

A pitot-static tube is a direct type of measuring instrument. It can be inserted into an air flow to measure the static and the total pressure as shown in Figure 4.5(a). The pressure in the entrance of the total pressure measuring tube, is called total or stagnation pressure. Ideally it is the pressure which results when the velocity is brought to zero and all the kinetic energy has been converted into pressure energy. From Bernoulli's equation

$$P_1 + \tfrac{1}{2}\ \rho \bar{u}_1^2 = P_2 + 0 \qquad \text{.....} \qquad [4.3]$$

Giving $\bar{u}_1 = \left(\frac{2(P_2-P_1)}{\rho}\right)^{\frac{1}{2}}$ ..... [4.4]

or $P_2-P_1 = \tfrac{1}{2}\ \rho \bar{u}_1^2 = q$

where, P_2 = total pressure P_1 = static pressure, u_1 = wind speed, q = dynamic pressure and ρ = density of the air = 1.225 Kg m^{-3} at normal temperature and pressure. The dynamic pressure can be measured directly using an inclined manometer.

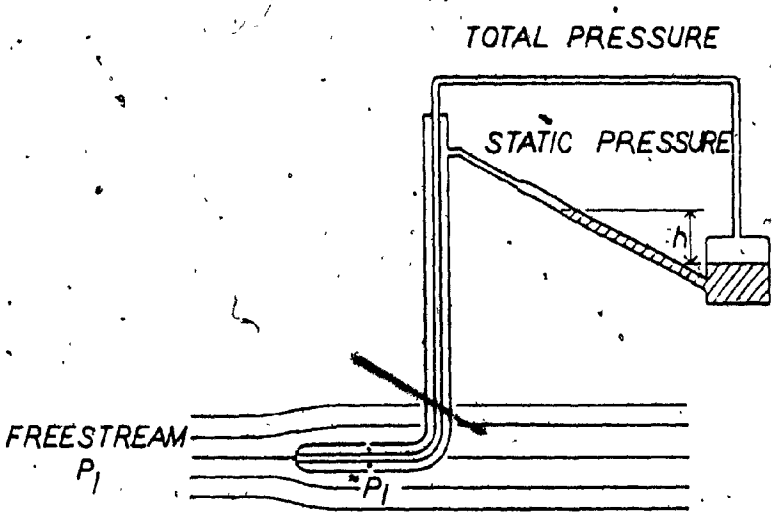

(a) A PITOT STATIC TUBE CONNECTED TO AN INCLINED MANOMETER (1)

(b) ANEMOMETER AND VOLTMETER

FIGURE 4.5 TEST INSTRUMENTS

The Pitot static tube is simple to operate but cannot be used for measurements very close to building or ground surfaces. It is not suitable for accurate measurements of velocity in highly turbulent flows because of its high damping characteristics. Also, it cannot measure turbulence.

In hot-wire anemometer the sensor is made of tungsten wire with thin platinum coating on surface and in hot-film anemometer it is essentially a conducting film on a ceramic substrate. A hot-wire anemometer operates on the principle of the change of resistance of an electrically heated wire with the temperature change due to the cooling effect of the moving airstream over the heated wire. The cooling of the wire by an airstream causes a change in its resistance proportional to the velocity. With appropriate calibration resistance measurement leads to the velocity measurement. The hot-film anemometer is rugged, stable and easy to maintain. It can provide very accurate results and at the same time it is convenient and flexible for wind tunnel measurements.

Measurements made with hot-film sensors may be subjected to deviations unless the direction of mean flow is known and thus separate measurements for determining flow direction are required. Hot-film anemometer measurements, however, become inaccurate if the turbulence intensity is greater than 20% (3). The hot-film cannot register the vertical component of the wind velocity. The possible accumulation of dirt on hot-film make its frequent calibration desirable (4).

The experimental set-up of the present work is shown in Figure 4.6.

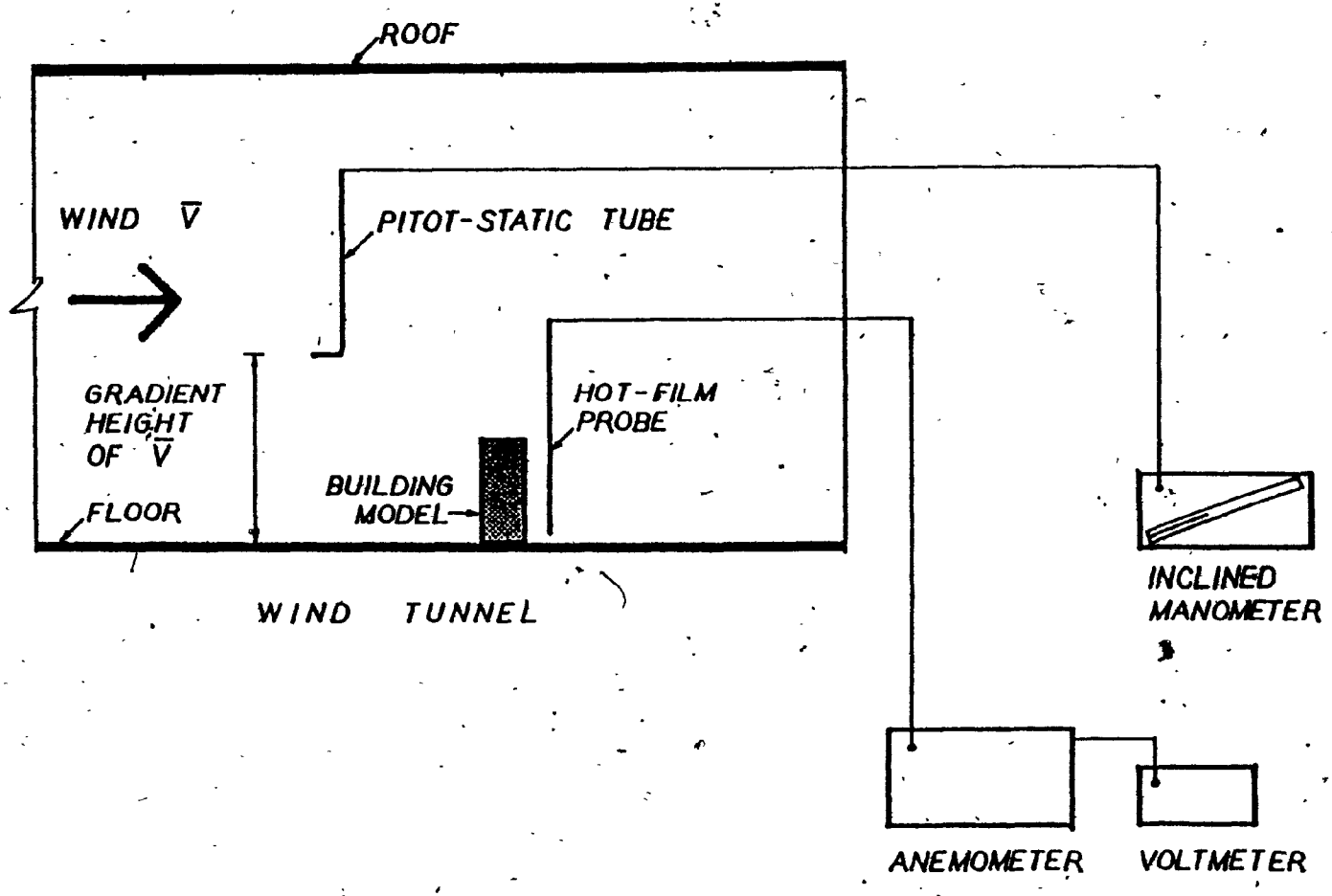

FIGURE 4.6 EXPERIMENTAL SET-UP

The pitot static tube was used to measure the average velocity at the gradient height via an inclined manometer. The gradient height is the height above which the wind velocity is assumed to be constant. The hot film probe connected to the anemometer was fixed at the point of measurement around the building model. The measurements of mean and rms values of wind speed were taken with the digital voltmeter and were recorded manually. Results are presented to express the relative increase or decrease of the mean wind speed and turbulence intensity. Measurements were carried out for a dense grid of points and the information provided was used to represent contours of 0.1 equal intervals for the velocity amplification ratio and contours of 0.5 equal intervals for the turbulence data. The velocity amplification ratio and the turbulence intensity ratio are the values measured in the presence of the building divided by the values measured at the same point in the absence of the building. This type of output format is consistent with the format used by other researchers and makes the comparison of the results easy and convenient.

4.5 INSTRUMENT CALIBRATION AND ACCURACY OF MEASUREMENTS

The use of the hot-film anemometer requires an accurate calibration which can be done as follows: First the Pitot-static tube measures the mean wind speed at gradient height above the centre of the turntable in an empty (without models) tunnel. Then the probe with a single horizontal sensor connected to the anemometer is fixed perpendicular to the

wind stream (because of directional sensitivity) at a point very close to the pitot-static tube. The linearised anemometer is carefully calibrated based on the reference reading of the air velocity as measured by the Pitot-tube at the gradient height. More details about calibration are given in reference 35. The grid of measurement locations is shown in Figure 4.7. The extent of the measurement location shown in the figure was found reasonable from strong wind point of view from the results of initial measurement locations. Kamei and Maruta (17) also used this size of area for their measurements. Beyond this zone wind conditions are not expected to change drastically by the presence of the building.

It was found difficult to measure wind speed and turbulence very close to the building faces because of the vibrations of the hot-film probe in wind flow. The nearest measurement taken from the building faces was at a distance of 10 mm (4m - full scale). Difficulties of measurement at 5mm (2m - full scale) above ground level were often experienced due to frequent breaking of hot-film sensor. In the particular case of the models studied the deviation of measurement results for a difference of ± 30° due to directional sensitivity of the hot-film sensor was found to be small - for most points within ± 2 to 3%. The anemometer model used in the present work has reading accuracy up to 0.5 %. The digital voltmeter is accurate for rms reading as ± 1% of the reading and for mean reading is ± 0.05% of reading. The deviations of measured values of wind speed due to sensor orientation and exact positioning and other technical problems occured in experimentation as well

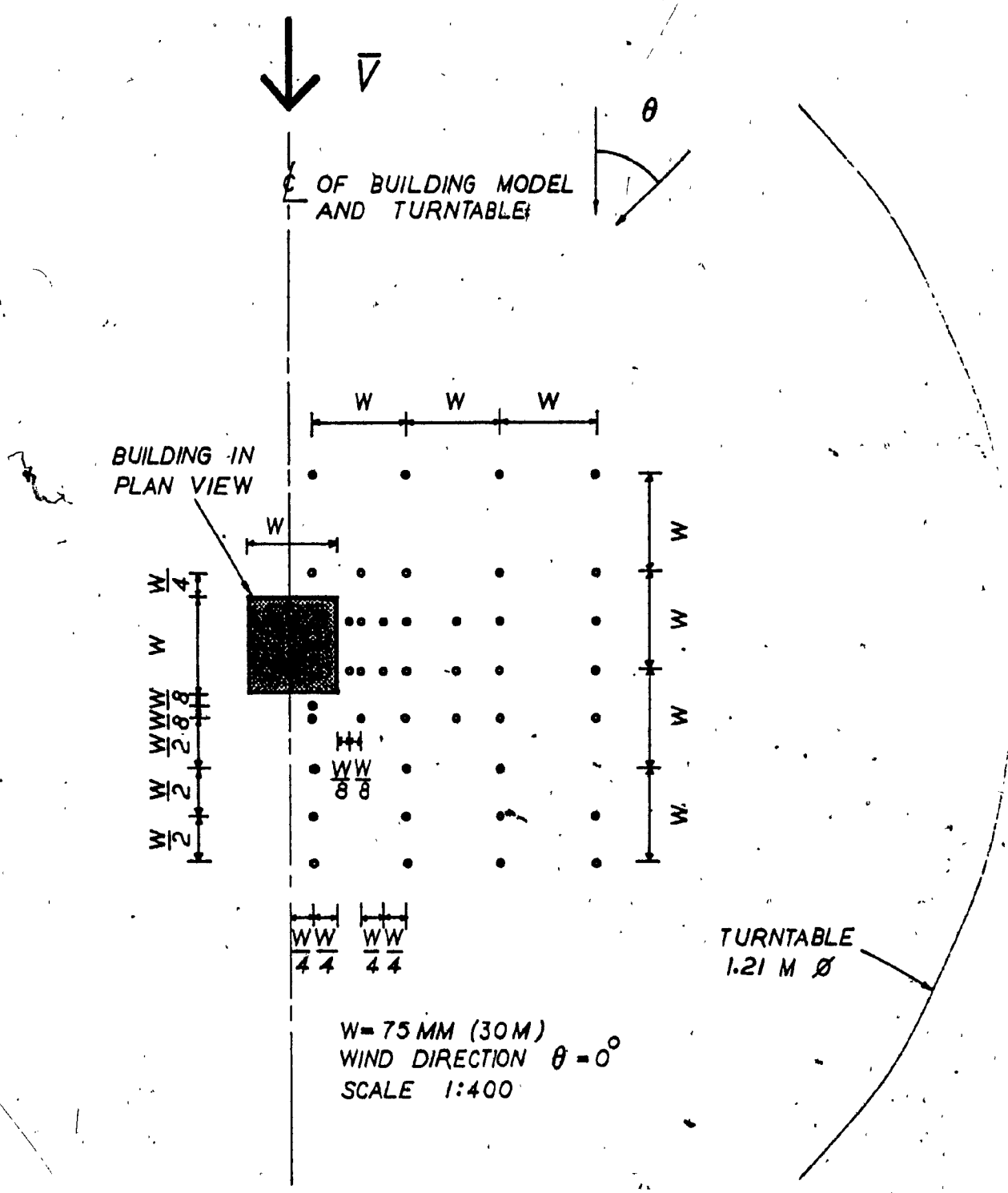

FIGURE 4.7 GRID OF MEASUREMENT LOCATIONS

yield a possible error of 3 to 4% as has been estimated by repeatability measurements.

4.6 BUILDING MODELS

Models were selected to represent square (30 m x 30 m) buildings of different heights. Modern buildings of square shape are often seen with their corners modulated as rounded and chamfered. The functions of these corner configurations are mainly justified for aesthetic purposes. Very few cases of buildings with their corners chamfered vertically are designed to serve environmental purposes. Square buildings of varying heights with one of their corners chamfered were modelled in the wind tunnel to investigate the effect of chamfering building corners on the wind environment at the plaza level. One corner of the model was cut vertically at 45° to its original faces. The minimum width dimension of a chamfered face is an equivalent of a sub modular dimension of the parking grid (i.e. 3m x 6m) for a building.

The modular increment in the chamfer width (t) generated a total of ten building configurations but only six configurations and the case of the square building were selected for tests as was found appropriate during initial experimentation. Basic model configurations are shown in Figure 4.8. They are denoted by numbers, which are used in the test results presented in Chapter 5.

Buildings with one chamfered corner may be seen in the downtown Montreal area (eg. St. Catherine, Dorchester and McGill streets). This is an outcome of building by-laws and maximum floor space utilization if

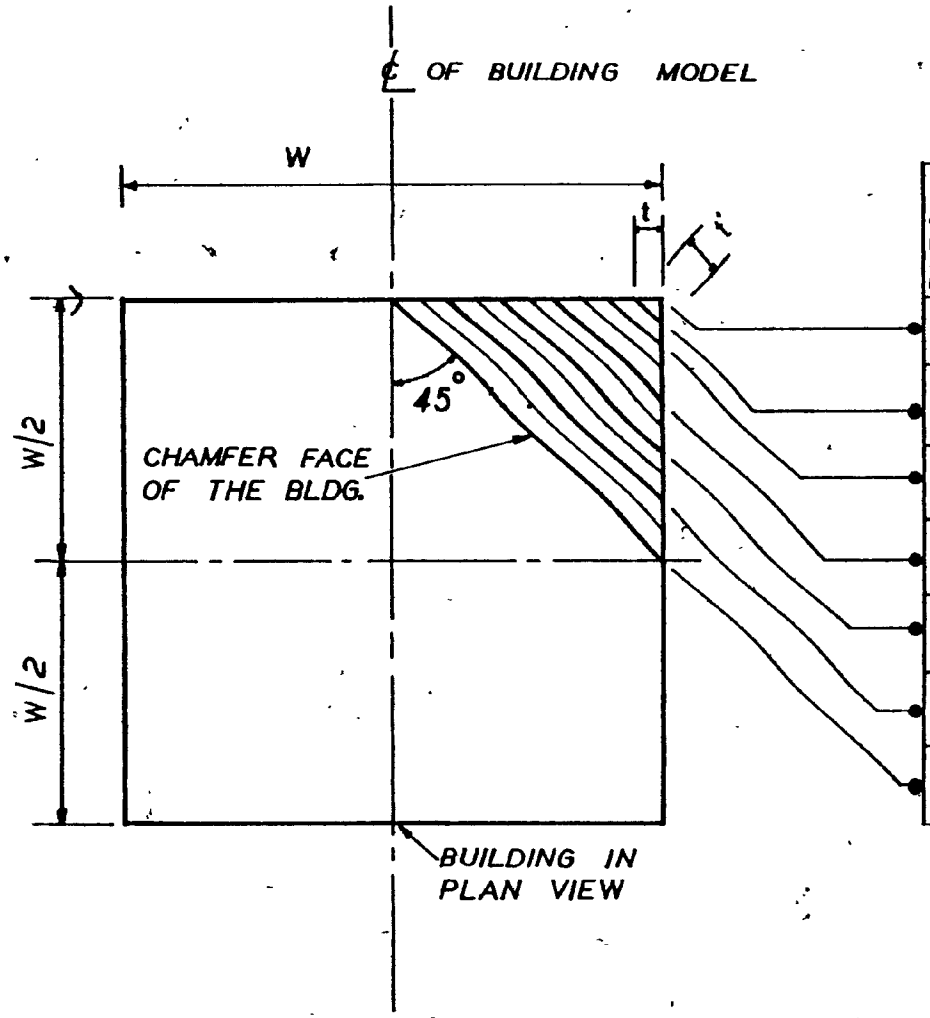

MODEL SCALE 1:400

BLDG. MODEL NO.	t' (mm) (m)	t (mm) (m)	W (mm) (m)	t/W	HEIGHT OF THE BUILDING (H) (mm) MODEL SCALE (m) FULL SCALE :
1	0.0 0.0	0.0 0.0	75 30	0.00	450, 300, 225, 150 180, 120, 90, 60
2	5.3 2.1	3.7 1.5	75 30	0.05	450, 300 180 120
3	10.6 4.2	7.5 3.0	75 30	0.10	450 150 180 60
4	21.2 8.5	15.0 6.0	75 30	0.15	450 150 180 60
5	31.8 12.8	22.5 9.0	75 30	0.30	450 150 180 60
6	42.4 17.0	30.3 12.0	75 30	0.40	450 150 180 60
7	53.0 21.2	37.5 15.0	75 30	0.50	450 150 180 60

FIGURE 4.8 BUILDING MODEL CONFIGURATIONS

the buildings of corner plot are located on the crossing of the streets. Penthouses on top of tall buildings or the fenestration of facades may not be modelled as they will probably have a small effect on the pedestrian level wind environment.

The models used in the tests were made of wood to a scale of 1/400. The model height was varied between 150 mm to 450 mm (60 m to 180 m full scale) corresponding to 20 to 60 storeys. The length of the chamfered face (t') varied from 5.3 mm to 53 mm (2.12 m to 21.2 m). The other chamfer dimensions, and the various heights of the building for the six configurations tested are also given in Figure 4.8. Two views of the building models used in the tests are shown in Figure 4.9. Experiments were also conducted on models of buildings with chamfered roofs to investigate their effect on wind environment at plaza level. Details about the tests are presented in Chapter 5. Note that the 1/400 geometric scale used for the models is not an absolute figure. Simulation tests show that similar results can be obtained for buildings made to 1/300 or 1/500 scale. This gives an idea about the tolerance of the representation of the test results for buildings of different size.

4.7 TEST PROGRAMME

The basic model configurations were combined with parameters such as building height, wind attack angle, and two different heights of measurement. Table 4.2 shows the test programme for the seven model configurations and their associated parameters in the tests.

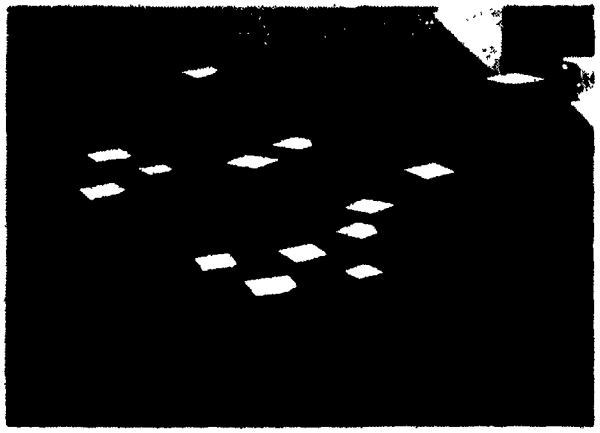

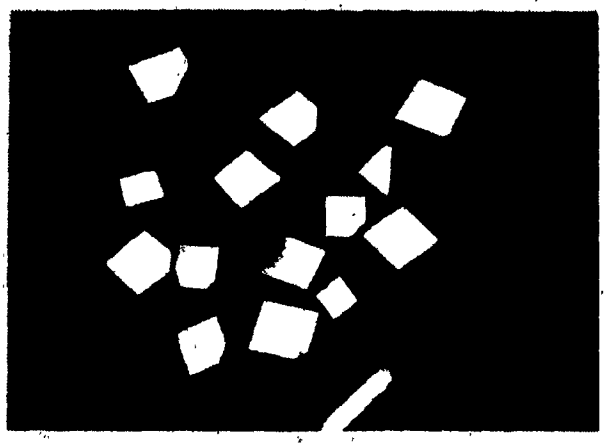

FIGURE 4.9 VIEWS OF BUILDING MODELS

MODEL SCALE 1:400

BLDG. MODEL NO.	SCALE	HEIGHT OF THE BUILDING (H)				HEIGHT OF MEASUREMENT		WIND ATTACK ANGLE, θ			
	MODEL (mm)	450	300	225	150	25	10	0°	30°	45°	60°
	FULL (m)	180	120	90	60	10	2				
1		•			•	•	•	•		•	
			•			•		•			
				•		•		•			
					•	•		•		•	
2		•	•			•		•			
3		•				•		•	•	•	•
		•					•	•			
					•	•		•			
4		•			•	•		•			
5		•			•	•		•			
6		•				•		•	•	•	•
		•					•	•			
					•	•		•			
7		•			•	•		•			

TABLE 4.2 BUILDING MODEL TEST PROGRAMME

Basic models number 1 to 7 were tested to investigate the effect of chamfering a 450 mm (180 m) tall building on the wind environment at 25 mm (10 m) height above ground level. Model number 3 and 6 were found to be more effective in assessing the effect of the chamfer on wind conditions and were chosen to investigate this effect at 10 mm (2 m) above ground level. Only selected measurements were taken at the low level, however, as it was found difficult to measure close to the ground surface. Model number 1 was tested at the lower measurement height of 10 mm above ground level for tall and low building heights to investigate the effect of different heights of the building on the wind environment.

The effect of low square buildings on wind environment at the base was found quite small in magnitude compared to that of higher buildings. It was difficult, time consuming and unnecessary to test every individual building configuration. Therefore only critical model configurations were tested as found necessary from earlier test results. Tests were carried out however, to investigate the effect of building height and also wind attack angle on wind conditions at the base of square and chamfered buildings.

The description of experiments in this chapter demonstrates the procedure to arrive at quantitative information of the wind environment at the base of tall buildings. The test results of the experiments on the wind environment expressed as relative increase or decrease in mean wind speed and the turbulence factors are presented in the next chapter.

CHAPTER 5

EXPERIMENTAL RESULTS AND DISCUSSION

Experimental test results on the wind environment around square and chamfered buildings are presented in this chapter. Comparison tests are shown to confirm the validity of the wind tunnel simulation. The results are illustrated for two measurement heights, different building heights and wind attack angles. Test results on the effect of a chamfered roof building on the pedestrian level wind enviornment are also presented.

5.1 COMPARISON TESTS

The objective of the comparison tests was to reproduce experimental results provided by other researchers before proceeding with the present study. Agreement between these results and those of the present experiments would confirm the validity of wind tunnel simulation and output.

It was decided to carry out some of the experiments reported by Kamei and Maruta (17) on wind environment around rectangular buildings. The decision was based on the simplicity of building model configurations and the similarity of other test parameters with these of present study. The scale of the building models was 1/300 and the measurements were taken at 10 m full scale equivalent height above ground level. Unfortunately, the experimental work of reference 17 provided data for mean wind speeds only with no information about turbulence conditions.

Therefore comparisons were made for mean wind speeds only. The effect of square buildings on the strong wind region in the corner stream with different exposures in both the crosswise and streamwise directions is presented in Figure 5.1.1. Velocity amplification ratios $\bar{V}_hP/\bar{V}_hA$ and the location of their occurrence do not vary much between urban and open country exposures.

In the present work, building models of the same geometry were made to a scale of 1/400. The measurements were taken at locations shown in Figure 4.7 at 25 mm (10 m full scale) above the ground level for an open country exposure. The results shown in Figure 5.1.2 are contours of the ratio of wind velocities affected by the presence of the building over those measured at the same point in the absence of the building to express the relative increase or decrease of mean wind velocities.

The maximum values of $\bar{V}_{10}P/\bar{V}_{10}A$ and the variation of wind flow pattern of the strong wind region around buildings of different heights measured by Kamei and Maruta show good agreement with the experimental results of the present study. This confirms the validity of the wind tunnel data and also increases confidence in the simulation of the atmospheric boundary layer wind characteristics in the wind tunnel.

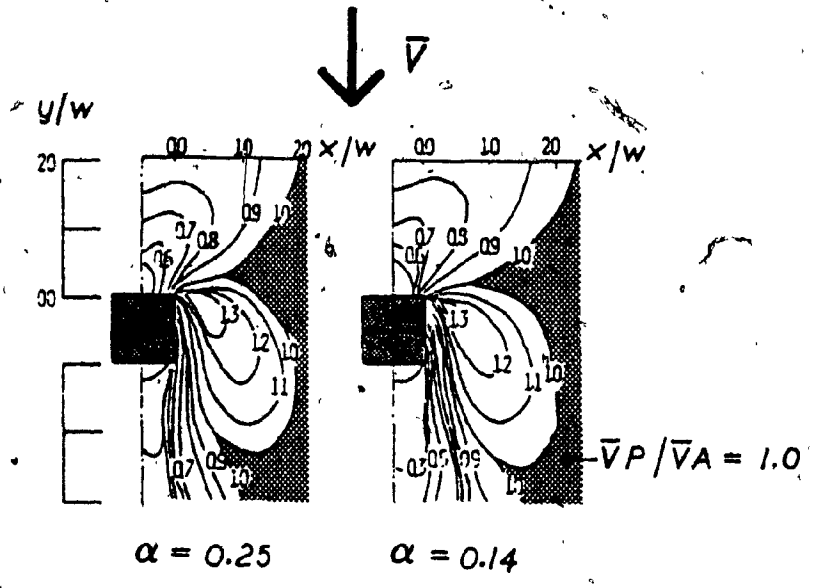

(a) EFFECT OF POWER-LAW EXPONENT OF VELOCITY PROFILE ON WIND ENVIRONMENT
MODEL HEIGHT H=20 CM(60 M), WIDTH W = 10 CM(30M) (17)

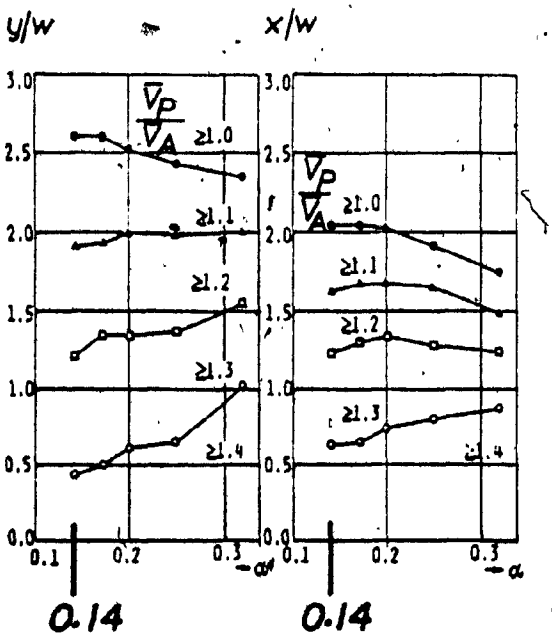

FIGURE 5.11(b) VARIATION OF THE STRONG WIND REGION WITH POWER-LAW EXPONENT α (17)

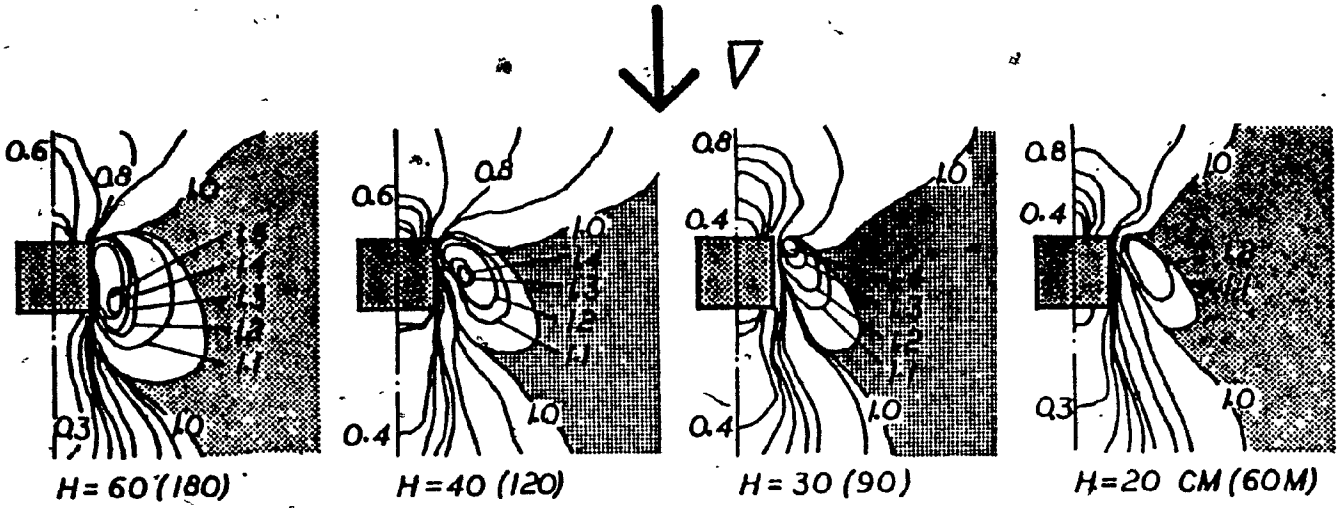

H = 60 (180) H = 40 (120) H = 30 (90) H = 20 CM (60M)

D=W= 10 CM (30M)
HEIGHT OF MEASUREMENT, 3.33 CM (10M)
SCALE 1:300

EXPERIMENTS BY KAMEI AND MARUTA (17)

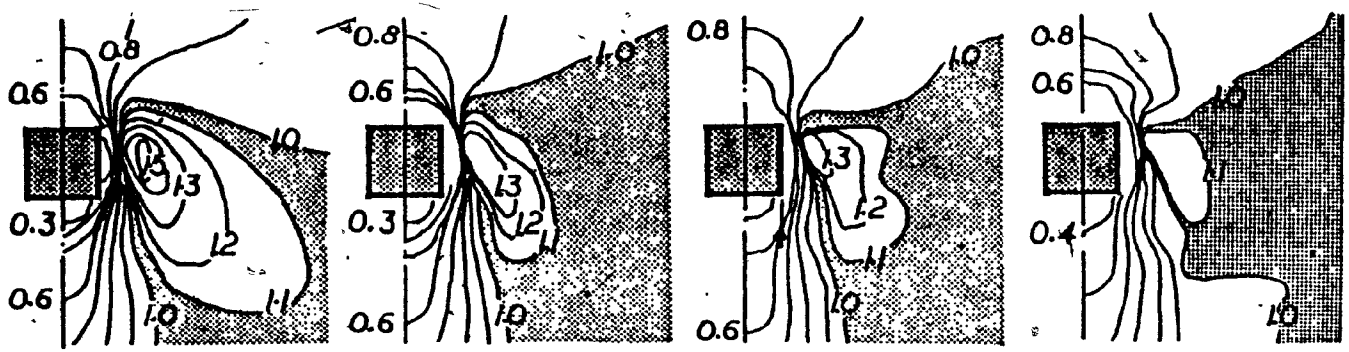

H = 45 (180) H = 30 (120) H = 22.5 (90) H = 15 CM (60M)

D=W = 7.5 CM (30M)
HEIGHT OF MEASUREMENT, 2.5 CM (10M)
SCALE 1:400

CBS RESULTS

FIGURE 5.1.2 COMPARISON OF TEST RESULTS

5.2 WIND FLOW FIELD AROUND BUILDINGS

Experimental results for mean velocity and turbulence conditions of the flow field around square and chamfered buildings of 180 m height are presented in this section.

5.2.1 Mean Velocity Conditions

Figure 5.2.1 shows the experimental results for models of 180 m tall square and chamfered buildings exposed to wind. Contours of 0.1 equal intervals represent the velocity amplification ratio $\bar{V}_{10}P/\bar{V}_{10}A$ (mean wind speed in the presence of the building/mean wind speed in the absence of the building) at 10 m above ground level. The wind flow field around the building can be divided into three basic regions, namely:

1. Low velocity on windward side;
2. Very low velocity on leeward side; and
3. High velocity in the corner stream of a building.

For a square building $\bar{V}_{10}P/\bar{V}_{10}A$ reaches a maximum value of 1.5 in the corner stream, a minimum value of 0.3 on the leeward side and a minimum value of 0.6 on the windward side. These values can be explained by considering the flow approaching a building. This flow is diverted both over the top as well as around the sides of the building with separation normally occuring at the leading sharp edges. Furthermore, the pressure

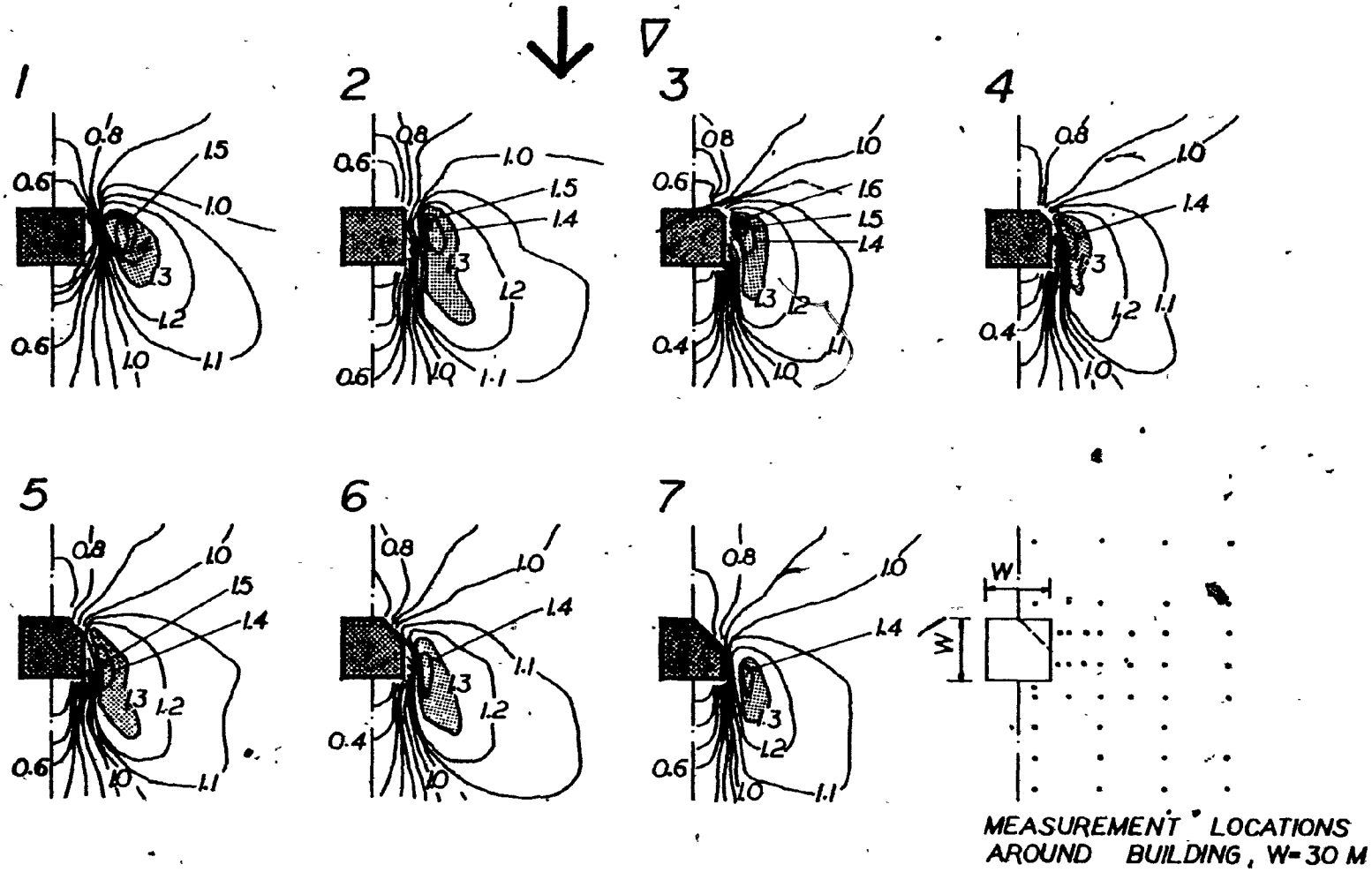

FIGURE 5.2.1 WIND FLOW FIELD AROUND TALL SQUARE AND CHAMFERED BUILDINGS

differences between low pressure wake regions (leeward face) and the relatively high pressure regions at the base of the windward face accelerate the flow around corners. The flow directed between these two regions around corners induces very high wind velocities in the corner stream. For a square 30 m x 30 m building 180m high, the mean wind speed in the corner stream increases up to 50 percent, as already mentioned. Similar results of velocity amplification for square buildings have been also found by Kamei and Maruta (17) (Figure 5.1.2) and discussed by other researchers (5,10,16,26).

The chamfered building does not reduce the maximum value of ratio $\bar{V}_{10}P/\bar{V}_{10}A$ much. This ratio reaches a maximum value of 1.4 for a building model of maximum chamfer face length. The reduction of the width of a building results in the location of the high velocity region close to the corner stream face of a building. In general, chamfering of a building corner reduces the width of the region of high velocities close to the corner stream face of a building.

The high velocity region around chamfered buildings may be explained in terms of pressure. The low wake pressure on the leeward side of the building depends on the velocity at the top of the building and therefore, no reduction of high velocities occurs for the same building height.

The gradient of the velocity amplification ratio for square and chamfered buildings is high very close to the corner stream face of a building. Figure 5.2.2 shows the variation of the velocity amplific-

ation ratio in a crosswise direction from the building face for the square and chamfered buildings. Maximum values of $\bar{V}_{10}P/\bar{V}_{10}A$ are found very close to the corner stream face of the chamfered building compared to square building. The maximum value of $\bar{V}_{10}P/\bar{V}_{10}A$ is very low for the square model but reaches up to 1.6 for chamfered model No. 3 and drops gradually for higher chamfers. The effect of chamfered buildings on the high velocity region is seen to be approximately equal to 1.25 W from the corner stream face in a cross wise direction. The highest values of the velocity amplification ratios in the streamwise direction for square and chamfered buildings are shown in Figure 5.2.3. The effect of chamfered buildings on the high velocity region also may be pointed out by comparing the peak values of a square building with chamfered building models at a point the same distance from the buildings face. The peak values which are found very low for square buildings have increased drastically for chamfer model No. 2 and become maximum for model No. 3. These peak values are found very close to the corner stream face of the building. The figure also shows the negligible effect of higher values of chamfered lengths on velocity amplification on windward and leeward sides of the buildings.

5.2.2 Turbulence Conditions

Motion of fluids in which local velocities and pressures fluctuate irregularly, in a random manner, is known as turbulence or turbulent flow. Turbulence is characterised by its intensity which is defined as the root mean square (rms) value of the wind velocity at a point divided by the mean wind velocity at the same point.

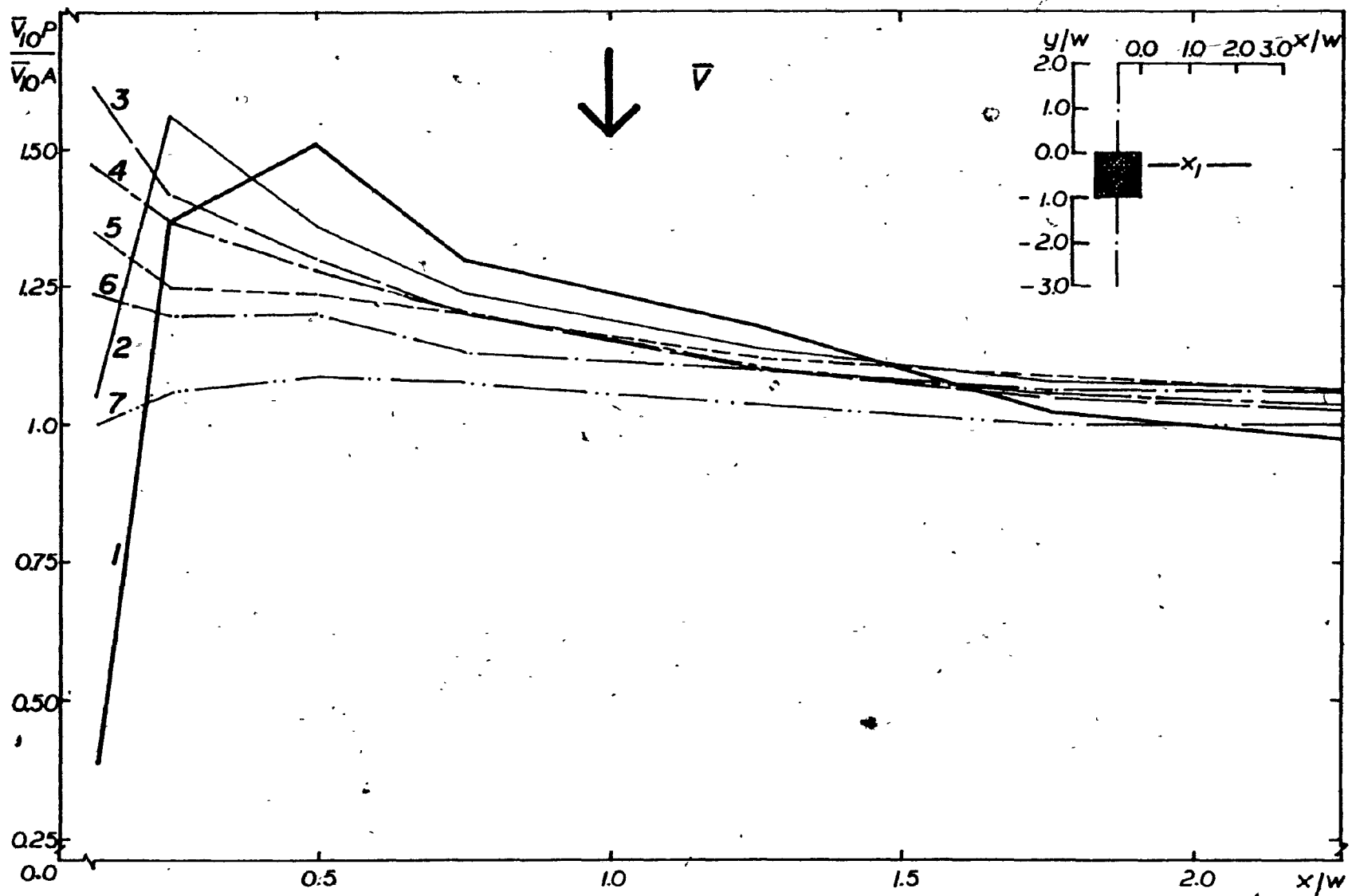

FIGURE 5.2.2 AMPLIFICATION OF VELOCITY CLOSE TO THE BUILDING FACE IN A CROSSWISE DIRECTION (AXIS $-x_1$)

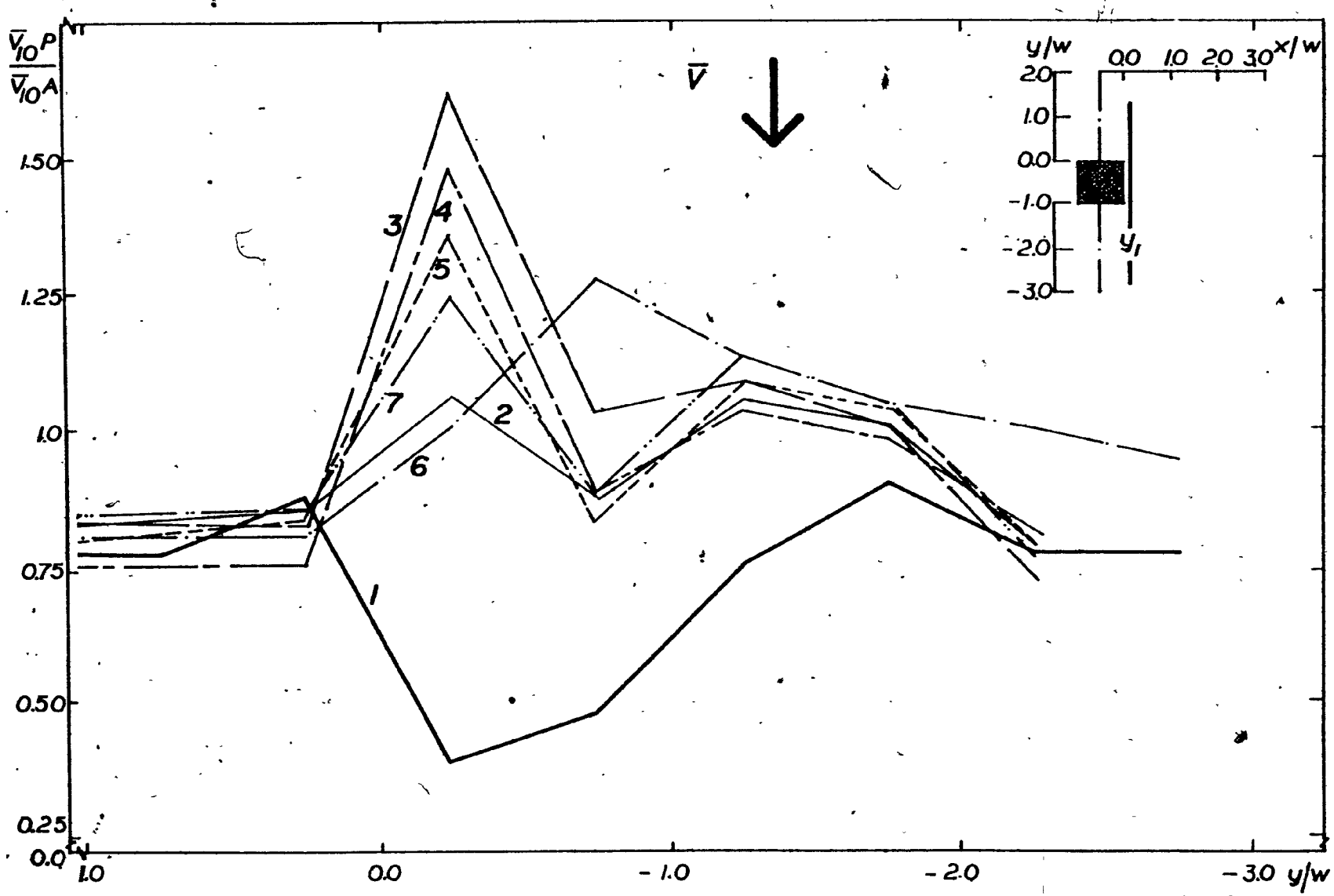

FIGURE 5.2.3 AMPLIFICATION OF VELOCITY CLOSE TO THE BUILDING FACE IN A STREAMWISE DIRECTION (AXIS-y_1)

Turbulence conditions around models of 180 m tall square and chamfered buildings are presented in Figure 5.2.4 in the same format as in Figure 5.2.1. Contours here represent the ratio $T_{10}P/T_{10}A$, i.e. turbulence intensity in the presence of the building divided by turbulence intensity in the absence of the building, and they are given in 0.5 intervals along with the contour corresponding to the lowest value.

The turbulence around square and chamfered buildings as observed in Figure 5.2.4 can be classified into three regions, namely:

1. Low turbulence in the corner stream region;
2. Higher turbulence on the windward side; and
3. Very high turbulence on the leeward side.

For a square building the ratio $T_{10}P/T_{10}A$ reaches maximum values of approximately 2.0 on the windward side, and 4.0 on the leeward side. A minimum value of 0.6 is reached in the corner stream.

The turbulence on the windward face of a square building joining the higher intensity turbulence on the leeward side, wrapping around the corner stream face of a building is directly associated with the intensity of the velocity flow field around the building as described in section 5.2.1. The spread of this joining passage around the corner stream face of a building depends on the high velocity flow fields in that region.

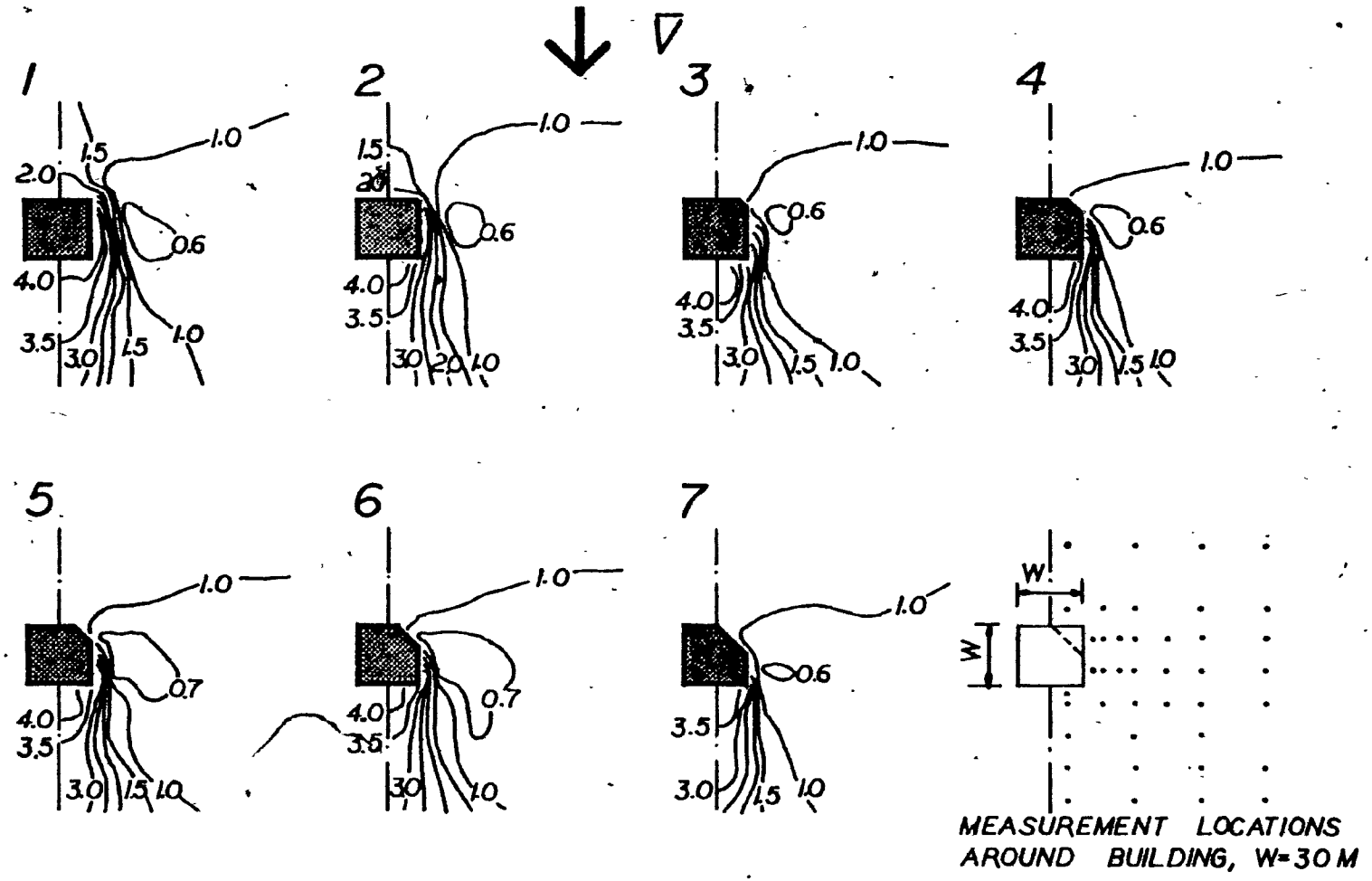

FIGURE 5.2.4 TURBULENCE CONDITIONS AROUND TALL SQUARE AND CHAMFERED BUILDINGS

For a square 30m x 30m building 180 m high, the turbulence intensity on the leeward side increases up to 4 times the value without the building. Comparison of these results with other studies is difficult because very few such data are available in the literature.

Similar results of turbulence conditions have been found for chamfered buildings. For higher values of chamfer length, some reduction in turbulence is observed close to the corner stream face. As the original width of the face reduces, the shape of a building changes considerably for higher chamfer lengths. This is easily understood as wider chamfered faces will be more sensitive to the velocity of the flow instead of turbulence at the base of the building.

Figure 5.2.5 shows the variation of turbulence intensity in the crosswise direction from the corner stream face of the building. The effect of the chamfer is seen only very close to the building face in corner stream. For example, for a square building the maximum value of $T_{10}P/T_{10}A$ reaches up to 4.1. A considerable reduction is seen for the chamfered buildings (models No. 3 and 7). Chamfering does not have any effect after approximately 0.5 W from the building face in corner stream. After this length from the face, the turbulence intensity varies within a range ± 20%.

Peak values of $T_{10}P/T_{10}A$ are often observed near the corner stream face of square and chamfered buildings. Figure 5.2.6 shows those values on the streamwise direction, which are quite low for chamfered buildings

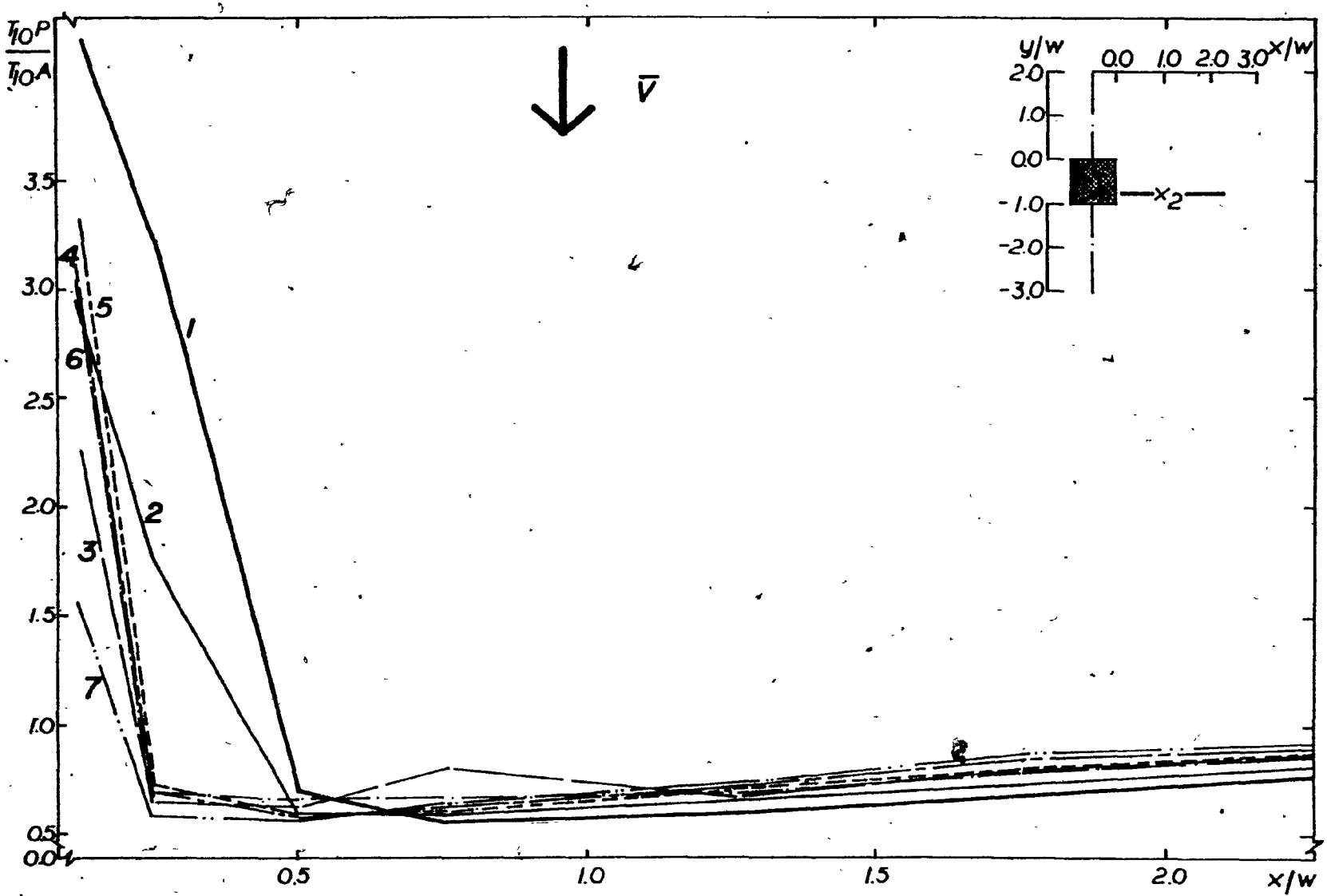

FIGURE 5.2.5 TURBULENCE CONDITIONS CLOSE TO THE BUILDING FACE IN A CROSSWISE DIRECTION (AXIS - x_2)

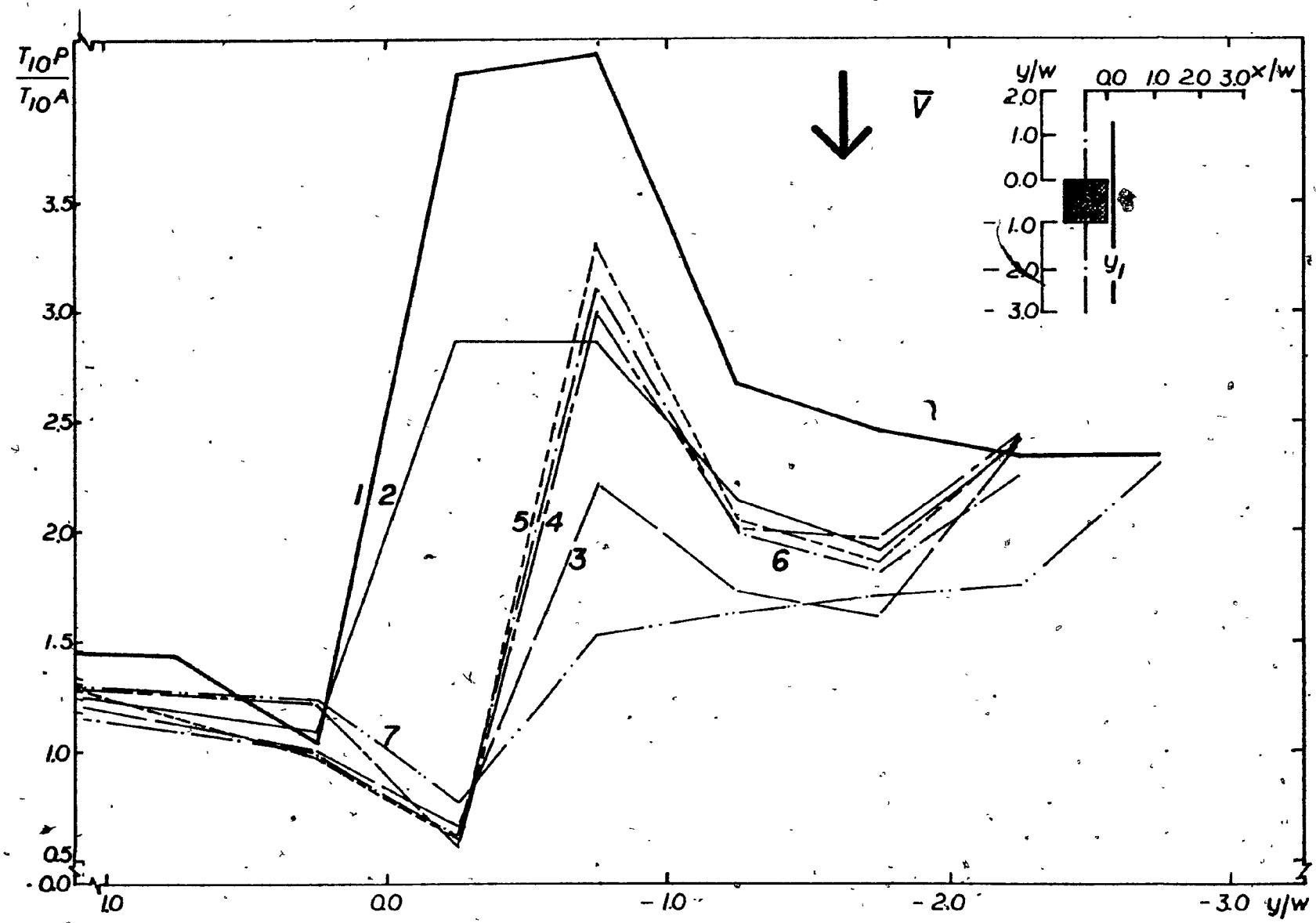

FIGURE 5.2.6 TURBULENCE CONDITIONS CLOSE TO THE BUILDING FACE IN A STREAMWISE DIRECTION (AXIS - y_1)

compared to the square building, but found to be high on the corner stream face of the buildings downstream.

It is interesting to note that higher velocity amplification ratios are always associated with low turbulence ratios. Figure 5.2.7 shows the areas of velocity amplification and turbulence reduction found around square and chamfered buildings 180 m high. The contour of 1.3 for $\bar{V}_{10P}/\bar{V}_{10A}$ representative of higher amplification, in a corner stream, is always associated with the contours of 0.6 or 0.7 for T_{10P}/T_{10A}. This has been observed for both square and chamfered buildings. Similar results regarding turbulence around buildings in general, have been pointed out by Davenport (16) and are also discussed in other studies (15, 25 and 27).

Chamfering a corner of a building does not affect the flow much on the windward and leeward sides of the building but largely reduces the extent of high velocity amplification in corner stream. Chamfered face lengths of a higher value than approximately 0.15 W do not show a significant reduction in the maximum value of velocity amplification in the corner stream except shifting those areas downstream close to the building face. Areas of velocity amplification are always areas of turbulence reduction. Higher values of turbulence intensity remain very close to the corner stream face of the chamfered buildings. The effect of the buildings and chamfer geometry on wind conditions at the base as pointed out in this section suggests the need for further investigation of only specific cases of chamfered building geometry. It also suggests

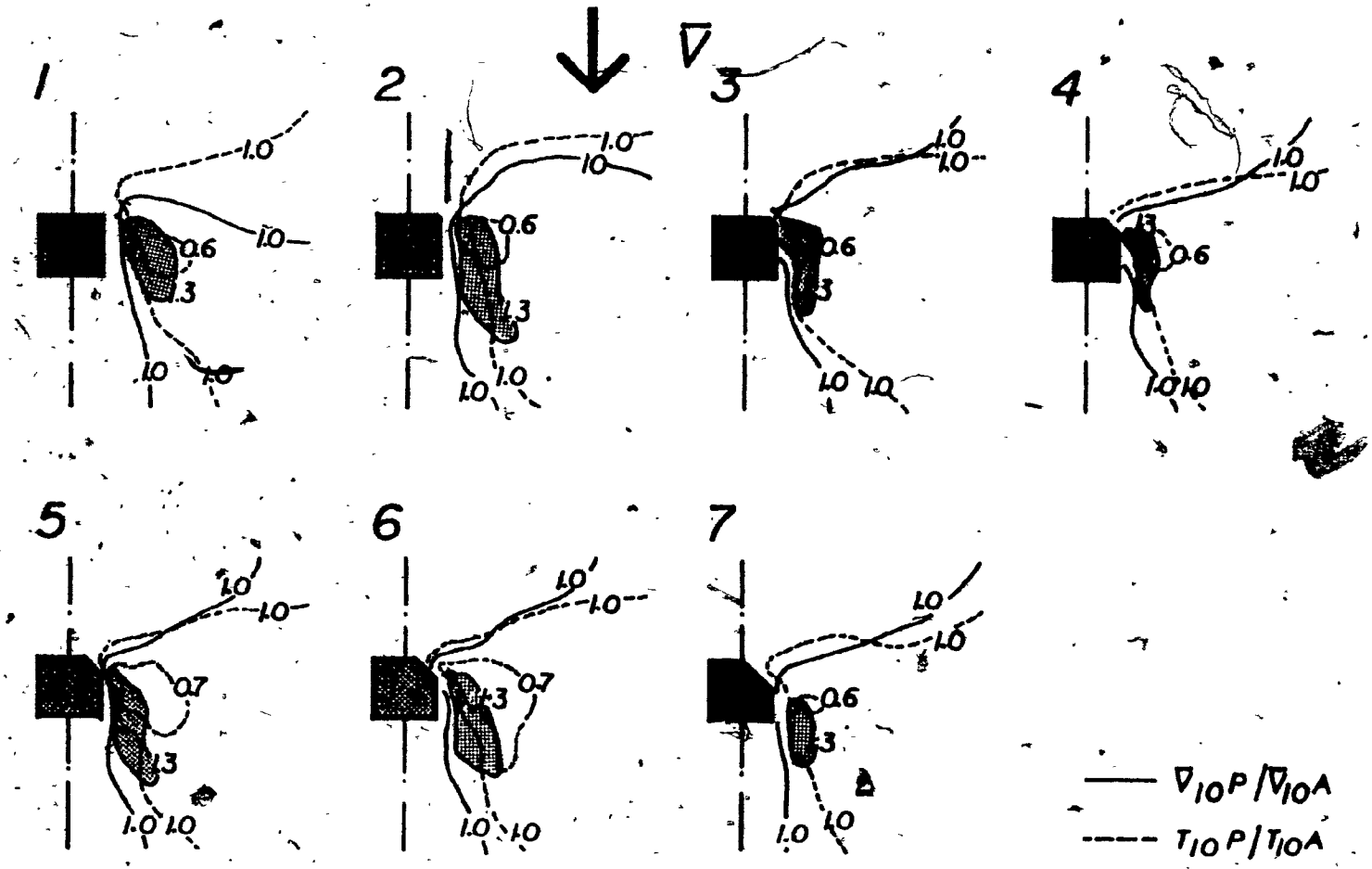

FIGURE 5.2.7 VELOCITY AMPLIFICATIONS AND TURBULENCE REDUCTIONS AROUND HIGH-RISE BUILDINGS (H = 180 M)

the need of more experiments on wind environment for different test parameters.

5.3 EFFECT OF MEASUREMENT HEIGHT ABOVE GROUND LEVEL

Effect on pedestrian level wind environment should be measured at 2 m above ground level but only specific tests were carried out at 2 m level. However, it was found technically difficult to measure very close to the ground surface and therefore the bulk of the measurements were carried out at a 10 m equivalent full scale height.

Measurements at a 2m equivalent full scale height were done only for characteristic cases and respective results were compared. This practice has also been applied in similar works as described in references 17 and 27.

Figure 5.3.1 compares results of the tests for a square building and two chamfered buildings (No. 3 and 6) for measurements made at 10 and at 2 meters above ground level. Contours of 0.1 equal intervals for $\bar{V}_{10}P/\bar{V}_{10}A$ are shown in the left half and for $\bar{V}_2P/\bar{V}_2A$ in the right-half of each sketch.

Turbulence contours around the same buildings are shown in Figure 5.3.2 in which all the parameters remain the same as in Figure 5.3.1. These contours are shown in 0.5 equal intervals and also correspond to lowest values as indicated for $T_{10}P/T_{10}A$ in the left half and for T_2P/T_2A in the right half of each sketch.

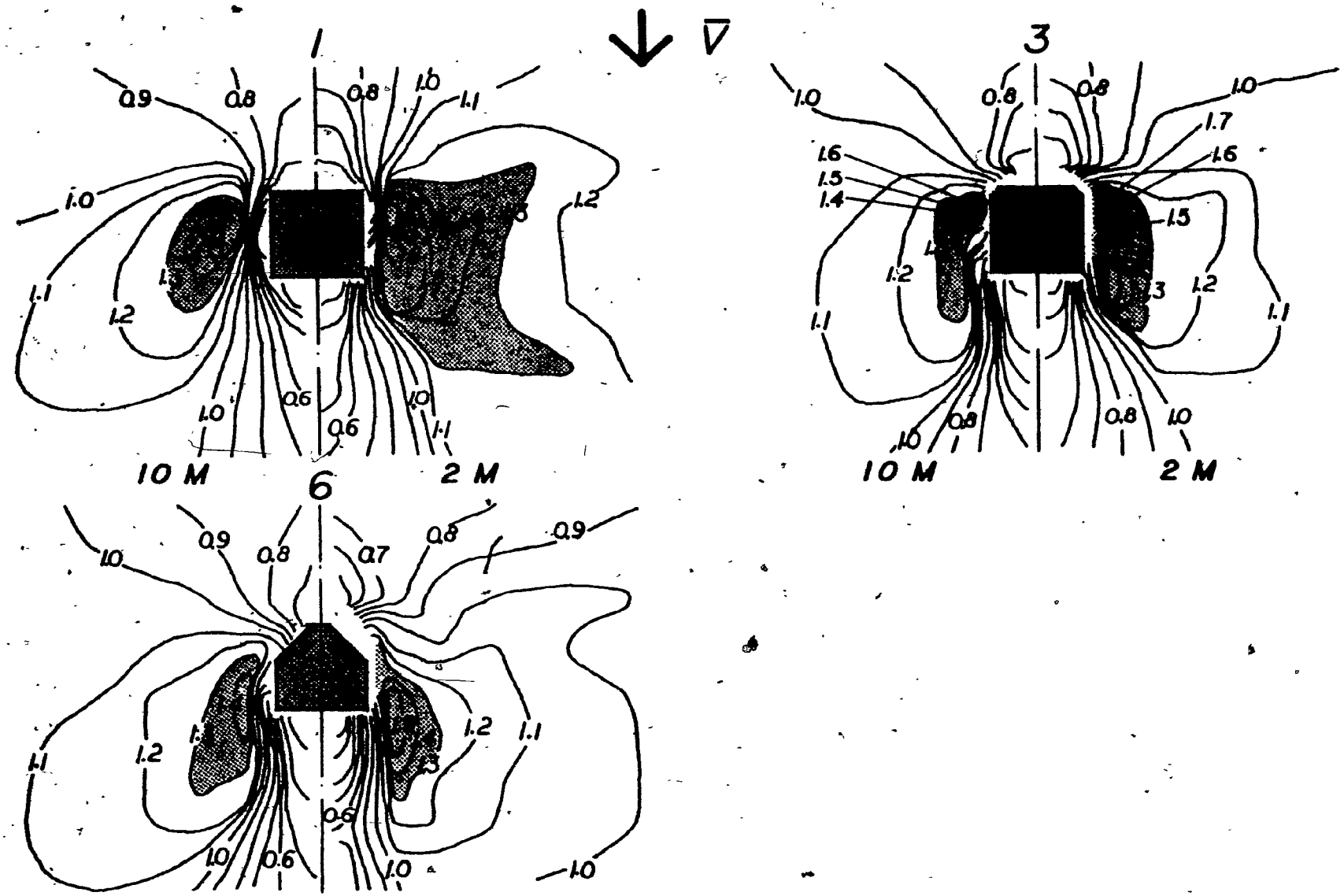

FIGURE 5.3.1 EFFECT OF MEASUREMENT HEIGHT ON VELOCITY AMPLIFICATION AROUND BUILDINGS (H=180 M)

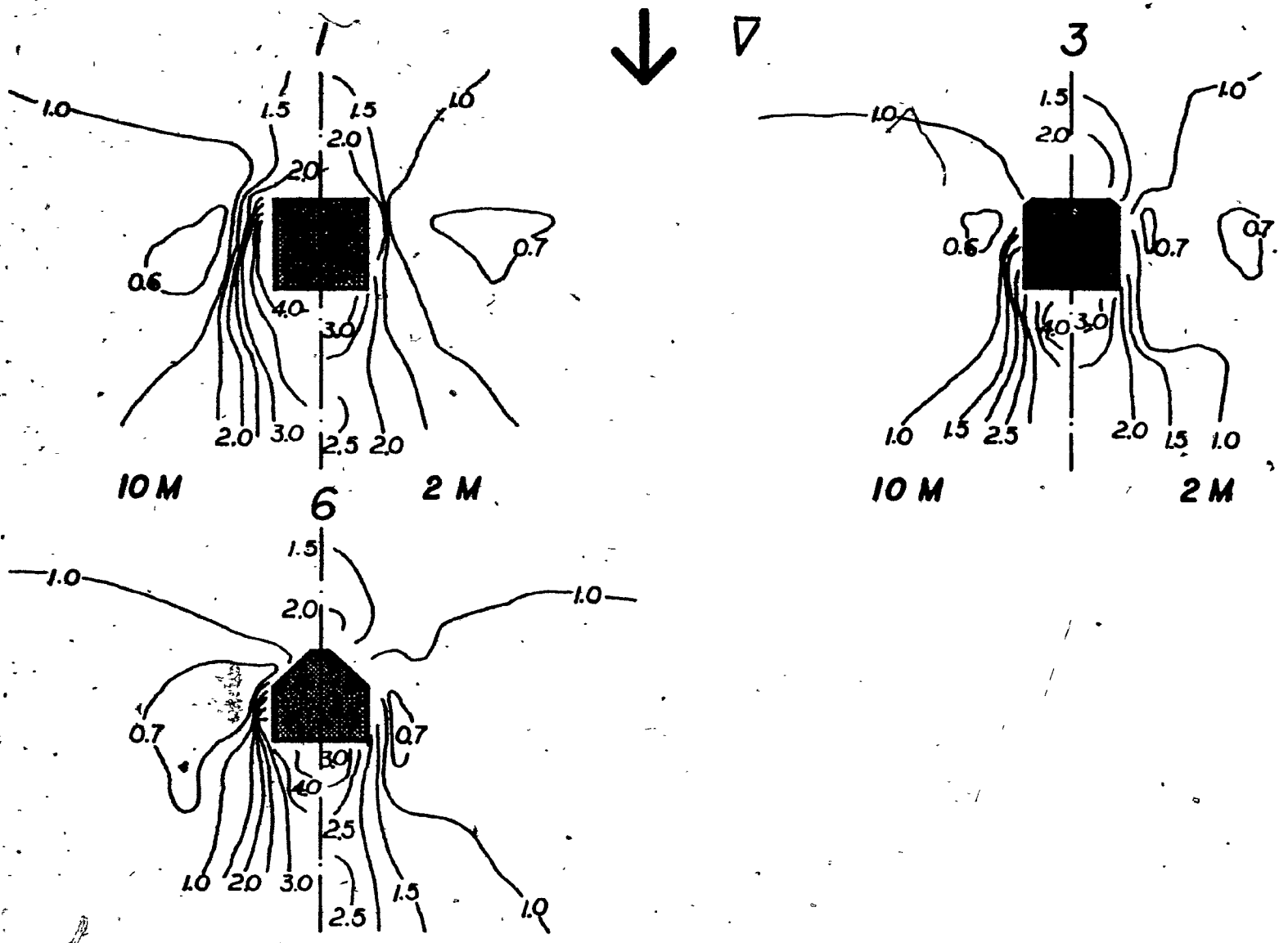

FIGURE 5.3.2 EFFECT OF MEASUREMENT HEIGHT ON TURBULENCE AROUND BUILDINGS (H=180 M)

It has been observed that for a square building, $\bar{V}_2P/\bar{V}_2A$ increases up to a maximum of 1.7 in the corner stream and the areas of high velocity amplification expand in the crosswise and streamwise directions more than for the ratios $\bar{V}_{10}P/\bar{V}_{10}A$. The values of low velocities on the windward and leeward sides do not change much from those measured at 10 m height. The turbulence on the windward and in the corner stream appears similar for the two measurement heights with a little reduction on the leeward side of the building at the 2 m height.

For chamfered buildings, the value of $\bar{V}_2P/\bar{V}_2A$ reaches a maximum of 1.7 for model No. 3 and 1.5 for model No. 6. The values of low velocities on the windward and leeward sides are not affected. However, a considerable reduction in the size of areas of high velocity amplification in the corner stream has been observed making the patterns obtained for the two heights comparable. The turbulence intensity increases to a maximum value of 2.0 and 3.0 for T_2P/T_2A on the windward and leeward sides of the chamfered buildings respectively.

Areas of velocity amplification are also areas of turbulence reduction at 2 m height. The effect on strong wind region at lower level of measurement in a corner stream of a building is also denoted by the contours of high velocity amplification ratios, equal or greater than 1.3. The contour of 1.3 reasonably represents a strong wind in magnitude and extent in the flow field at the base of the building. This is illustrated in Figure 5.3.3 for building models No. 1, 3 and 6 with contours of 1.0 and 1.3 for $\bar{V}_2P/\bar{V}_2A$ and 1.0 and 0.7 for T_2P/T_2A.

Here, the contours of 1.0 show relatively good agreement, except for a little deviation downstream in the corner stream region. The higher velocity amplification area in the corner stream of a 180 m high square building increases in extent at the 2 m compared to 10 m height of measurement. For chamfered buildings, the increase in intensity and extent of higher velocity amplification area is very small at the 2 m height. The turbulence increases on the windward side of both the square and chamfered buildings at lower level of measurement. Similar results for velocity amplification for square buildings are discussed by Kamei and Maruta (17) and they have been presented in Figure 2.5 (a).

Results presented for the square and two chamfered buildings for a strong wind area in a corner stream in Figure 5.3.4 show contours of 1.3 and 1.0 for $\bar{V}_{10}P/\bar{V}_{10}A$ and $\bar{V}_2P/\bar{V}_2A$. Contours of the highest value, lowest value and 1.0 as indicated for $T_{10}P/T_{10}A$ and T_2P/T_2A are presented in the bottom sketches.

A procedure for plotting and comparing the strong wind areas in the corner stream of a building as outlined in Figure 5.3.4 is presented in the top sketch of Figure 5.3.5. The sketch shows the notation and terminology used in this procedure. A similar methodology is used by Penwarden and Wise (31) and is also presented in reference 17.

Figures 5.3.5, 5.3.6 and 5.3.7 show the relative distances from the building faces of the strong wind area in the corner stream in the crosswise and streamwise directions as denoted by the contour of 1.3 for $\bar{V}_{10}P/\bar{V}_{10}A$. The values at the 2 m height of measurement for square and chamfered buildings No. 3 and 6 are also shown in the Figures.

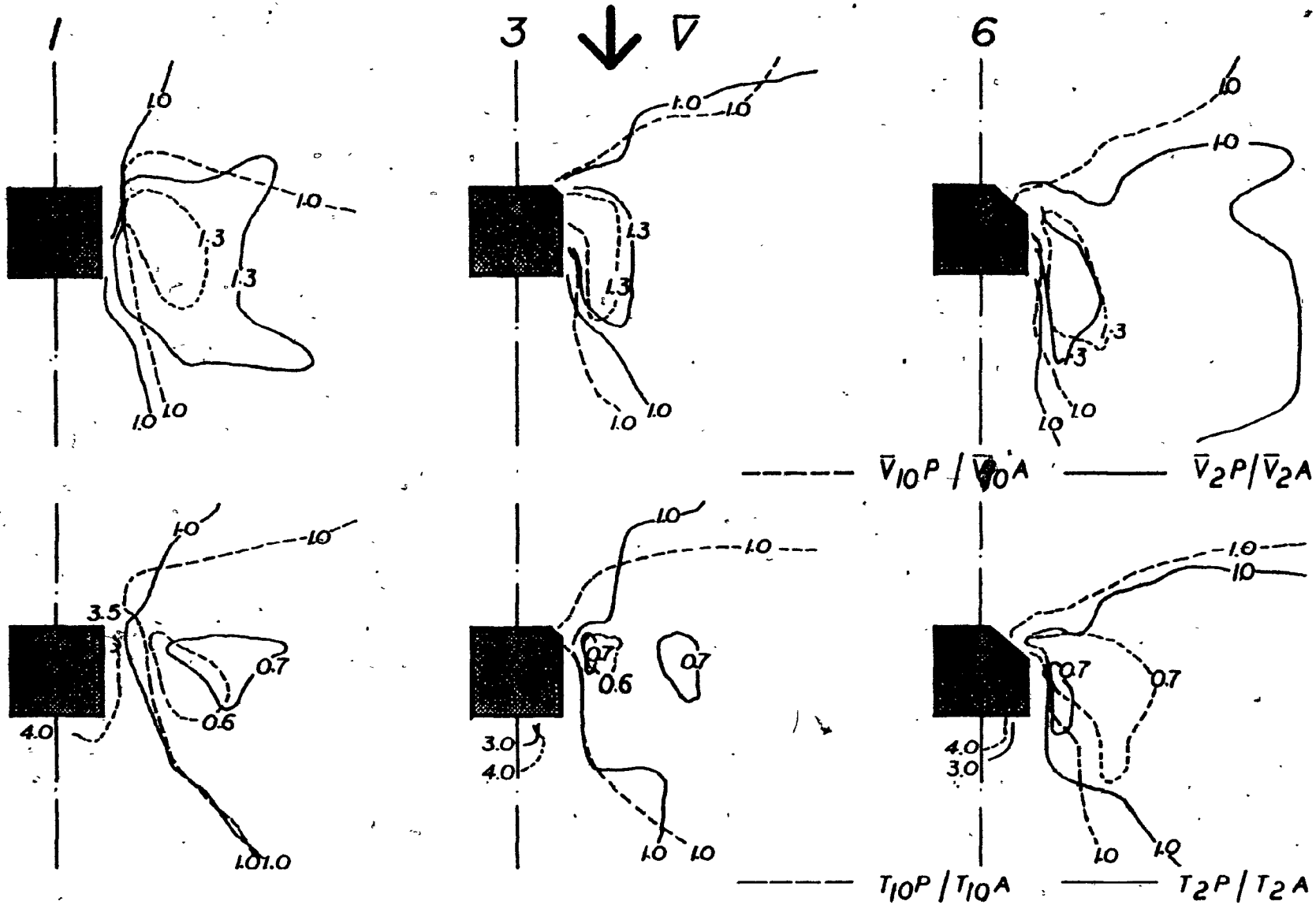

FIGURE 5.3.4 EFFECT OF LOWER MEASUREMENT HEIGHT ON STRONG WIND AREA IN A CORNER STREAM (H = 180 M)

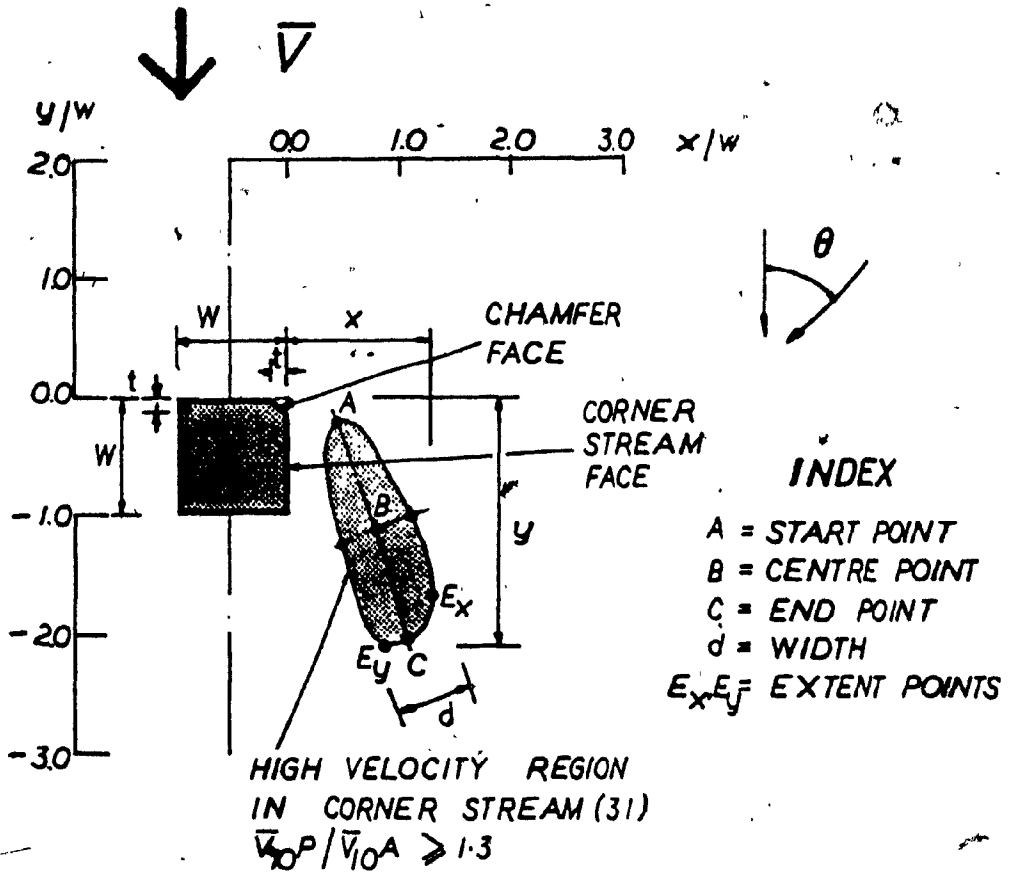

NOTATION AND TERMINOLOGY

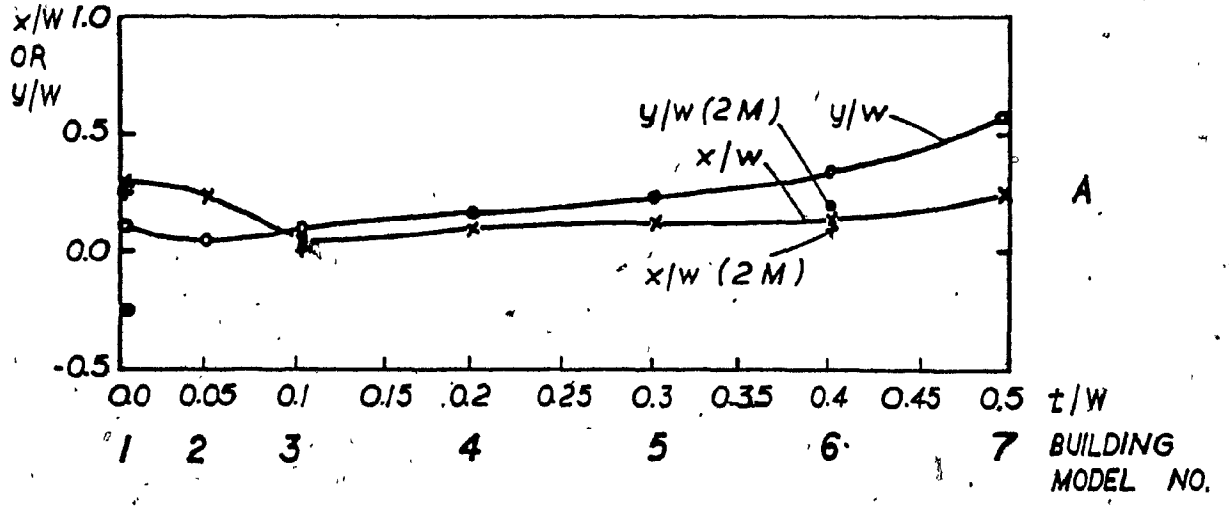

FIGURE 5.3.5 EFFECT OF CHAMFER ON STRONG WIND AREA IN A CORNER STREAM OF THE BUILDING

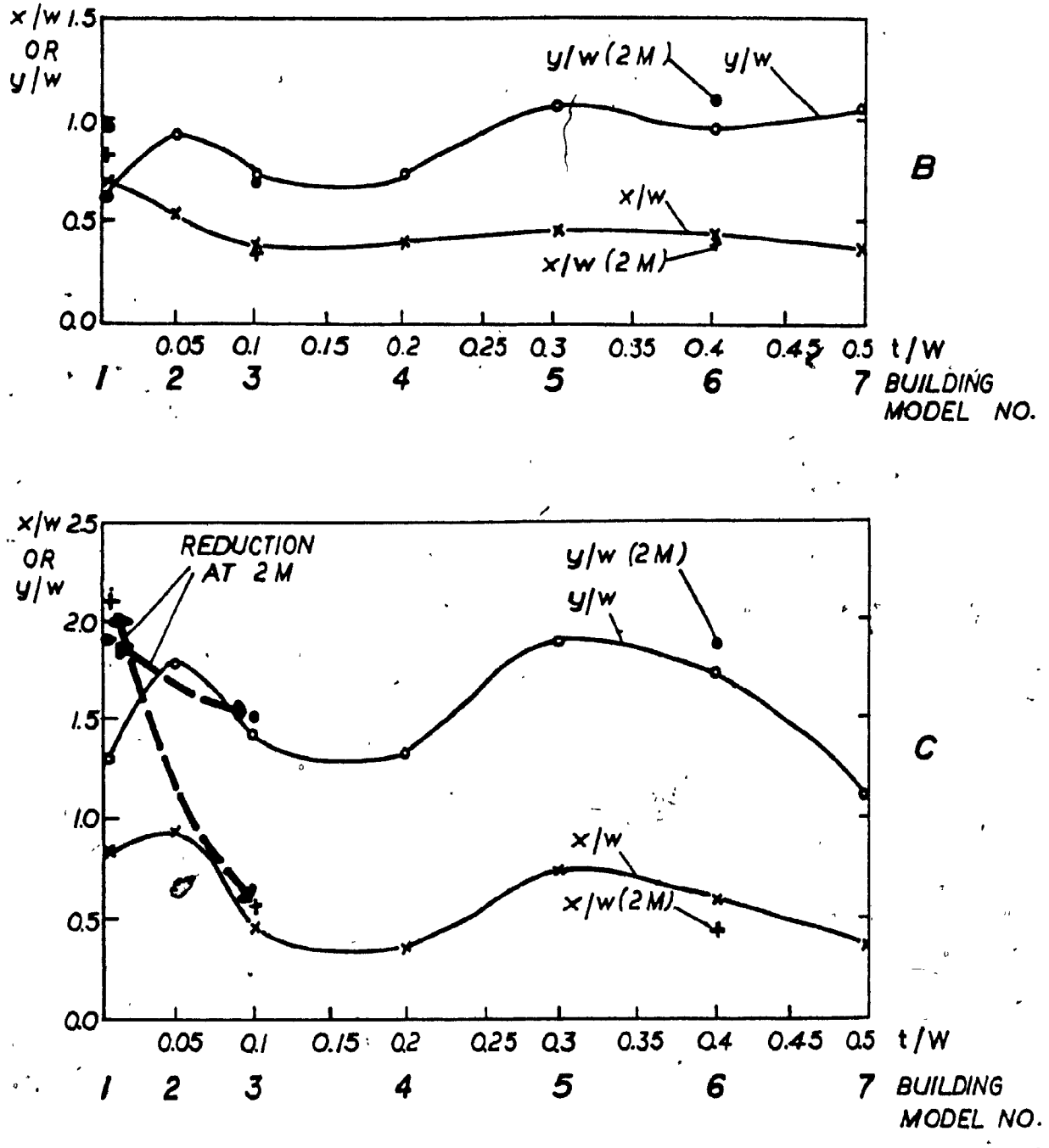

FIGURE 5.3.6 EFFECT OF CHAMFER ON STRONG WIND AREA IN A CORNER STREAM OF THE BUILDING

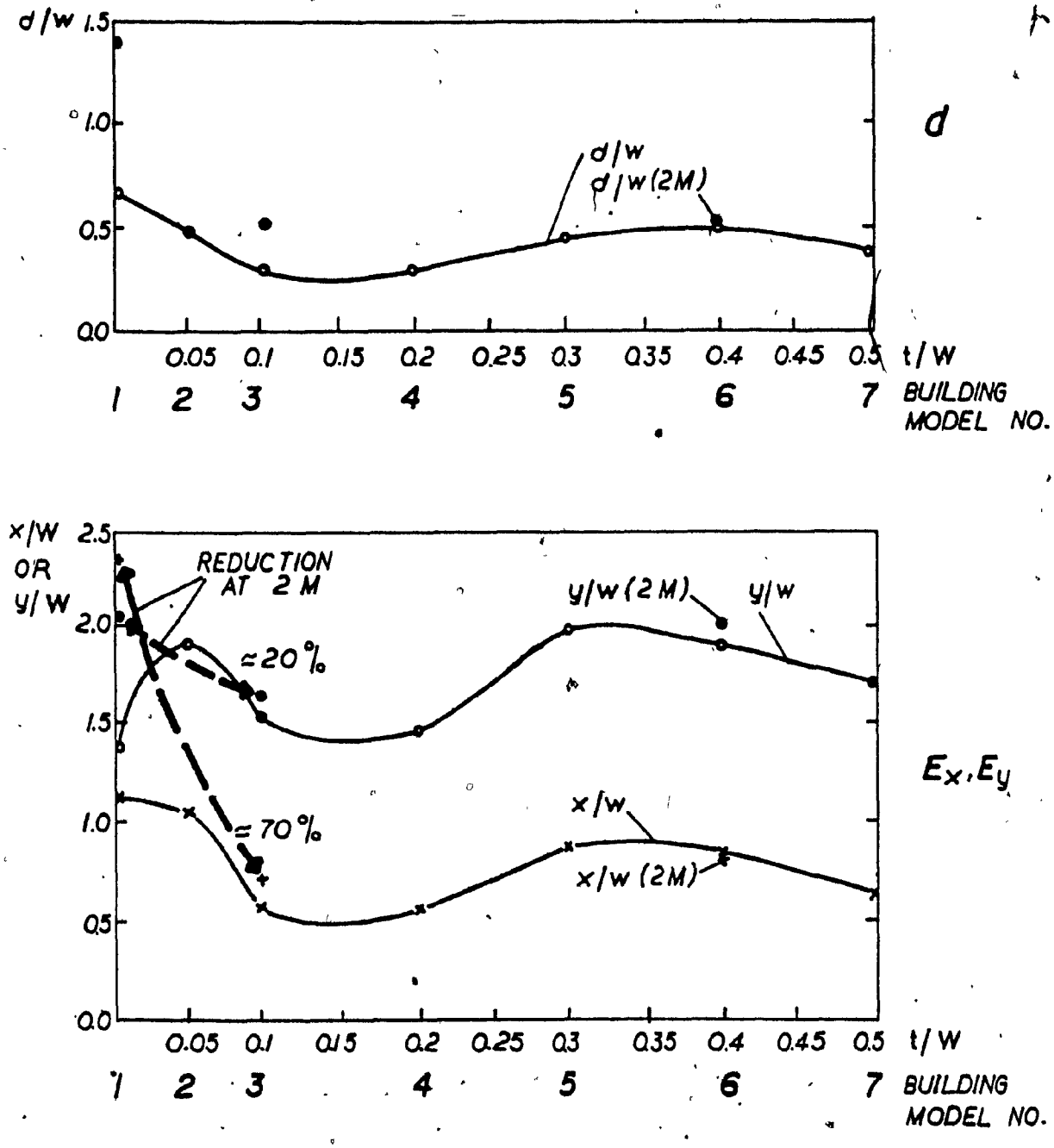

FIGURE 5.3.7 EFFECT OF CHAMFER ON STRONG WIND AREA IN A CORNER STREAM OF THE BUILDING

It has been observed that at the 10 m height of measurement the starting point, A of the strong wind area remains close to the corner stream face in the crosswise direction and moves downstream for higher values of chamfer length. The coordinates of A, for the strong wind area for models No. 1,3 and 6 do not deviate much at the 2 m height of measurement compared to the values at 10 m height.

For larger chamfers the area becomes more elongated in shape. The centre of the area B, moves in the streamwise direction and remains approximately constant in the cross-wise direction. At the lower height of measurement the variation in areas is not much. The end dimension C, of a strong wind area has been reduced considerably in the crosswise direction at 2m height up to model No. 3. No further reductions have been noticed for higher values at chamfer widths.

The width dimension, d, of a strong wind area reduces up to model No. 3, and then increases for model No. 6. A considerable reduction in the width of the strong wind area is observed at the 2 m height of measurement up to building model No. 3. The extent points Ex and Ey as in Figure 5.3.7 show significant reduction in the extent of strong wind area up to model No. 3, specially in the cross-wise direction at the 2m height of measurement. The higher values of chamfer length do not show much deviation at the 2 m height of measurement.

The chamfering of a corner at 45° to its original faces of a 180 m tall square building reduces the strong wind area in the corner stream by approximately 75% at the 2 m height. Figure 5.3.8 shows the location

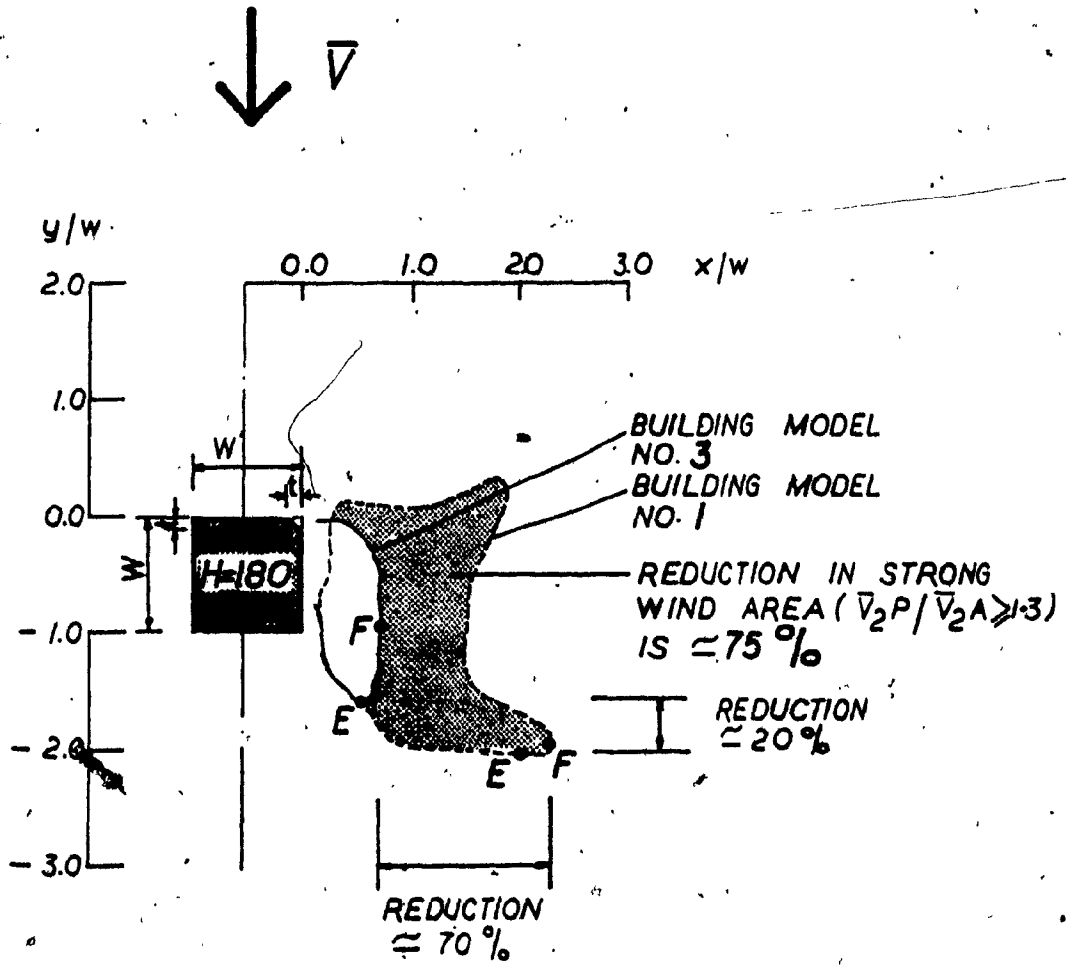

FIGURE 5.3.8 REDUCTION IN STRONG WIND AREA AT PEDESTRIAN LEVEL

of the strong wind area in the corner stream of a 180 m tall square and chamfered building at 2 m above ground level. In the crosswise direction the reduction is approximately 70% (i.e. 1.6 times the width (W) dimension) and approximately 20% in the streamwise direction (i.e. 0.4 times the width (W)) for a chamfered width (t), approximately equal to 1/10 of the original width (W) of a square building.

Larger chamfers do not have great influence in the reduction of a strong wind area at the pedestrian level. Chamfered corners of a building reduce the turbulence close to the corner stream face of the building but do not have much effect on the leeward side of the building. Experiments on wind environment have shown that the reduction in strong wind area becomes more at lower level of measurement. However, the 10 m height is mostly used instead of 2 m for most of the tests because of the measurement difficulties mentioned earlier in the section.

5.4 COMPARISON OF COMFORT CRITERIA

Comfort criteria relate with both the wind velocity and the turbulence field around a building, as has been discussed in Chapter 3. This section presents the analysis of the experimental data and the results for the comfort parameters found in the corner stream of square and chamfered buildings.

The non-dimensional comfort parameter (ψ) suggested by Gandemer (10) has been used in the present work. This parameter includes the effect of turbulence and is defined as:

$$\psi_h = \frac{\bar{V}_hP + Vrms_hP}{\bar{V}_hA + Vrms_hA} = \frac{Q\,(1+T_hP)}{1+T_hA} \qquad \text{----------[5.4.1]}$$

where ψ_h = comfort parameter at height, h, above ground (2 or 10m),

Q = $\bar{V}_hP/\bar{V}_hA$, velocity amplification ratio,

$\bar{V}_hP$ = mean wind speed in the presence of the building at height h,

$Vrms_hP$ = rms value of wind speed in the presence of the building at height h,

$\bar{V}_hA$ = mean wind speed in the absence of the building at h height,

$Vrms_hA$ = rms value of wind speed in the absence of the building at height h,

T_hP = Turbulence intensity in the present of the building at height h and

T_hP = Turbulence intensity in the absence of the building at height h.

Figure 5.4.1 shows contours of ψ_{10} factors for the square and chamfered buildings No. 3, 4 and 6, all 180 m high. For the square building the strong wind area in corner stream defined by ψ_{10} does not deviate much from $\bar{V}_{10}P/\bar{V}_{10}A$. The contours of high values from ψ_{10} and $\bar{V}_{10}P/\bar{V}_{10}A$ are compared in the corner stream region of the building. Similarly, higher values of strong wind area as defined in the figure do not deviate for chamfered buildings also.

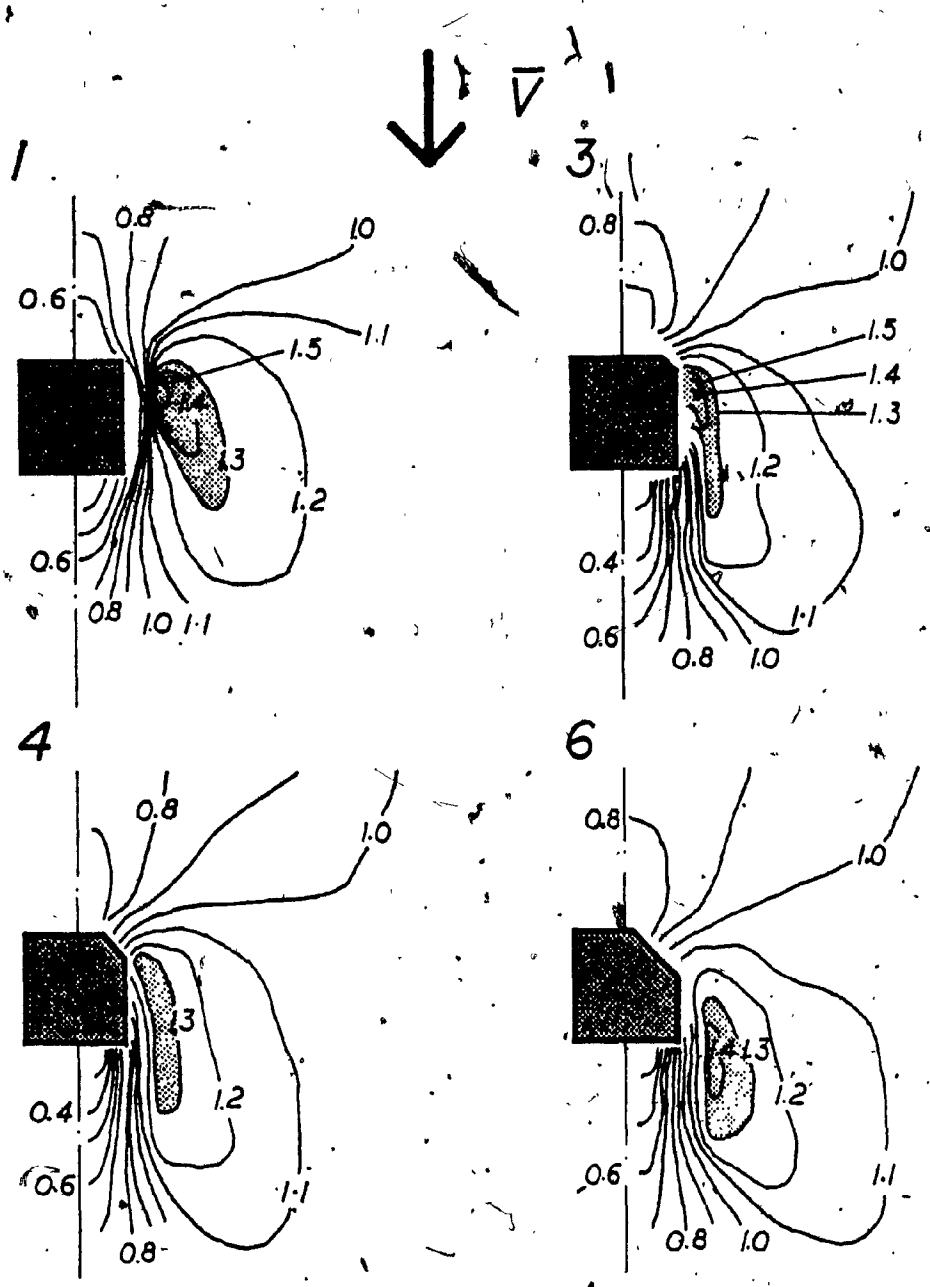

FIGURE 5.4.1 CONTOURS OF ψ_{10} FACTORS FOR SQUARE AND CHAMFERED BUILDINGS

The differences between ψ_{10} and $\bar{V}_{10}P/\bar{V}_{10}A$ for both square and chamfered buildings are small because the turbulence in the flow $T_{10}P$, in the corner stream of a building is approximately equal to turbulence $T_{10}A$ in absence of the building. A detailed the comparison between ψ_{10} and $\bar{V}_{10}P/\bar{V}_{10}A$ for the strong wind area in the corner stream is presented in Table 5.4.1. The strong wind area is represented by the contour of 1.3 for both ψ_{10} and $\bar{V}_{10}P/\bar{V}_{10}A$. Details about the location of the strong wind area from building faces are given in the top sketch of Table. The comparison shows generally little deviation between strong wind regions defined by ψ_{10} and $\bar{V}_{10}P/\bar{V}_{10}A$. Consequently, the intensity and extent of the strong wind region in the corner stream of square and chamfered buildings does not depend much on the turbulence in the flow at 10 m height.

The comparison of comfort criteria at the lower level of measurement (2m) is presented for the square and chamfered buildings No. 3 and 6 in Figure 5.4.2. The parameters in the figure remain the same as in Figure 5.4.1. The strong wind area in the corner stream based on ψ_2 is again similar to that defined by $\bar{V}_2P/\bar{V}_2A$ for both square and chamfered buildings.

Superposition of strong wind areas denoted by the 1.3 contour for both ψ and mean wind speed is shown in Figure 5.4.3 for the 2 m and 10 m heights. Also shown in the Figure is the deviation of ψ and mean wind speed for contours of 1.0 (no influence of the buildings on the wind environment) at both measurement heights. A detailed comparison of the

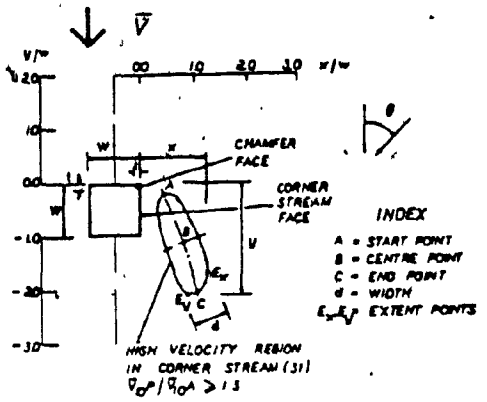

PLAN VIEW OF A BUILDING NOTATION AND TERMINOLOGY

Model No.	t/w	d/W	
		$\frac{\bar{V}_{10P}}{\bar{V}_{10A}}$	ψ_{10}
1	0.0	0.7	0.52
3	0.1	0.3	0.17
4	0.2	0.35	0.2
6	0.4	0.5	0.4

d

Model No.	t/w	x/w		y/w	
		$\frac{\bar{V}_{10P}}{\bar{V}_{10A}}$	ψ_{10}	$\frac{\bar{V}_{10P}}{\bar{V}_{10A}}$	ψ_{10}
1	0.0	0.4	0.4	0.1	0.05
3	0.1	0.05	0.05	0.1	0.1
4	0.2	0.1	0.1	0.15	0.15
6	0.4	0.15	0.25	0.35	0.5

A

Model No.	t/w	x/w		y/w	
		$\frac{\bar{V}_{10P}}{\bar{V}_{10A}}$	ψ_{10}	$\frac{\bar{V}_{10P}}{\bar{V}_{10A}}$	ψ_{10}
1	0.0	0.82	0.8	1.3	1.25
3	0.1	0.45	0.3	1.45	1.35
4	0.2	0.35	0.35	1.35	1.5
6	0.4	0.6	0.5	1.75	1.7

C

Model No.	t/w	x/w		y/w	
		$\frac{\bar{V}_{10P}}{\bar{V}_{10A}}$	ψ_{10}	$\frac{\bar{V}_{10P}}{\bar{V}_{10A}}$	ψ_{10}
1	0.0	0.7	0.6	0.62	0.62
3	0.1	0.4	0.3	0.75	0.65
4	0.2	0.4	0.3	0.75	0.85
6	0.4	0.42	0.38	1.0	1.15

B

Model No.	t/w	x/w		y/w	
		$\frac{\bar{V}_{10P}}{\bar{V}_{10A}}$	ψ_{10}	$\frac{\bar{V}_{10P}}{\bar{V}_{10A}}$	ψ_{10}
1	0.0	1.1	0.85	1.3	1.2
3	0.1	0.5	0.4	1.45	1.4
4	0.2	0.55	0.45	1.4	1.5
6	0.4	0.8	0.65	1.8	1.75

Ex, Ey

TABLE 5.4.1 - COMPARISON BETWEEN STRONG WIND AREAS IN THE CORNER STREAM OF TALL BUILDINGS AS DEFINED BY ψ_{10} AND $\bar{V}_{10P}/\bar{V}_{10A}$

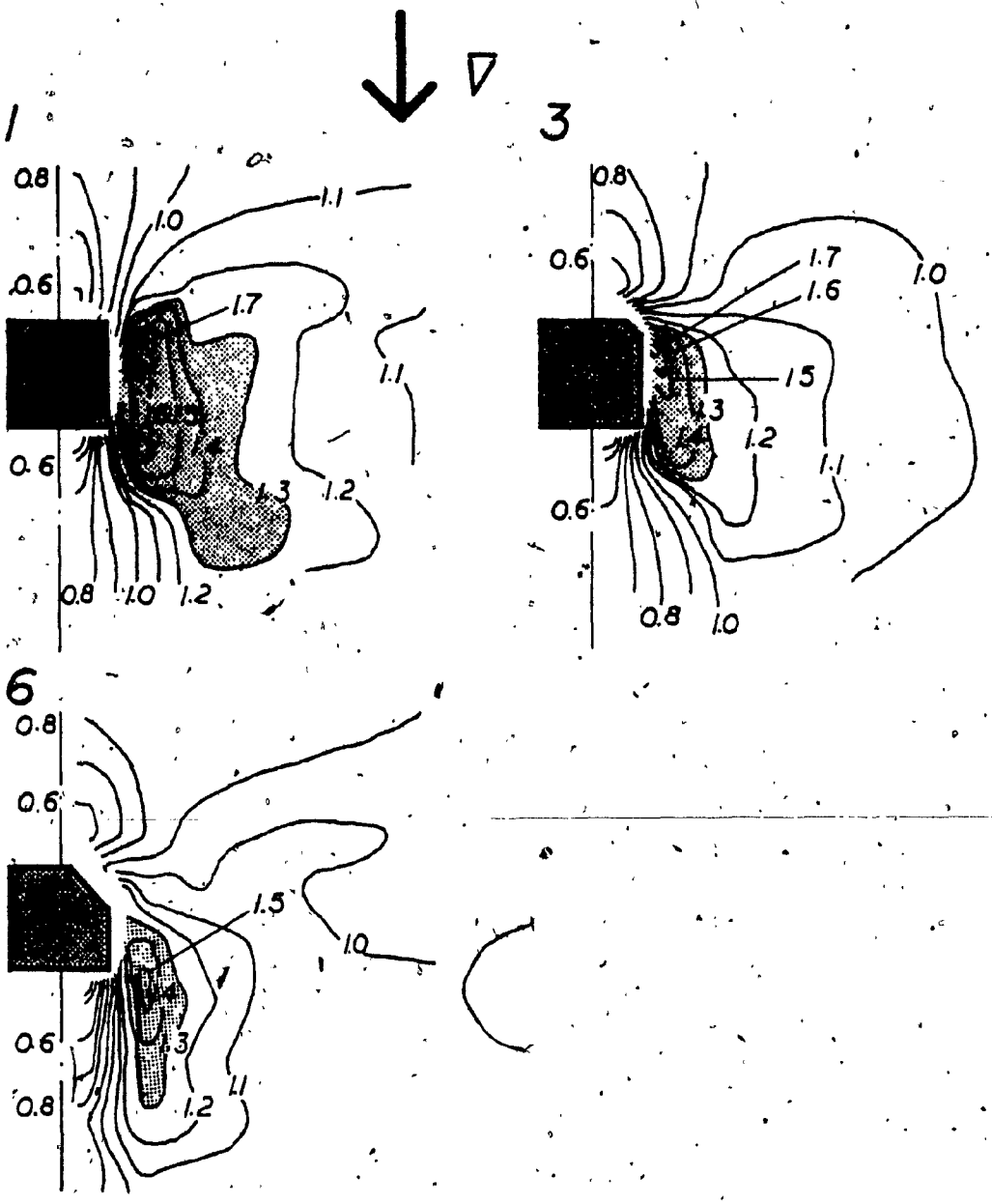

FIGURE 5.4.2 CONTOURS OF ψ_2 FACTORS FOR SQUARE AND CHAMFERED BUILDINGS

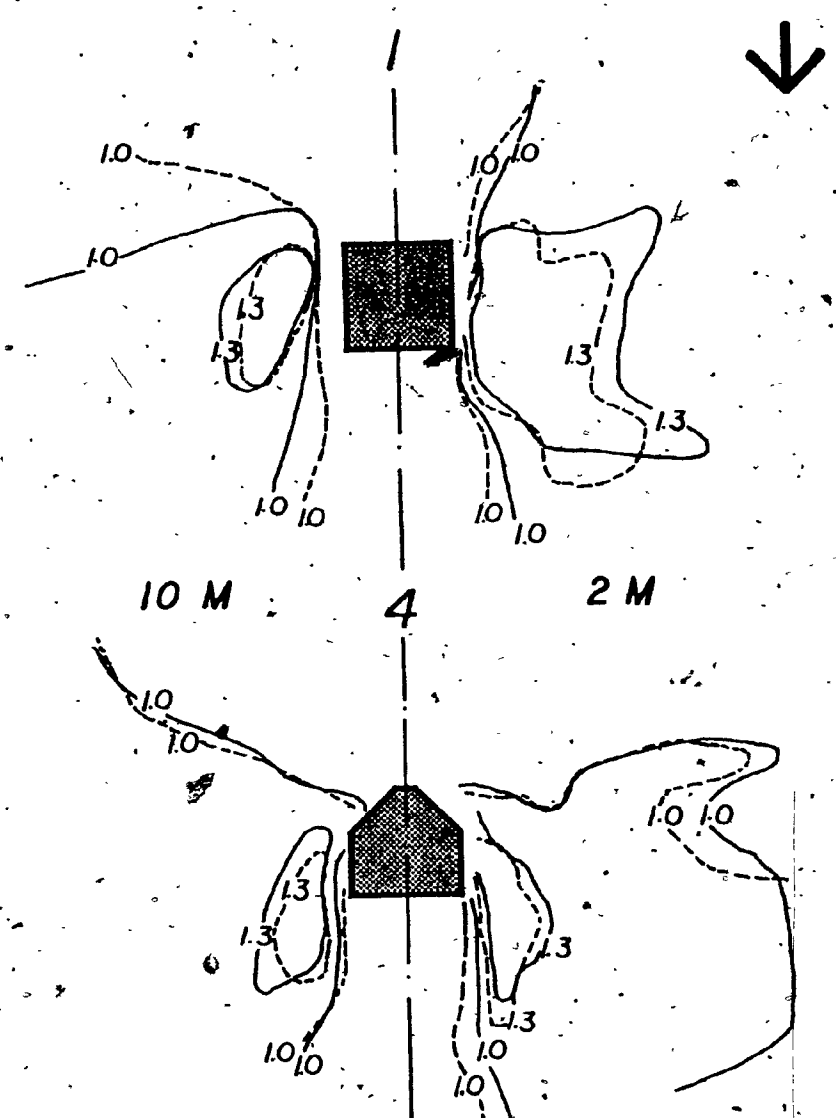

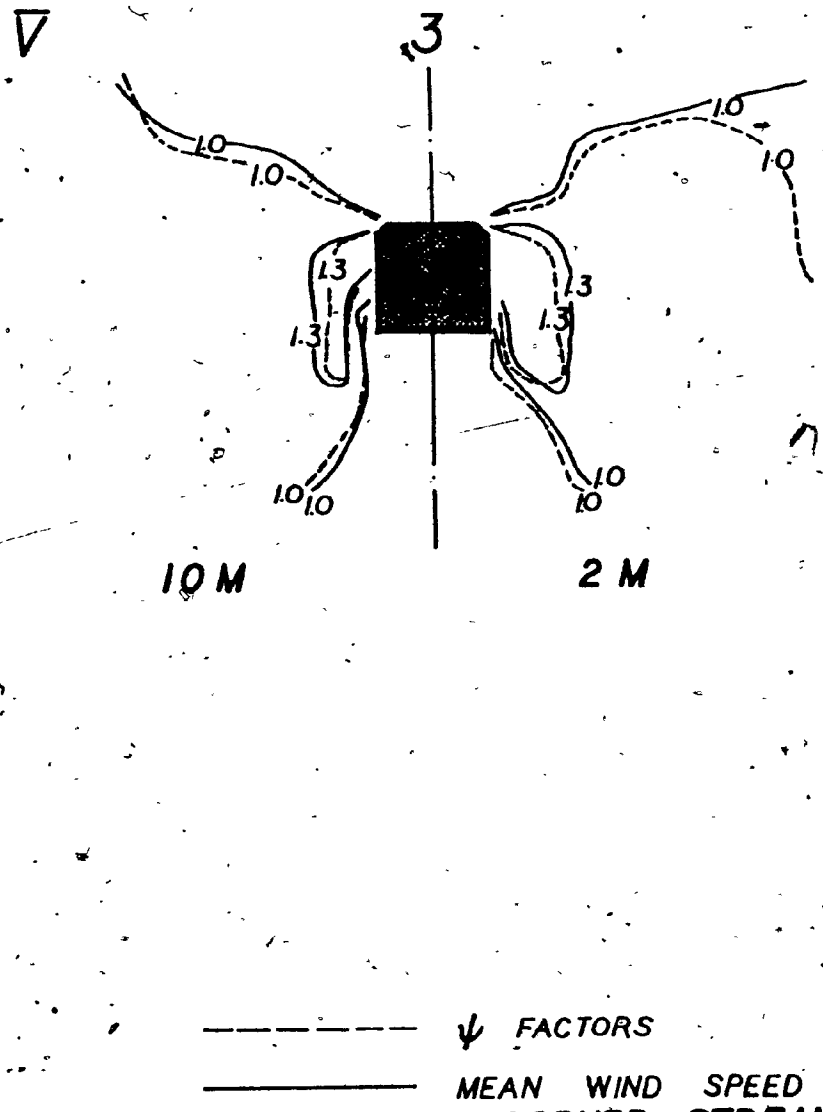

FIGURE 5.4.3 DEVIATION OF STRONG WIND AREAS IN THE CORNER STREAM OF TALL SQUARE AND CHAMFERED BUILDINGS AS DEFINED BY ψ_h AND $\bar{V}_h P / \bar{V}_h A$

---------- ψ FACTORS

———————— MEAN WIND SPEED

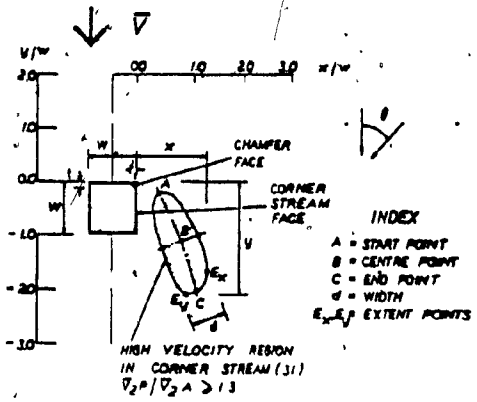

PLAN VIEW OF A BUILDING NOTATION AND TERMINOLOGY

Model No.	t/w	x/w		y/w	
		$\frac{\bar{V}_2P}{\bar{V}_2A}$	ψ_2	$\frac{\bar{V}_2P}{\bar{V}_2A}$	ψ_2
1	0.0	0.23	0.23	-0.25	0.02
3	0.1	0.04	0.02	0.5	0.5
6	0.4	0.1	0.1	0.2	0.43

A

Model No.	t/w	x/w		y/w	
		$\frac{\bar{V}_2P}{\bar{V}_2A}$	ψ_2	$\frac{\bar{V}_2P}{\bar{V}_2A}$	ψ_2
1	0.0	0.82	0.7	1.0	1.02
3	0.1	0.38	0.3	0.58	0.7
6	0.4	0.4	0.4	1.12	1.25

B

Model No.	t/w	d/W	
		$\frac{\bar{V}_2P}{\bar{V}_2A}$	ψ_2
1	0.0	1.45	1.2
3	0.1	0.52	0.5
6	0.4	0.52	0.5

d

Model No.	t/w	x/w		y/w	
		$\frac{\bar{V}_2P}{\bar{V}_2A}$	ψ_2	$\frac{\bar{V}_2P}{\bar{V}_2A}$	ψ_2
1	0.0	2.17	1.4	1.95	2.1
3	0.1	0.5	0.5	1.53	1.4
6	0.4	0.45	0.35	1.95	2.17

C

Model No.	t/w	x/w		y/w	
		$\frac{\bar{V}_2P}{\bar{V}_2A}$	ψ_2	$\frac{\bar{V}_2P}{\bar{V}_2A}$	ψ_2
1	0.0	2.2	1.65	1.95	2.15
3	0.1	0.7	0.62	1.6	1.48
6	0.4	0.75	0.65	1.9	2.12

Ex, Ey

TABLE 5.4.2 - COMPARISON BETWEEN STRONG WIND AREAS IN THE CORNER STREAM OF TALL BUILDINGS AS DEFINED BY ψ_2 AND $\bar{V}_2P/\bar{V}_2A$.

relative distances for the extent of strong wind area from building face is presented for the square and chamfered buildings in Table 5.4.2 in the same format with Table 5.4.1 presented previously. Numerical values for both the crosswise and streamwise directions in the Table show a small difference between Ψ_2 and $\bar{V}_2P/\bar{V}_2A$ in the corner stream of a building. Consequently, the turbulence intensity does not influence the extent of the strong wind region around square and chamfered buildings at 2 m height. This may justify the use of the velocity amplification factors only for the definition of comfort criteria.

5.5 EFFECT OF BUILDING HEIGHT

In this section test results are presented for various heights of square and chamfered buildings.

Figure 5.5.1 shows contours of $\bar{V}_{10}P/\bar{V}_{10}A$ and $T_{10}P/T_{10}A$ in top and bottom sketches respectively for a square building of 30 m x 30 m and heights of 180, 120, 90 and 60 m. In general, a consistent increase in the magnitude and the area of high velocities can be observed in the corner stream of the building as the building height increases. The values for $\bar{V}_{10}P/\bar{V}_{10}A$ reach maxima of 1.5, 1.3, 1.3 and 1.1 for 180, 120, 90 and 60 m heights respectively.

The local wind dynamic velocity pressure increases with height. Low wake pressure is dependent on the free stream velocity at the top of the building, as already discussed in Chapter 2. Taller buildings will have a lower wake pressure and they will directly correspond to the wind velocities around the sides and corners (26). The values of

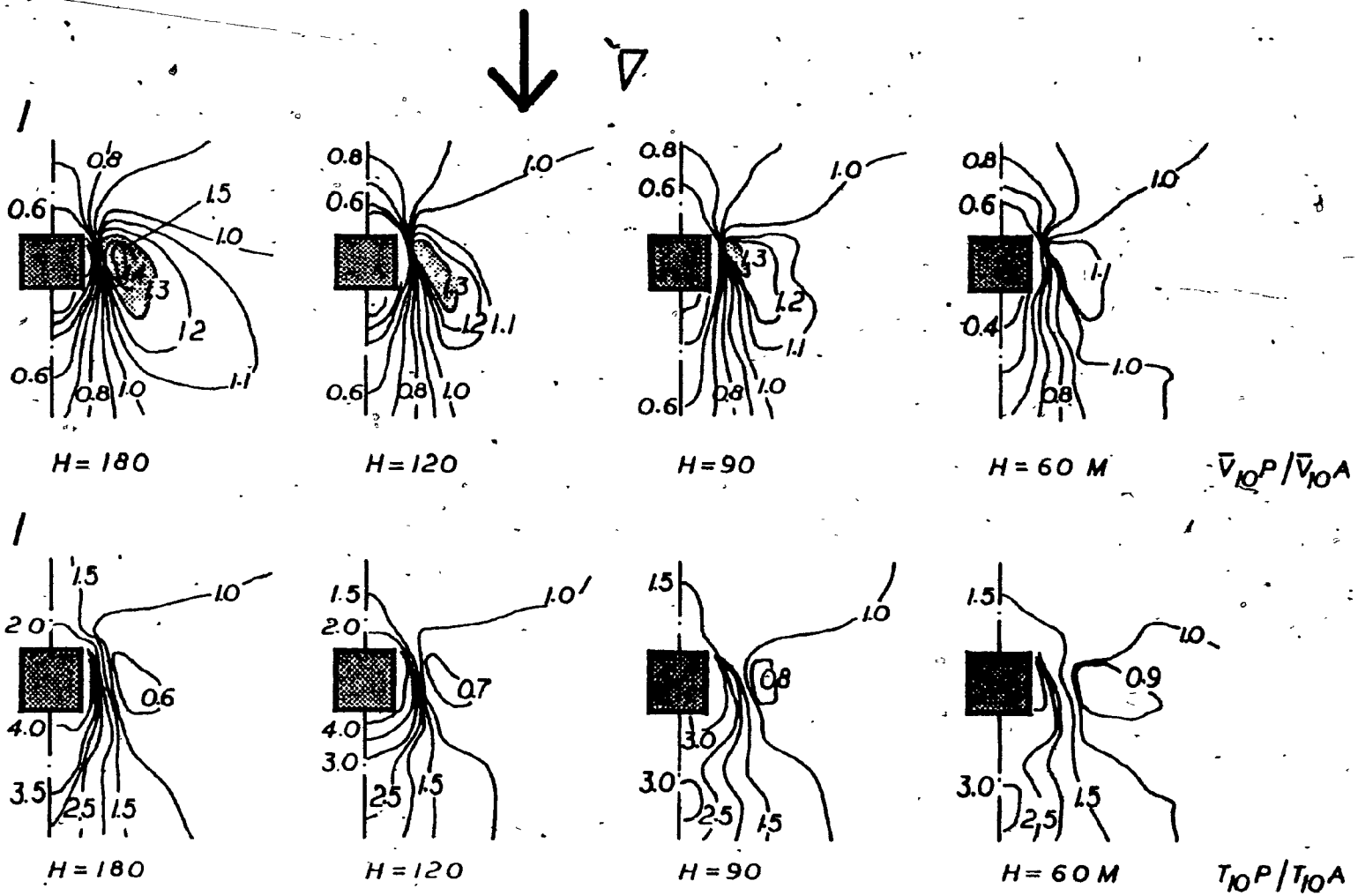

FIGURE 5.5.1 VELOCITY AND TURBULENCE INTENSITY AMPLIFICATION FACTORS AROUND SQUARE BUILDINGS OF DIFFERENT HEIGHTS

$\bar{V}_{10}P/\bar{V}_{10}A$ on the leeward and windward sides reach around 0.4 and 0.6 respectively when varying the building height. Similar results for velocity amplification in the corner stream of the square building have been found by Kamei and Maruta (17) and have been shown in Figure 5.1.2.

The turbulence is not significantly affected by increasing building height. For the lowest building height, $T_{10}P/T_{10}A$ reaches a maximum of 3.0 on the leeward side and a maximum of 1.5 on the windward side. In the corner stream, the turbulence intensity reduces from 0.9 to 0.6 as the building height increases.

Typical results showing the effect of chamfered building height on velocity amplification are shown in Figure 5.5.2. Data are presented in the same format as in Figure 5.5.1 for chamfered buildings No. 3, 5 and 7. Contours of $\bar{V}_{10}P/\bar{V}_{10}A$ are presented for buildings 180 m and 60 m high. For the lowest building, (60 m), the value of $\bar{V}_{10}P/\bar{V}_{10}A$ reaches a maximum of 1.3 for model No. 3, 1.2 for No. 5 and 1.1 for No. 7. The values of $\bar{V}_{10}P/\bar{V}_{10}A$ on the windward and leeward sides remain approximately the same as for 180 m high buildings.

Figure 5.5.3 shows the effect of 60 m high square and chamfered buildings on velocity amplification. The values of $\bar{V}_{10}P/\bar{V}_{10}A$ vary up to 0.5 W from the building face in the crosswise direction. The peak values are very close to the corner stream face of the building. Furthermore, the effect of greater chamfering on wind environment is not noticable after a distance of about 0.5 W from the building face.

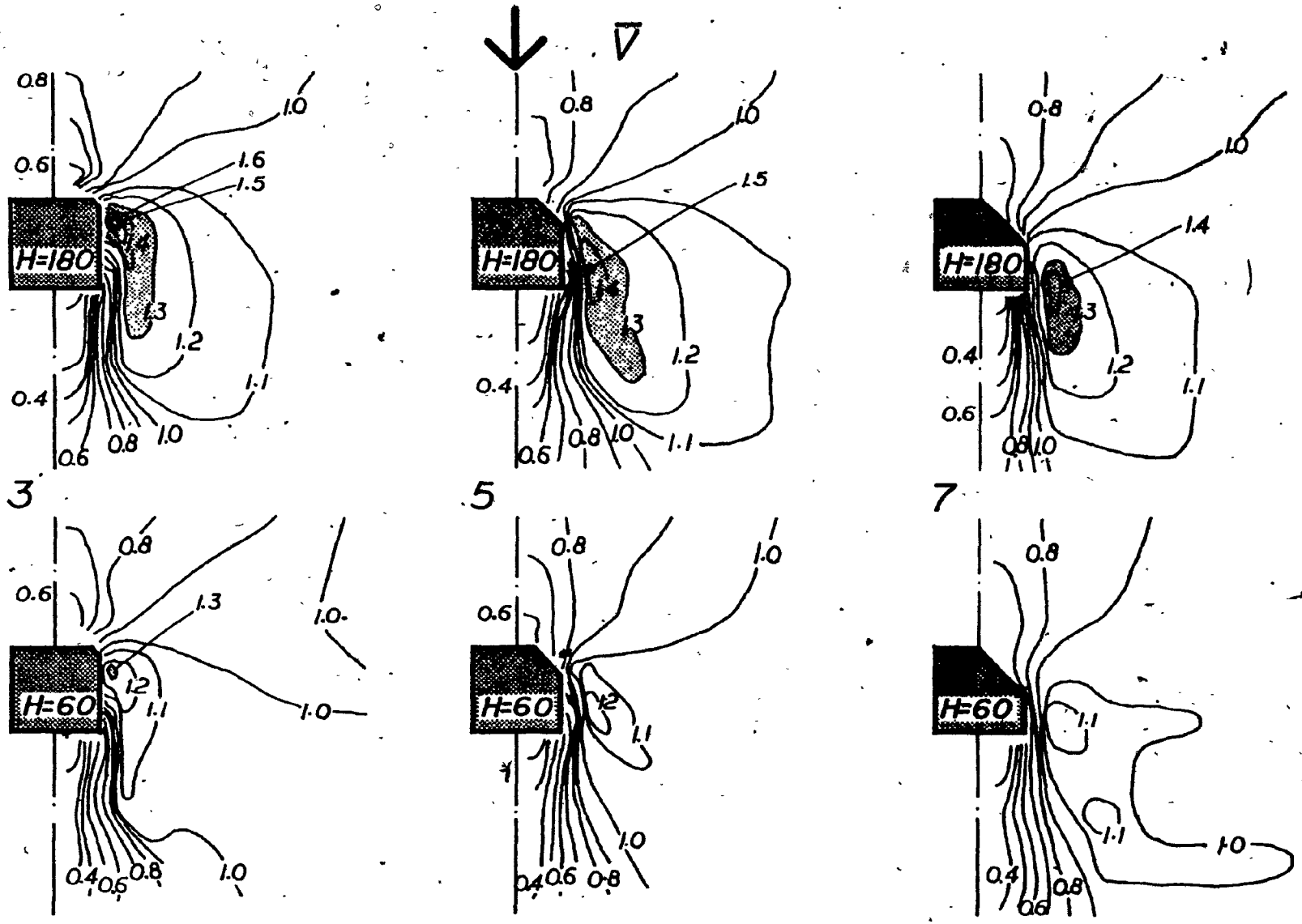

FIGURE 5.5.2 EFFECT OF VARYING HEIGHT OF CHAMFERED BUILDINGS ON VELOCITY AMPLIFICATION

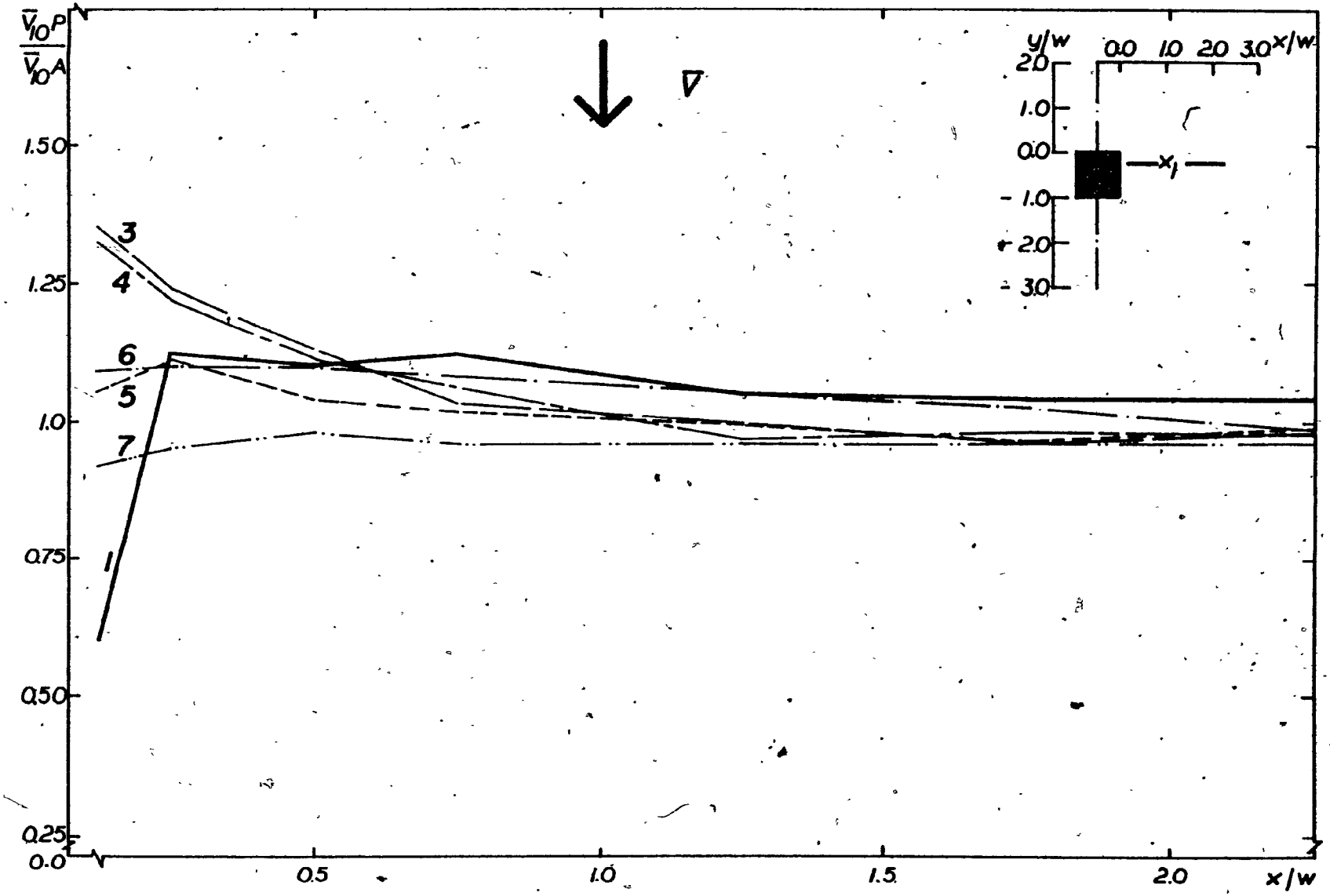

FIGURE 5.5.3 AMPLIFICATION OF VELOCITY CLOSE TO THE FACE OF LOW BUILDINGS (AXIS - x_1)

Figure 5.5.4 shows contours of turbulence intensity for chamfered buildings No. 3, 5 and 7. Data presented are in the same format with those of Figure 5.5.1. The value of $T_{10}P/T_{10}A$ reaches a maximum of 3.5 for 60 m and 4.0 for 180 m heights on the leeward side. A small increase in values of $T_{10}P/T_{10}A$ was observed on the windward sides of the 60 m high buildings.

In the crosswise direction as shown in Figure 5.5.5, the values of $T_{10}P/T_{10}A$ around a 60 m high square building reach a maximum of 3.5 and do not differ greatly from the maximum values of around 4.0 for the 180m high building. Turbulence intensity is very low in the corner stream region for both square and chamfered buildings. Higher values are often observed close to the corner stream face for square building. Greater chamfer lengths do not reduce turbulence significantly around a 60 m high building. The effect of varying height on turbulence conditions is very small on the windward and leeward sides of both square and chamfered buildings.

5.6 EFFECT OF WIND ATTACK ANGLE, θ.

This section presents experimental results for different wind attack angles for 180 and 60 m high square and chamfered buildings. These heights were selected since they were fround to cause quite different effects on the strong wind region.

Figure 5.6.1 shows contours of $\bar{V}_{10}P/\bar{V}_{10}A$ for square and chamfered buildings (No. 3 and 6) for 0° and 45° azimuths. The maximum values of

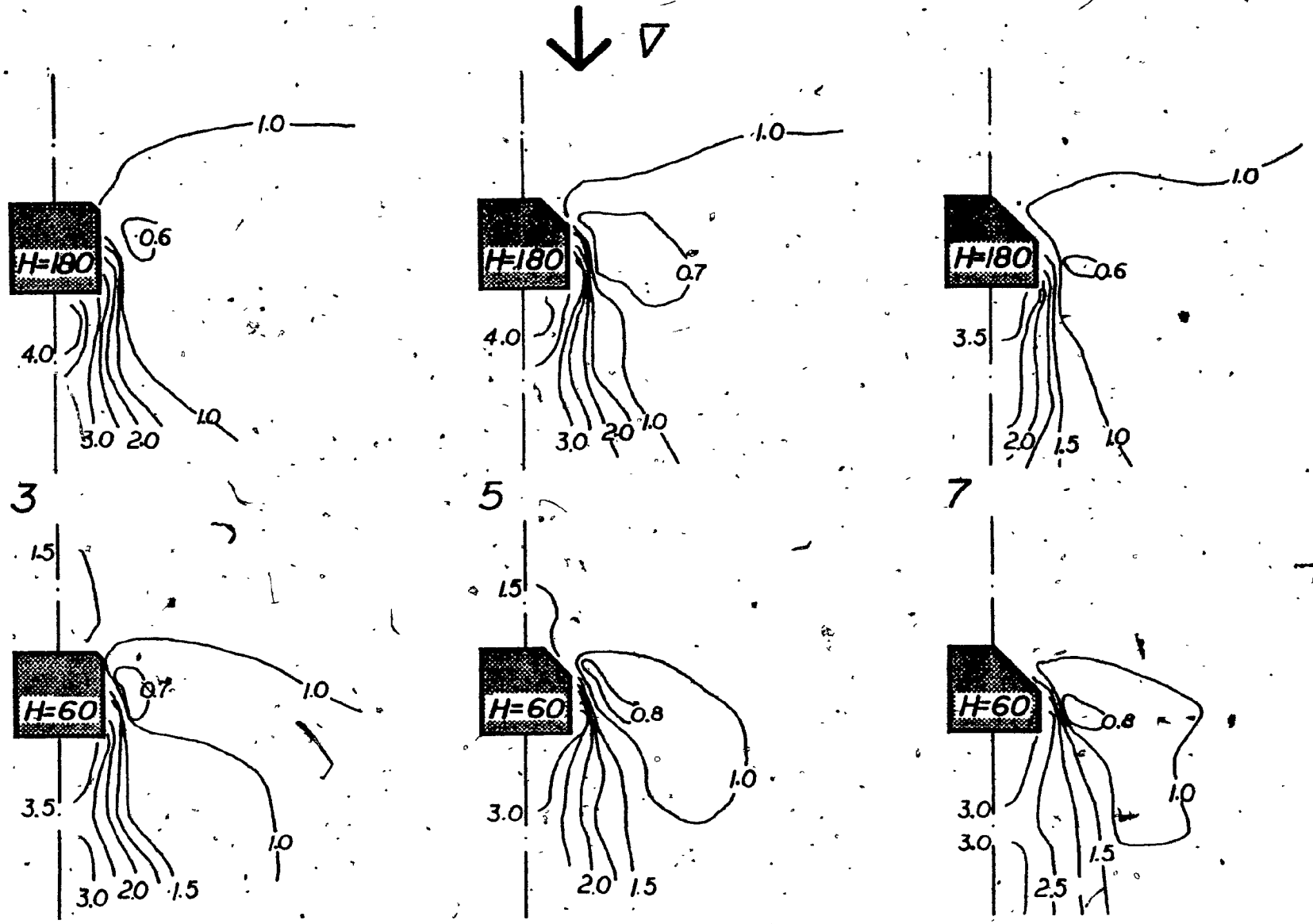

FIGURE 5.5.4 EFFECT OF VARYING HEIGHT OF CHAMFERED BUILDINGS ON TURBULENCE CONDITIONS

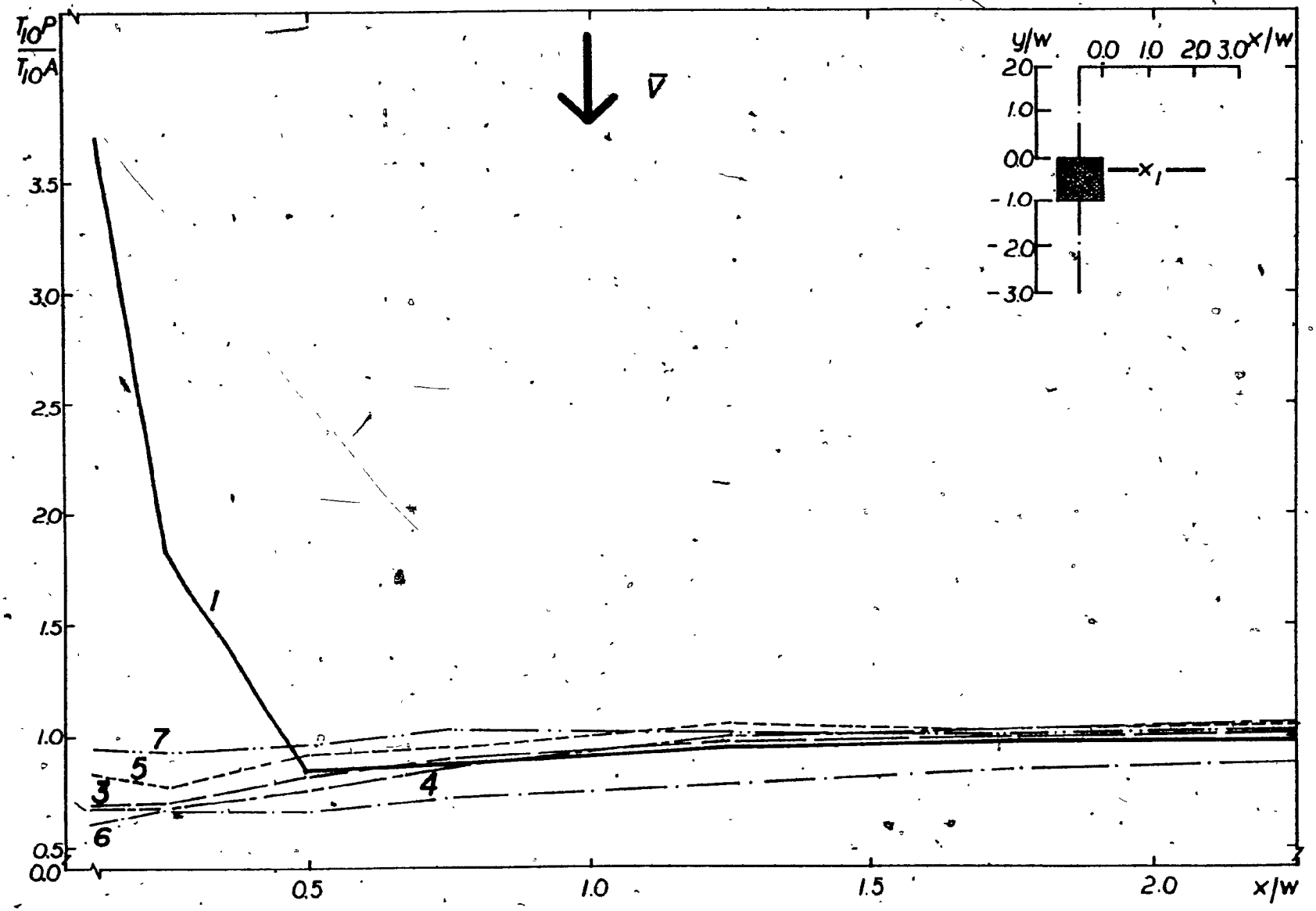

FIGURE 5.5.5 TURBULENCE CONDITIONS CLOSE TO THE FACE OF LOW BUILDINGS (AXIS-x_1)

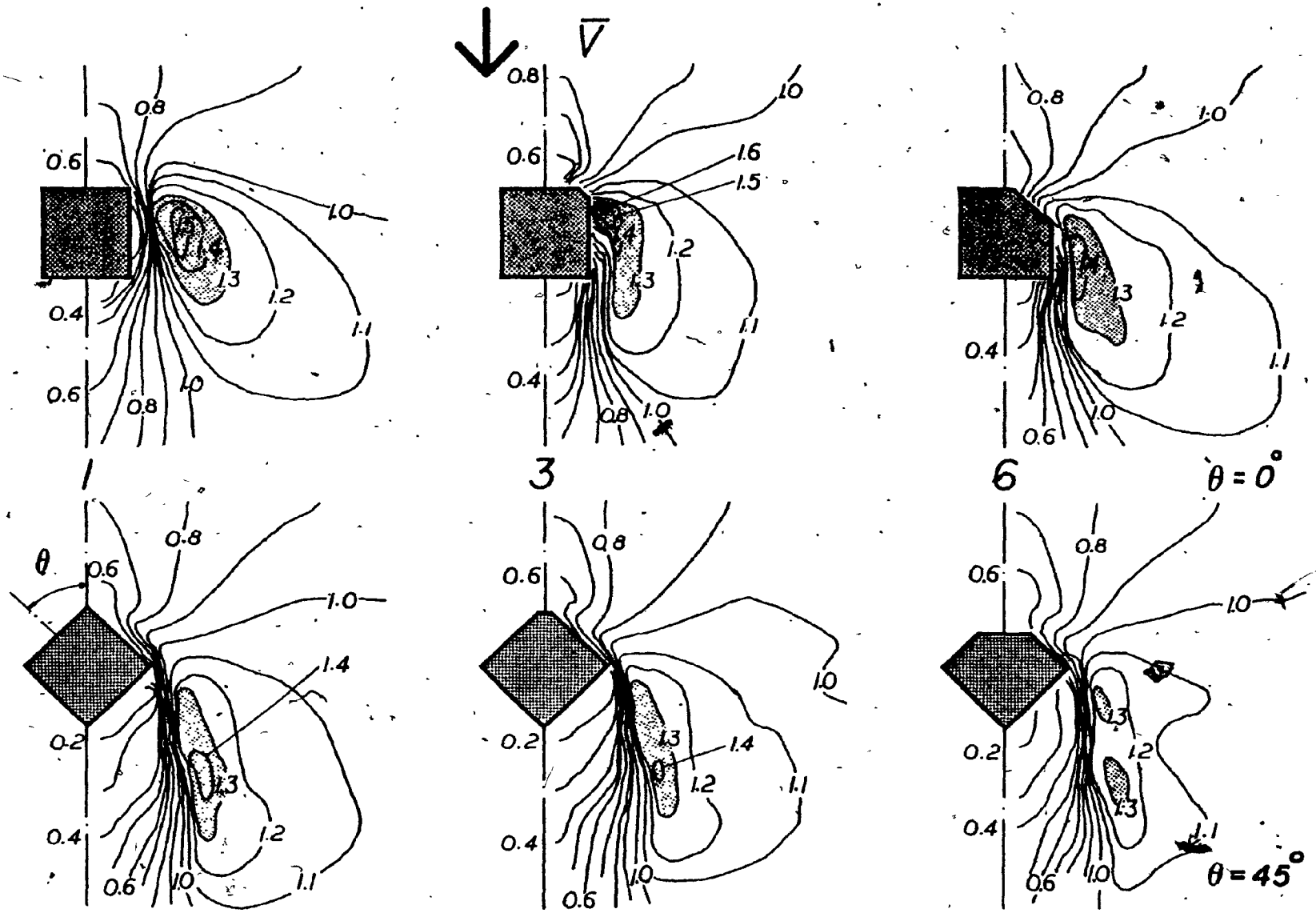

FIGURE 5.6.1 EFFECT OF WIND ATTACK ANGLE, θ, ON VELOCITY AMPLIFICATION AROUND THE SQUARE AND CHAMFERED BUILDINGS (H=180 M)

the velocity amplification factors are almost independent of wind direction, as can be easily noticed from the diagrams. This has also been found by Kamei and Maruta (17) and Lawson and Penwarden (22) for a number of wind directions for square buildings only.

Figure 5.6.2 shows contours of turbulence intensity $T_{10}P/T_{10}A$ for the same building models. The magnitude of the maximum value of turbulence intensity depends little on the wind azimuth but the location of occurrence of this value is drastically affected by the wind direction. This was expected by considering the flow pattern around a building. The flow separation occuring at the sharp edges on windward side of the square building has been found changed for 45° azimuth. The flow pattern becomes more turbulent in character around corners.

Table 5.6.1 shows the values of $\bar{V}_{10}P/\bar{V}_{10}A$ and $T_{10}P/T_{10}A$ for chamfered building No. 3 and 6 for varying wind azimuths including 30° and 60°. Measurements taken are presented in the sketch for six locations close to the corner stream face of the 180 m high chamfered building. The maximum value of $\bar{V}_{10}P/\bar{V}_{10}A$ is not affected significantly by wind direction. The differences between these values are small for 0°, 30°, 45° and 60° azimuths but the locations where these values occur change considerably. The values of $T_{10}P/T_{10}A$ also shown in the Table show a very low turbulence intensity in the areas of high velocity amplification.

The effect of building height for $\theta = 45°$ on the wind flow field around the square building is shown in Figure 5.6.3. Results are

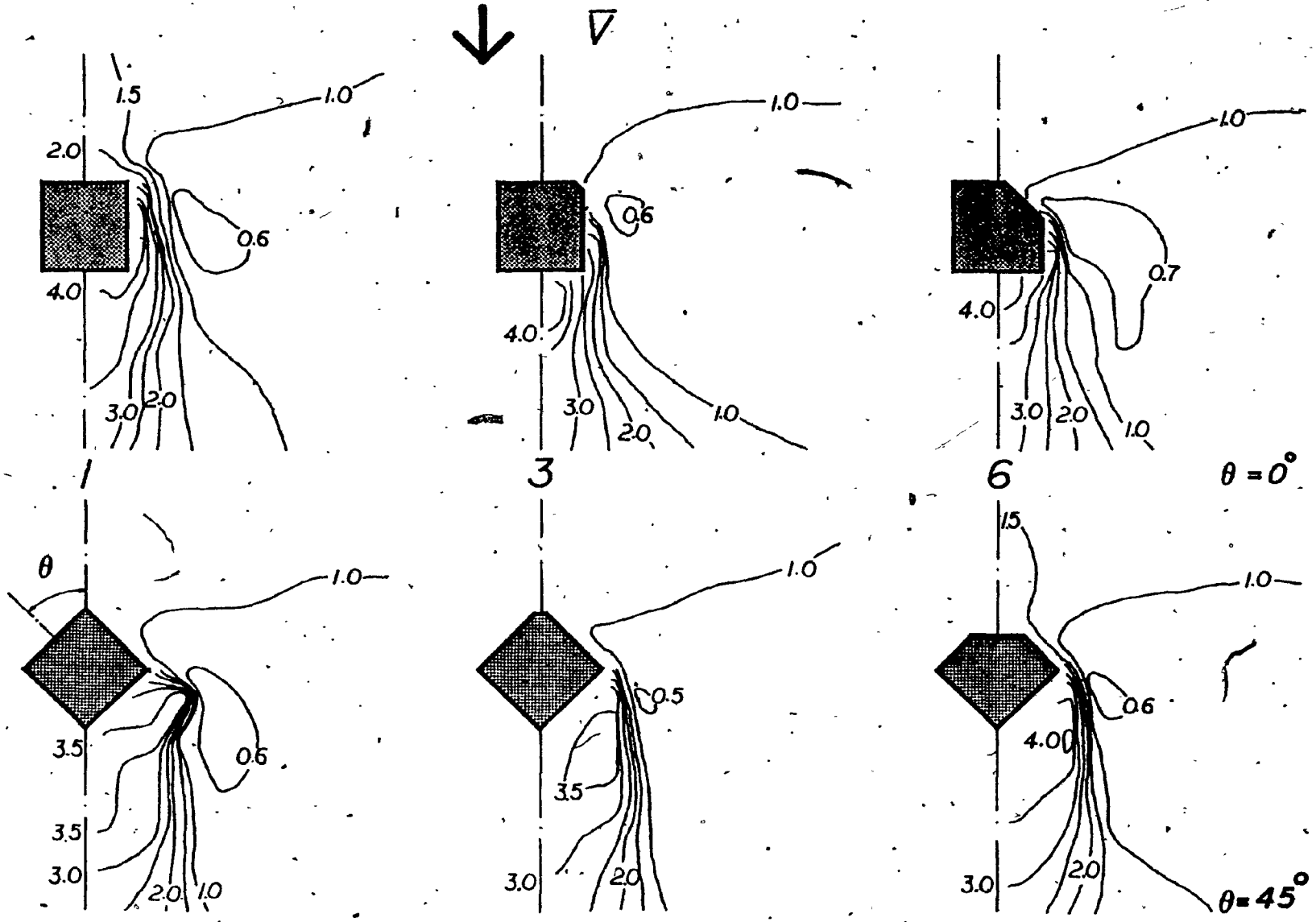

FIGURE 5.6.2 EFFECT OF WIND ATTACK ANGLE, θ, ON TURBULENCE CONDITIONS AROUND THE SQUARE AND CHAMFERED BUILDINGS. (H = 180 M)

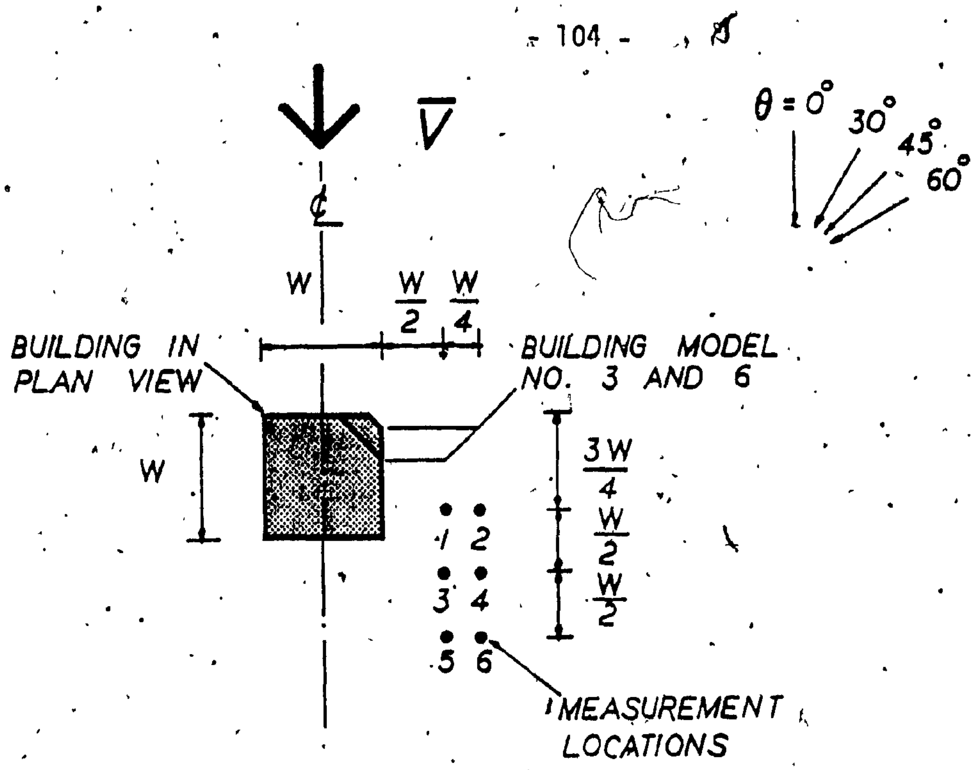

Building Model No.	Wind Attack Angle, θ	MEASUREMENTS AT POINTS											
		1		2		3		4		5		6	
		$\bar{V}_{10P}/\bar{V}_{10A}$	T_{10P}/T_{10A}	$\bar{V}_{10P}/\bar{V}_{10A}$	T_{10P}/T_{10A}	$\bar{V}_{10P}/\bar{V}_{10A}$	T_{10P}/T_{10A}	$\bar{V}_{10P}/\bar{V}_{10A}$	T_{10P}/T_{10A}	$\bar{V}_{10P}/\bar{V}_{10A}$	T_{10P}/T_{10A}	$\bar{V}_{10P}/\bar{V}_{10A}$	T_{10P}/T_{10A}
3	0°	1.3	0.62	1.23	0.8	1.29	0.84	1.22	0.78	1.21	0.94	1.21	0.88
	30°	1.27	0.5	1.2	0.57	1.37	0.53	1.29	0.54	1.38	0.86	1.37	0.6
	45°	1.34	0.46	1.23	0.53	1.3	1.04	1.35	0.54	0.92	2.76	1.42	0.65
	60°	1.4	0.57	1.28	0.55	1.07	1.92	1.37	0.54	1.02	1.94	1.42	0.71
6	0°	1.33	0.6	1.25	0.64	1.35	0.99	1.3	0.65	1.28	1.0	1.32	0.7
	30°	1.24	0.6	1.12	0.66	1.33	0.64	1.24	0.61	1.35	0.83	1.31	0.67
	45°	1.34	0.5	1.21	0.59	1.26	1.13	1.27	0.61	1.2	1.45	1.38	0.72
	60°	1.34	0.6	1.21	0.57	1.07	2.1	1.3	0.65	1.14	1.88	1.37	0.78

TABLE 5.6.1 - EFFECT OF VARYING WIND ATTACK ANGLE, θ, ON VELOCITY AND TURBULENCE AMPLIFICATION FACTORS OF TALL CHAMFERED BUILDINGS.

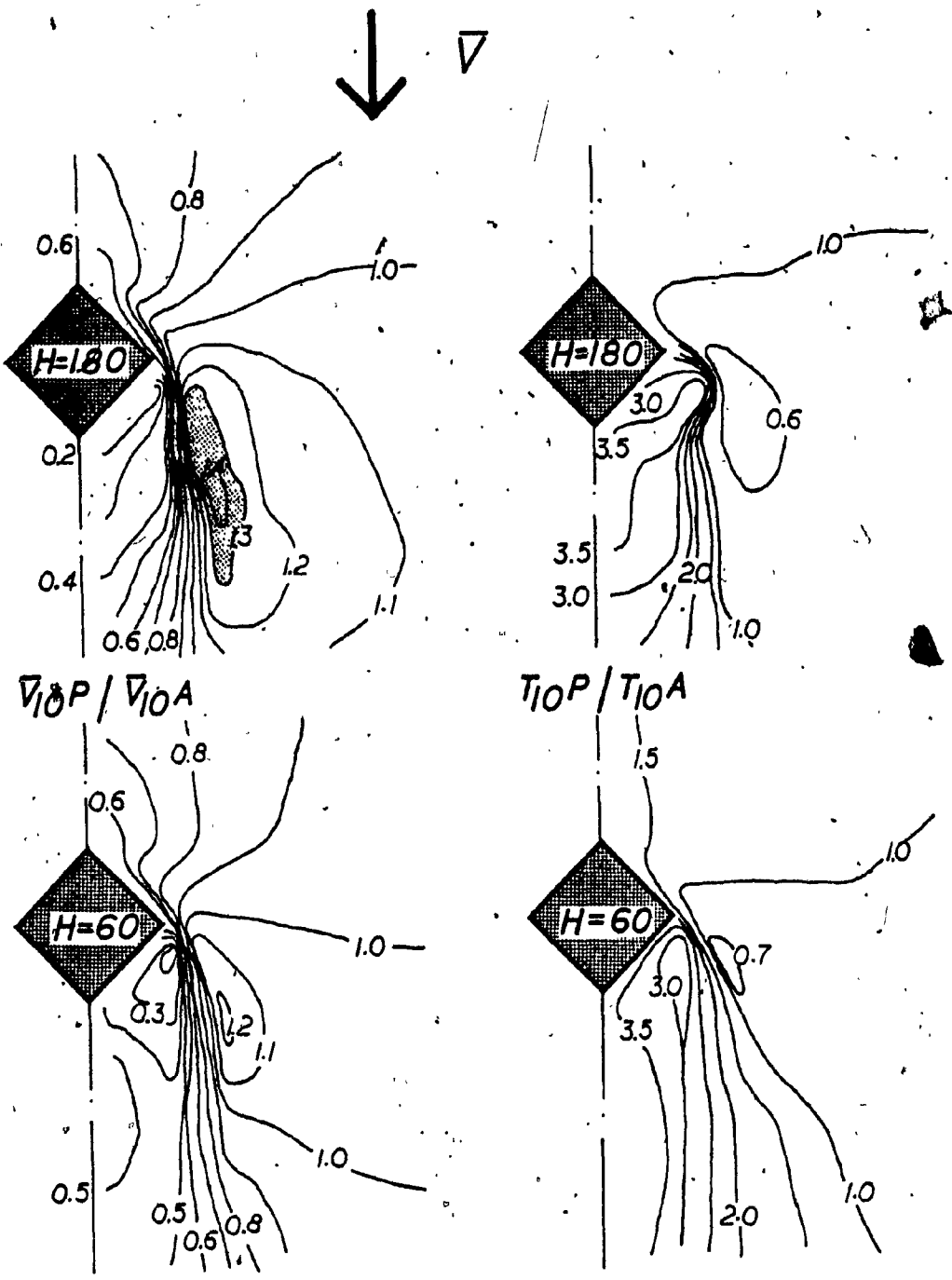

FIGURE 5.6.3 EFFECT OF BUILDING HEIGHT ON VELOCITY AND TURBULENCE AMPLIFICATION FACTORS AROUND SQUARE BUILDING FOR $\theta = 45^{\circ}$

presented for $\bar{V}_{10}P/\bar{V}_{10}A$ and $T_{10}P/T_{10}A$ for the lowest and highest buildings at a 45° azimuth.

For the lowest building (60 m high) the maximum value of $\bar{V}_{10}P/\bar{V}_{10}A$ reaches up to 1.2 for a 45° azimuth which is very close to the value for a 0° azimuth. However, the locations of these values change for varying azimuth. For the highest building (180 m high) the maximum value of $\bar{V}_{10}P/\bar{V}_{10}A$ for a 45° azimuth is also close to the maximum value measured for a 0° azimuth. The size of the strong wind area increased on the leeward side of the building for a 45° azimuth. The values of low velocities on windward and leeward sides did not change significantly for varying building height. The maximum value of $T_{10}P/T_{10}A$ reaches approximately 3.5 on the leeward sides of both the lowest and highest buildings. The magnitude and size of the strong wind area in the corner stream of a building remains independent of wind attack angle.

The effect of wind direction for different building heights at the lower level of measurement (2 m) is presented in Figure 5.6.4. The figure shows results for square buildings 180 and 60 m high. Contours of $\bar{V}_2P/\bar{V}_2A$ and T_2P/T_2A are shown in left and right hand sketches respectively for $\theta = 45°$. The maximum value of $\bar{V}_2P/\bar{V}_2A$ reaches up to 1.8 and 1.4 for 180 and 60 m high buildings respectively. This difference is expected at the lower level of measurement as already discussed in section 5.3, for a 0° azimuth. Higher values of velocity amplification at the 2 m level may be noticed by comparing values of $\bar{V}_2P/\bar{V}_2A$ as presented in Figure 5.3.1 for 0° azimuth. The comparison of $\bar{V}_2P/\bar{V}_2A$ values

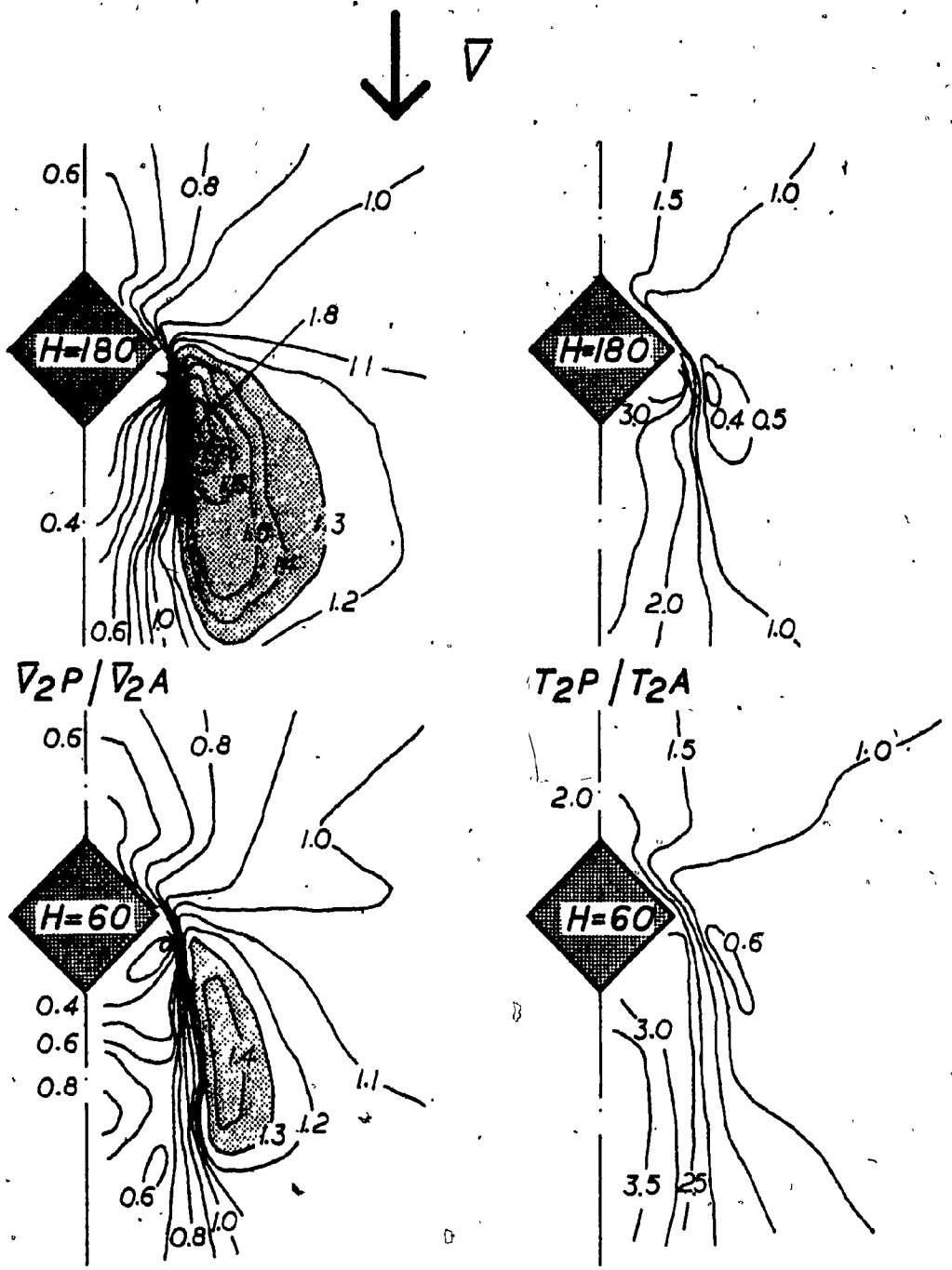

FIGURE 5.6.4 EFFECT OF BUILDING HEIGHT ON VELOCITY AND TURBULENCE AMPLIFICATION FACTORS AROUND SQUARE BUILDINGS AT LOWER HEIGHT OF MEASUREMENT ($\theta = 45^{\circ}$)

for $\theta = 45°$ is not necessary for chamfered buildings as small differences have been resulted from the tests at 10 m level as indicated in Table 5.6.1. Comparison of $\bar{V}_2P/\bar{V}_2A$ as values at 45° azimuth for lower and higher buildings shows considerable differences in intensity and extent of the strong wind region in the corner stream. At the lower level of measurement for a 45° azimuth, a considerable increase in the velocity amplification factor is found for both highest and lowest buildings. The maximum value of turbulence intensity increases up to 2.0 at the lower height of measurement on the windward face of a low building. In general, a small reduction in turbulence intensity on the leeward side of a square building is observed at the lower level of measurement for the 45° azimuth.

5.7 COMMENT ON CHAMFERED ROOF BUILDING

Additional experiments were carried out to investigate the wind conditions around square tall buildings with chamfered roofs. The model used for these tests represents a 180 m high square 30 m x 30 m building. The ratio of chamfer face width over the width of the building is 0.1. The chamfered face makes an angle of 45° to the roof and vertical (windward) face of the building. Chamfer dimensions correspond to building model No. 3 as they are described in Figure 4.7.

The results are compared in Figure 5.7.1 with a non-chamfered building of the same height. Contours of $\bar{V}_{10}P/\bar{V}_{10}A$ are shown in the

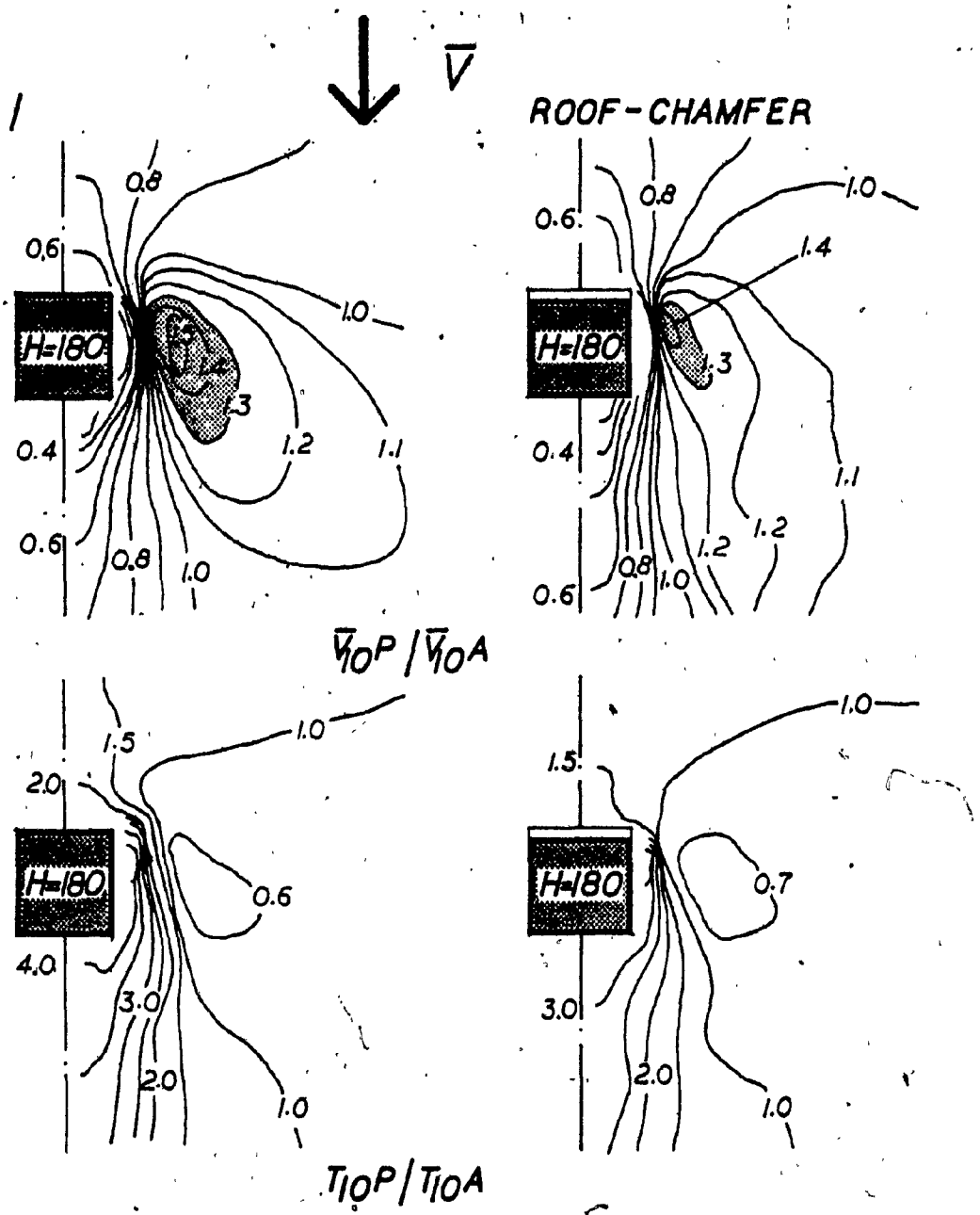

FIGURE 5.7.1 COMPARISON OF VELOCITY AND TURBULENCE INTENSITY CONDITIONS AROUND SQUARE AND ROOF-CHAMFERED BUILDINGS

top diagrams while contours for $T_{10}P/T_{10}A$ are presented in bottom diagrams.

The maximum value of $\bar{V}_{10}P/\bar{V}_{10}A$ reaches up to 1.4 for the chamfered building, a value not much different from that for the square building. A significant reduction in the maximum values of $\bar{V}_{10}P/\bar{V}_{10}A$ was observed but no specific change on windward and leeward sides was noticed for low values of velocity and turbulence intensity factors. A considerable reduction in the maximum value of $T_{10}P/T_{10}A$ was also noticed on the leeward side of the chamfered roof building.

Although limited tests were carried out for chamfered roof buildings, some conclusions may be drawn. A significant reduction in the extent of the strong wind area is achieved. However, the velocity flow fields in the corner stream region are changed compared to non-chamfered roof buildings and they become more elongated in the streamwise direction.

The model test results presented in this chapter suggest chamfered geometry as an important criterion to be considered in the design of new plaza areas from the pedestrian's comfort point of view. The application of the information derived from wind tunnel tests for prediction of wind conditions is presented in Chapter 6.

CHAPTER 6

APPLICATION OF WIND ENVIRONMENT DATA FOR STATISTICAL PREDICTION OF WIND CONDITIONS AROUND BUILDINGS

A procedure for evaluating predicted plaza level wind speeds with frequencies of occurrence to check the criterion of acceptability for various pedestrian activities is described in this chapter. Wind speeds without their frequencies of occurrence would not be useful for evaluating plaza level wind conditions. Also, the frequency of occurrence of wind within a given azimuth is important at locations where a change in wind direction occurs, locally in the presence of other buildings. For example, different frequencies of occurrence may be associated with the same wind speed for different geographical locations. Different exposures within geographical locations change the level of turbulence associated with the wind speed.

In order to estimate the frequencies of wind speed in a built up area, one requires real wind data as well as wind tunnel findings. The frequency of occurrence (at a particular location) of wind speeds $\bar{V}_{10}A$ larger than $\bar{V}_{10}P$ from any wind direction becomes:

$$P(>\bar{V}_{10}P) = \sum_{\text{all sectors}} A(\theta)\, e^{-[\bar{V}_{10}P/C(\theta)]^{K(\theta)}} \quad \text{(16)} \quad \ldots\ldots\ldots [6.1]$$

in which $A(\theta)$ = relative frequency of occurrence for each azimuth θ by definition $\sum_{\text{all sectors}} A(\theta) = 1$, $C(\theta)$, $k(\theta)$ = Weibull coefficients which can be

evaluated from the relative frequency records of wind speeds at 10 m level provided for the standard sixteen compass directions.

A useful basis for the estimation of frequencies of $\bar{V}_{10}A$ may be provided by weather station records of wind speeds and directions published in local climatological data sheets. It is desirable, in practice, to consider frequency estimates based on several years of data to represent the correct wind climate. Information on frequencies of wind speeds at a weather station (f $\bar{V}_{10}A$) are available for various cities. They may be presented either diagramatically or in the form illustrated in Table 6.1 for the city of Montreal. They may be also reorganized in the format of Table 6.2 including percentages. In certain applications it may be of interest to estimate frequencies for individual seasons, or for a grouping of seasons. Estimation of such frequencies of specific application is described by Isyumov and Davenport (16). The numerical examples of these application procedures for existing plaza buildings are given in references 16 and 31.

Wind climate data emphasizing frequencies of wind speed versus direction may be used column-by-column for calculation of wind conditions as a function of the wind direction. In some cases however, the conditions emphasizing frequencies based on wind direction may be omitted (33). In the present work it was felt appropriate to calculate total frequencies without regard to direction. This can be justified since the emphasis of this study was on the geometry of the building rather than on its interaction with the built-up environment. It has

WIND SPEED VS DIRECTION 1953 - 1980

Wind Direction		Wind Speed Classes (km/h) 1 - 10	11-20	21-30	31-40	41-50	51-60	61-70	71-80	81-90	91-100	101-999	MEAN	PERCENTAGE OF OCCURRENCES BY DIRECTION	% OF SPEEDS LIMIT
NNE	21,172	5,944	9,085	4,450	1,324	277	68	15	9				16.5	8.6	0.0
NE	16,544	3,843	6,425	4,215	1,536	382	117	22	4				18.5	6.7	0.0
ENE	6,016	1,983	2,526	1,163	283	51	10						15.2	2.5	0.0
E	5,859	2,925	2,377	490	62	5							11.4	2.4	0.0
ESE	5,734	2,755	2,171	712	93	3							12.2	2.3	0.0
SE	9,609	3,782	3,675	1,692	406	45	8		1				14.2	3.9	0.0
SSE	11,614	4,057	4,732	2,204	551	64	6						15.0	4.7	0.0
S	9,510	5,024	3,714	677	84	7	3	1					11.1	3.9	0.0
SSW	14,940	5,086	6,983	2,356	432	73	6	4					14.3	6.1	0.0
SW	29,792	7,351	12,041	7,426	2,404	444	92	27	5	2			17.7	12.1	0.0
WSW	34,103	6,955	12,047	9,607	4,211	1,001	222	47	13				19.9	13.9	0.0
W	30,063	6,881	10,580	8,213	3,551	679	122	31	6				19.1	12.2	0.0
WNW	12,324	3,647	4,590	2,894	1,037	131	21	4					16.8	5.0	0.0
NW	9,105	3,628	3,035	1,148	269	22	3						13.0	3.3	0.0
NNW	6,471	3,486	2,104	767	109	2	3						11.5	2.6	0.0
N	12,174	6,540	4,213	1,179	210	30	1	1					11.4	5.0	0.0
CALM/	11,418													4.7	
TOTAL	245,448	73,887	90,298	49,193	16,562	3,216	682	152	38	2			15.55	*100.00%	* 0.0%

* Total number of occurances before selection: 245,448
16 Points distribution from 10's of degrees is weighted in the 4 cardinal points

TABLE 6.1 - FREQUENCY OF OCCURRENCE OF WIND SPEED IN MONTREAL (6)

WIND SPEED VS DIRECTION
MONTREAL INT'L A QUEBEC - YEARS 1953 - 1980

Frequencies of wind speeds at 10 m above ground in open terrain (in percentage of total time)

Wind Direction	1 NNE	2 NE	3 ENE	4 E	5 ESE	6 SE	7 SSE	8 S	9 SSW	10 SW	11 WSW	12 W	13 WNW	14 NW	15 NNW	16 N	ALL DIRECTIONS TOTAL (%)	CUMULATIVE TOTAL *(%)
WIND SPEED (m/s)																		
CALM	-	-	-	-	-	-	-	-	-	-	-	-	-	-	-	-	4.7	99.9758
0.3 - 2.9	2.4	1.6	0.8	1.2	1.1	1.5	1.6	2.0	2.1	3.0	2.8	2.8	1.5	1.5	1.4	2.7	30.1	95.2758
3.0 - 5.6	3.7	2.6	1.0	1.0	0.9	1.5	1.9	1.5	2.8	4.9	4.9	4.3	1.8	1.2	0.8	1.7	36.8	65.1758
5.7 - 8.4	1.8	1.7	0.5	0.2	0.3	0.7	0.9	0.3	0.9	3.0	3.9	3.4	1.2	0.5	0.3	0.5	20.1	28.3758
8.5 - 11.2	0.5	0.6	0.1	0.02	0.04	0.2	0.2	0.03	0.2	1.0	1.7	1.4	0.4	0.1	0.04	0.08	6.6	8.2758
11.3 - 13.9	0.1	0.1	0.02	0.002	0.001	0.02	0.03	0.002	0.08	0.2	0.4	0.3	0.05	0.009	0.0008	0.01	1.3	1.6758
14.0 - 16.8	0.03	0.05	0.004	-	-	0.003	0.002	0.001	0.002	0.04	0.1	0.05	0.008	0.001	0.001	0.0004	0.3	0.3758
16.9 - 19.5	0.006	0.009	-	-	-	-	-	0.0004	0.001	0.01	0.02	0.01	0.002	-	-	0.0004	0.06	0.0758
19.6 - 22.3	0.004	0.002	-	-	-	0.004	-	-	-	0.002	0.005	0.002	-	-	-	-	0.015	0.0158
22.4 - 25.0	-	-	-	-	-	-	-	-	-	0.0008	-	-	-	-	-	-	0.0008	0.0008
TOTAL																	100.0%	

16 Point distribution from 10's of degrees is weighted in the 4 cardinal points.

* Cumulative frequencies calculated by progressive addition of values in the previous column, starts from highest Beaufort's No.

TABLE 6.2 - MONTREAL WIND CLIMATE

also been found that the magnitude of wind speed in the corner stream at the plaza level is not affected by the wind direction, although the location of the strong flow fields does change.

In the procedure illustrated below, the aerodynamic information used, rather than being a function of wind direction, is limited to the building cases and the wind direction studied in this work. Total frequencies for the Montreal area are given in Table 6.2 in the 'all directions' column. Based on these data, the cumulative frequency distribution (CDF function) has been plotted in Figure 6.1 for 10 m and 2 m heights above ground level. The process of interpolation has been aided by fitting a smooth curve through the points as shown in the figure. In order that $\bar{V}_{10}P$ exceeds 5 m/s (as discussed in Chapter 3, the wind at the meteorological site, $\bar{V}_{10}A$, is calculated as follows (31):

$$\bar{V}_{10}A > 5/(\bar{V}_{10}P/\bar{V}_{10}A) \text{ m/s} \quad \ldots\ldots\ldots\ldots \quad [6.2]$$

$\bar{V}_{10}A > 5/(1.8)$ m/s (A value to be derived from wind tunnel tests in form of a ratio to express relative increase or decrease of wind speed)

$\bar{V}_{10}A > 2.7$ m/s

The frequency of such winds can be taken from Figure 6.1. Frequencies of winds associated with various values of velocity amplification ratio at 10 m and 2 m heights of measurements are presented in Table 6.3.

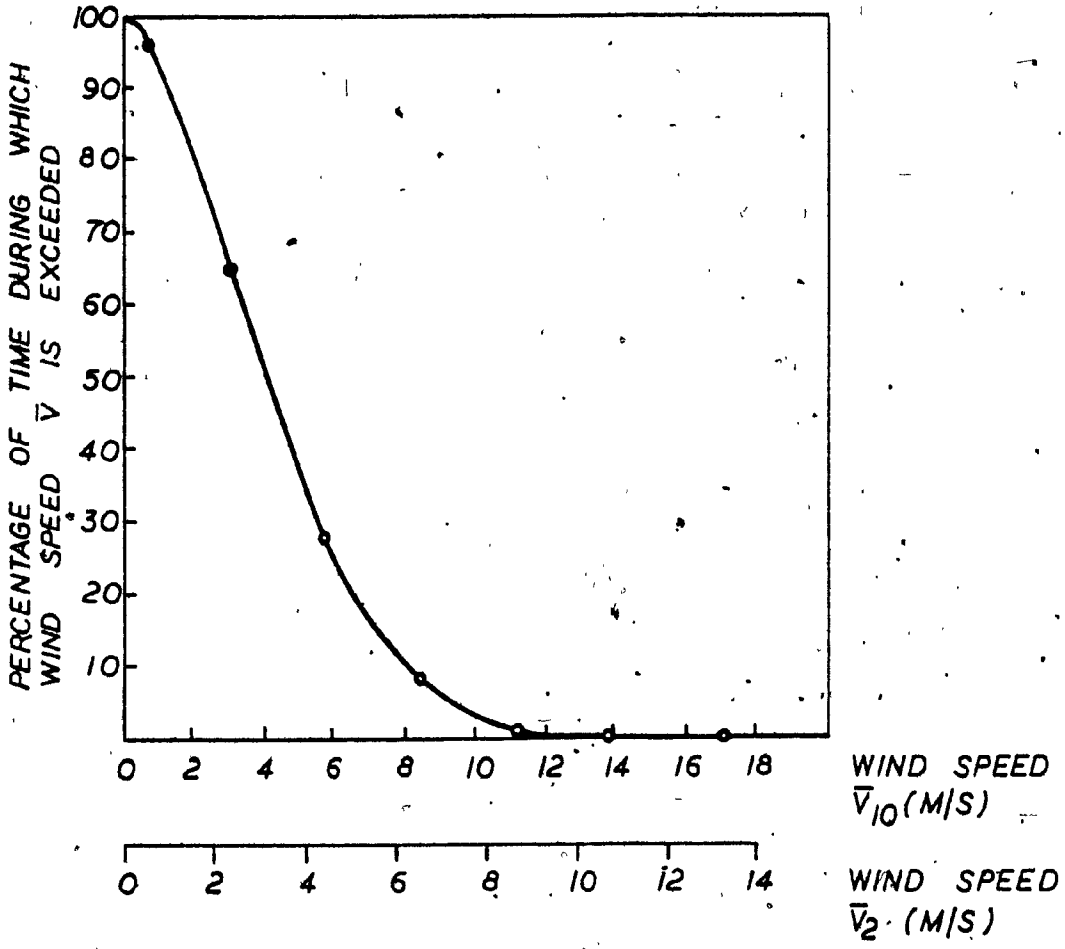

FIGURE 6.1 CUMULATIVE FREQUENCY OF WIND SPEED, $\bar{V}$
(FROM DATA IN TABLE 6.2)

VELOCITY AMPLIFICATION RATIO: $\bar{V}_hP/\bar{V}_hA$ h = 2 or 10 m	IN ORDER THAT $\bar{V}_hP$ 5 > m/s, $\bar{V}_hA > 5/(\bar{V}_hP/\bar{V}_hA)$ m/s.(31) (Discomfort begins at a mean wind speed of 5 m/s(31)).	FREQUENCIES OF THE WIND SPEED $\bar{V}_hA > 5/(\bar{V}_hP/\bar{V}_hA)$ m/s, from Figure 6.1	
		$\bar{V}_{10A}$ = (%)	$\bar{V}_{2A}$ = (%)
1.8	2.7	67	56
1.7	2.9	65	52
1.6	3.1	63	50
1.5	3.3	60	45
1.4	3.6	55	40
1.3	3.8	53	38
1.2	4.2	50	30
1.1	4.5	45	25
1.0	5.0	37	20
0.9	5.5	30	15
0.8	6.2	23	10

TABLE 6.3 - WIND TUNNEL RESULTS COMBINED WITH MONTREAL WIND CLIMATE.

Any discomfort level can be accommodated with this procedure. For example, superposition of wind frequencies associated with equal velocity amplification ratio ($\bar{V}_{10P}/\bar{V}_{10A}$) are presented in Figure 6.2. The contours shown in top left sketch of the figure are for a 180 m tall square (30 m x 30 m) building indicating the percentage of time during which the wind speed $\bar{V}_{10P}$ exceeds 5 m/s. (Montreal location). A similar presentation for the 2 m height of measurement is shown in Figure 6.3.

One may evaluate the areas around the buildings at plaza level as described in Figures 6.2 and 6.3 from the point of view of the pedestrian's comfort. The suggested plaza areas in the corner stream of a tall square building, as shown in the top right sketches for different pedestrian activities, are based on the comfort criteria proposed by Davenport (7). Details about comfort criteria for pedestrian activities as walking fast, strolling, standing and sitting for short exposure and long exposure applicable to different areas at plaza level have been presented in Table 3.2.

The effect of chamfered buildings on strong wind areas is shown in the bottom sketches of Figures 6.2 and 6.3. These sketches show the reductions of the areas rated as dangerous and/or unpleasant for pedestrian activities. The reductions of these areas at the pedestrian level are demonstrated for a chamfered building with a chamfered face approximately equal to 10% of the width of the original face of the building.

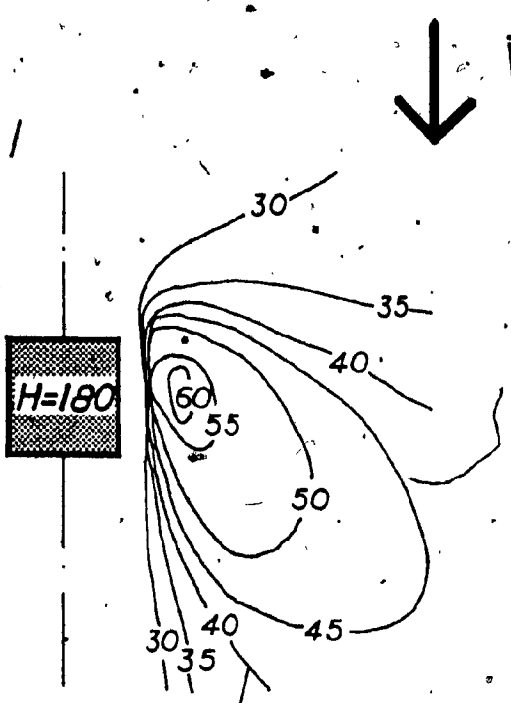

PERCENTAGE OF TIME DURING WHICH WIND SPEED $\bar{V}_{10} > 5$ M/S

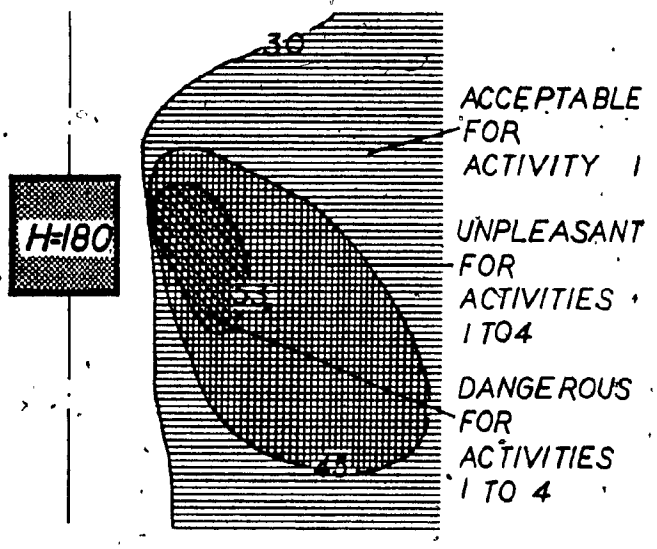

STRONG WIND AREAS IN A CORNER STREAM OF A SQUARE BUILDING

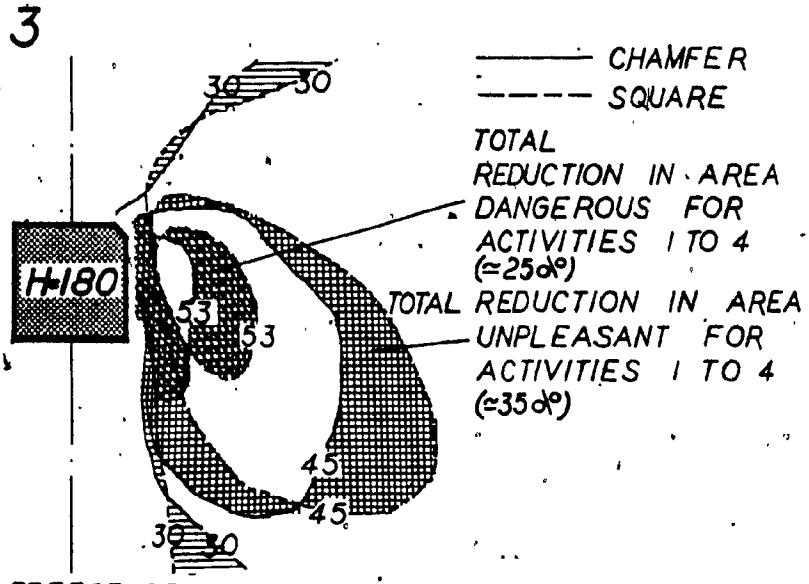

EFFECT OF CHAMFERED BUILDING ON THE STRONG WIND AREA IN A CORNER STREAM

ACTIVITY
1 WALKING FAST
2 STROLLING
3 STANDING, SITTING - SHORT EXPOSURE
4 STANDING, SITTING - LONG EXPOSURE

FIGURE 6.2 EFFECT OF CHAMFER ON PLAZA LEVEL WIND ENVIRONMENT AROUND A 180 M TALL BUILDING IN MONTREAL

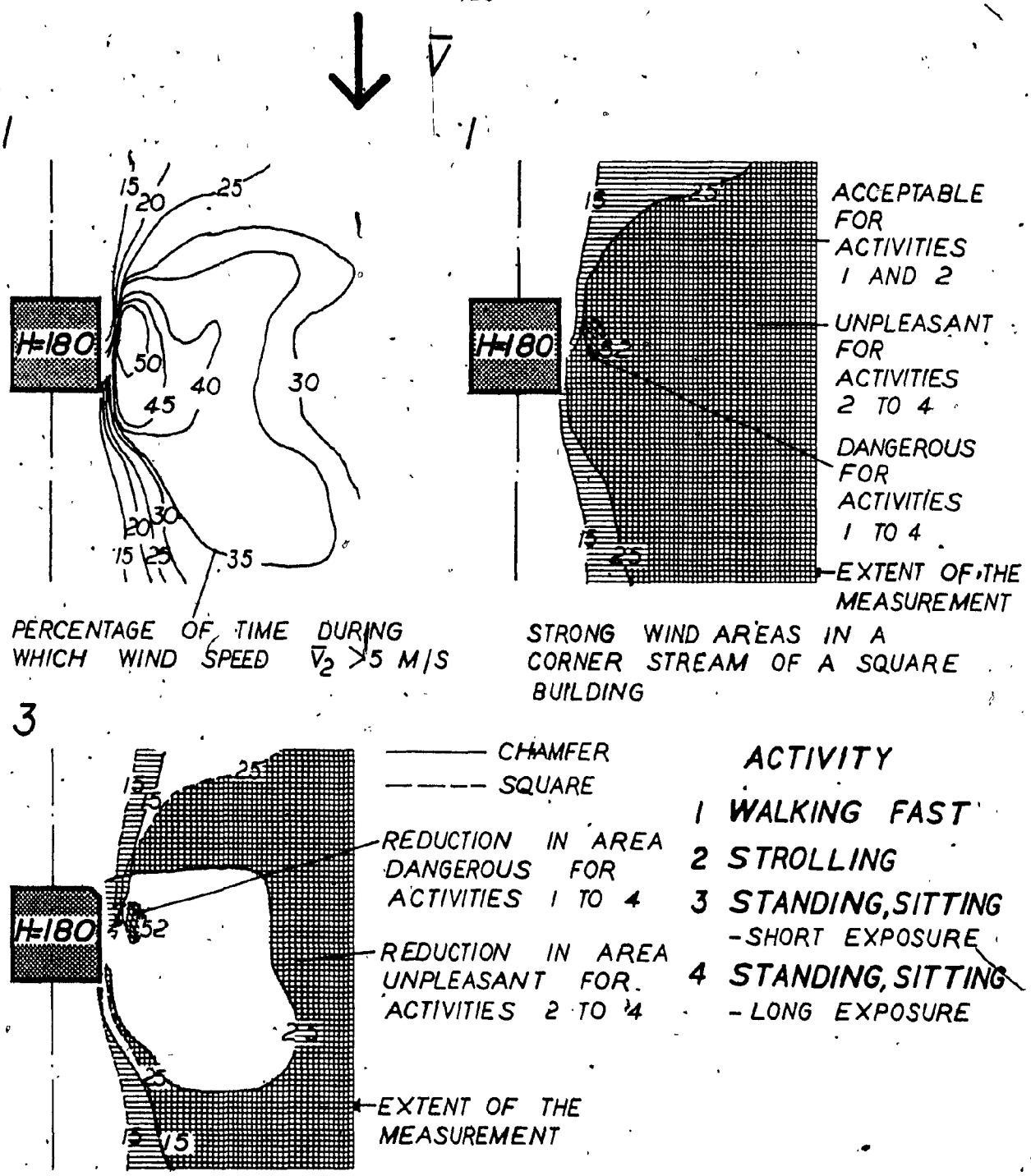

FIGURE 6.3 EFFECT OF CHAMFER ON THE PEDESTRIAN LEVEL WIND ENVIRONMENT AROUND A 180 M TALL BUILDING IN MONTREAL

The procedure shows the application of wind tunnel results for the statistical prediction of wind conditions at the pedestrian level around a tall building. The utilization of plaza areas for various pedestrian activities may be estimated for proposed locations as presented here. The procedure gives a detailed picture of these areas and their locations relative to the building geometry. Model test results have already proved the chamfered corners as one of the parameters in designing plaza areas for acceptable wind environment. With this procedure chamfered building geometry useful in reducing strong wind areas may be easily incorporated in new designs.

CHAPTER 7

CONCLUSIONS AND RECOMMENDATIONS FOR FUTURE STUDY

Based on the experimental results of this study the following conclusions can be made.

1. For a tall square building the mean wind speed in a corner stream increases up to 50 percent of free wind speed while turbulence on the leeward side increases up to 4 times its value without the building. The intensity and the size of the strong wind area increases considerably for both low and high square building at the low level of measurements (2m).

2. Chamfering of a corner at 45° to its original faces of a tall square building reduces the strong wind area in the corner stream by approximately 75 percent of the area accounted for a square building at the pedestrian level. A ratio of (chamfered width/original face width) higher than about 0.15 does not show significant reduction in the intensity and the extent of the strong wind area in the corner stream.

3. Chamfered buildings always have higher values of velocity and turbulence amplification factors close to the corner stream face than square buildings. Higher values of chamfered length reduce the turbulence close to the corner stream face but do not have much effect on the leeward side of the building.

4. Areas of velocity amplification are also areas of turbulence reduction.

5. As the building height increases, high velocities and the size of the corner stream of both square and chamfered buildings increase consistently whereas the turbulence is not much affected.

6. The maximum values of velocity amplification factor and the size of the strong wind area in the corner stream of a building are almost independent of wind direction. The maximum value of turbulence intensity depends little on the wind direction but the location of occurrence of this value is drastically affected by the wind direction.

RECOMMENDATIONS FOR FUTURE STUDY

In the present study building models and some parameters used in the tests may require further investigations. Based on the findings of this work the following may be suggested:

1. A study to investigate the effect of the size of the building on the strong wind area at pedestrian level would be interesting. The results of this study may be used for establishing chamfered geometry as a design parameter for the comfort of pedestrians at the base of tall buildings.

2. More tests on chamfered building models would be necessary for an urban exposure. The higher values of turbulence may show significant effects on the size of the strong wind area at the pedestrian level.

3. Results of the chamfered-roof model tests suggest additional experimentation on the wind environment for a variety of parameters including low building height, lower height of measurement and more values of chamfered-roof width.

REFERENCES:

(1) Aynsley, R.M., Vickery, B., Melbourne, W., "Architectural Aerodynamics", Applied Science Publishers Ltd., London, 1980.

(2) Baines, W.D., "Effect of Velocity Distribution on Wind Loads of Flow Patterns of Buildings", Symposium Wind Effects on Building Teddington, England, 1963.

(3) Bradbury, L.J.S., "Measurements with a Pulsed-Wire and a Hot-Wire Anemometer in the Highly Turbulent Wake of a Normal Flat Plate", Journal of Fluid Mechanics, Vol. 177, 1976.

(4) Bradshaw, P., "An Introduction to Turbulence and its Measurements", Pergamon Press, Oxford, 1971.

(5) Beranek, W.J. and Vankoten, H., "Visual Techniques for the Determination of Wind Environment", Journal of Industrial Aerodynamics, 295-306, 4, 1979.

(6) Canadian Climate Normals, Volume 5, Wind, 1951-80, A Publication of Canadian Climate Program, 1982.

(7) Davenport, A.G., "An Approach to Human Comfort Criteria for Environmental Wind Conditions", Proceedings Colloquium on Building Climatology, Stockholm, Sweden, 1972.

(8) Durgin, F.H., and Chowk, A.W., "Pedestrial Level Wind: A Brief Review", Journal of the Structural Division Vol. 108 No. ST8, Aug. 1982.

(9) Dye, R.C.F., "Comparison of Full Scale and Wind Tunnel Model Measurements of Ground Winds Around a Tower Building", Journal of Wind Engineering and Industrial Aerodynamics, 6, 1980, 311-326.

(10) Gandemer, J., "Wind Environment Around Buildings: Aerodynamic Concepts", Proceedings 4th International Conference on Wind Effects on Buildings and Structures, Heathrow, 1975.

(11) Gilling, D., Miller, P.O., and Whitebread, R.E., "The Influence of a Wind Tunnel Study on the Design for the Quantas Centre, Sydney, Australia", Proceedings 3rd Int. Conf. on Wind Effects on Buildings and Structures, Tokyo, 1971.

(12) Hunt, J.C.R., "Wind Tunnel Experiments on the Effects of Wind on People", A Report to the Building Research Establishment; September, 1974.

(13) Hunt, J.C.R, Poulton, E.C., and Mumford, J.C., "The Effects of Wind on People; New Criteria Based on Wind Tunnel Experiments", Building and Environment, Vol. 11, Pergamon Press, 1976.

(14) Irwin, H.P.A.H., "A Simple Omnidirectional Sensor for Wind Tunnel Studies of Pedestrian-Level Winds", Journal of Wind Engineering and Industrial Aerodynamics, 219-239, 7, 1981.

(15) Isyumov, N., "Studies of the Pedestrian Level Wind Environment at the Boundary Layer Wind Tunnel Laboratory of the University of Western Ontario", Journal of Industrial Aerodynamics, 187-200, 3, 1978.

(16) Isyumov, N. and Davenport, A.G., "The Ground Level Wind Environment in Built up Areas", Proc. 4th International Conference on Wind Effects on Buildings and Structures, Heathrow, 1975.

(17) Kamei, I. and Maruta, E., "Study on Wind Environmental Problems Caused Around Buildings in Japan", Paper Presented at the 3rd Colloquium on Industrial Aerodynamics, Aachen, June 14-16, 1978, Journal of Industrial Aerodynamics, 307-331, 4, 1979.

(18) Lawson, T.V., "Wind Environment of Buildings: A Logical Approach to the Establishment of Criteria", Report No. TVL 7321, University of Bristol, Bristol, England, Dept. of Aerodynamics Engineering, 1973.

(19) Lawson, T.V., "Wind Effects on Buildings", Vol. I, Applied Science Publishers Ltd., (Chapter 10, 15), London 1980.

(20) Lawson, T.V., "Wind Effects on Buildings", Vol. II Applied Science Publishers Ltd., (Chapter 12), London 1980.

(21) Lawson, T.V., "External and Internal Environment", Technical Study, Architects Journal, December, 1968.

(22) Lawson, T.V. and Penwarden, A.D., "The Effects of Wind on People in the Vicinity of Buildings", Proc. 4th International Conference on Wind Effects on Buildings and Structures, Heathrow, 1975.

(23) MacGregor, J., "Why the Wind Howls Around those Plazas Close to Skyscrapers", The Wall Street Journal, Feb. 1971.

(24) Melbourne, W.H., "Criteria for Environmental Wind Conditions", Journal of Industrial Aerodynamics, 241-249, 3, 1978.

(25) Melbourne, W.H., "Wind Environment Studies in Australia", Journal of Industrial Aerodynamics, 201-214, 3, 1978.

(26) Melbourne, W.H. and Joubert, P.N., "Problems of Wind Flow at the Base of Tall Buildings", Proc. 3rd International Conference on Wind Effects on Buildings and Structures, Tokyo, 1971.

(27) Murakami, S., Uehara, K. and Komine, H., "Amplification of Wind Speed at Ground Level Due to Construction of High-Rise Building in Urban Area", Journal of Industrial Aerodynamics, 343-370, 4, 1979.

(28) Nagib, M.H., "Visualization of Turbulent and Complex Flows Using Controlled Sheets of Smoke Streaklines", Proc. Int. Symp. on Flow Visualization, Tokyo, 1977.

(29) Penwarden, A.D., "Acceptable Wind Speeds in Towns", Building Science, Vol. 8, pp. 259-267, Pergamon Press, 1973.

(30) Penwarden, A.D., "Wind Environment Around Tall Buildings", Building Research Establishment Digest No. 141, May 1972.

(31) Penwarden, A.D., and Wise, A.F.E., "Wind Environment Around Buildings", Building Research Establishment Report, Vol. 141, May 1975.

(32) Sealey Antony, "An Introduction to Building Climatology", Published by Commonwealth Association of Architects - 1979.

(33) Simiu, E. and Scanlan, R.H., "Wind Effects on Structures: An Introduction Wind Engineering", John Wiley & Sons, (Chapter No. 10), 1978.

(34) Stathopoulos, T., "Design and Fabrication of a Wind Tunnel for Building Aerodynamics", Proc. 5th Colloquium on Industrial Aerodynamics, Aachen, 1982.

(35) TSI 1076, Hot-Wire Anemometer System, Thermo System Inc.

(36) Wise, A.E.F., "Effects Due to Groups of Buildings", The Canadian Architect /Noy., pp. 28-40, 1971.

(37) Wise, A.E.F., Sexton, D.E. and Lillywhite, M.S.T., "Studies of Air Flow Round Buildings", Architects Journal, pp. 1185-1189, 19th May, 1965.

APPENDIX I - NOTATION

The following symbols are used in this thesis:

$A(\theta)$ = relative frequency of occurrence of wind being within the sector;

$C(\theta)$ = Weibull coefficient;

Cg = surface drag coefficient;

f = frequency of wind speed;

H = building height;

K = a constant reflecting the degree to which the effect of wind speed fluctuations are significant;

$K(\theta)$ = Weibull coefficient;

k = Von Karman's constant;

Q = velocity amplification ratio at h height;

r = ratio of the velocity at a particular point to the mean wind velocity at the top of the building;

T_2A = turbulence intensity in the absence of the building at 2 m height;

$T_{10}A$ = turbulence intensity in the absence of the building at 10 m height;

T_hA = turbulence intensity in the absence of the building at h height;

T_2P = turbulence intensity in the presence of the building at 2 m height;

$T_{10}P$ = turbulence intensity in the presence of the building at 10 m height;

T_hP = turbulence intensity in the presence of the building at h height;

t = width of the chamfered face;

t' = length of the chamfered face;

V^e = effective wind speed;

V_g = wind speed at gradient height;

V_{rms} = root mean square value of wind speed;

$V_{rms\ 10A}$ = root mean squere value of wind speed at 10 m height in absence of the building;

$V_{rms\ hA}$ = root mean square value of wind speed at h height in absence of the building;

$V_{rms\ 10P}$ = root mean square value of wind speed at 10 m height in presence of the building;

$V_{rms\ hP}$ = root mean square value of wind speed at h height in presence of the building;

$\bar{V}$ = mean wind speed;

$\bar{V}_2A$ = mean wind speed in absence of the building at 2 m height;

$\bar{V}_{10}A$ = mean wind speed in absence of the building at 10 m height;

$\bar{V}_hA$ = mean wind speed in absence of the building at h height;

$\bar{V}_H$ = mean wind speed at roof height;

$\bar{V}_2P$ = mean wind speed in presence of the building at 2 m height;

$\bar{V}_{10}P$ = mean wind speed in presence of the building at 10 m height;

$\bar{V}_hP$ = mean wind speed in presence of the building at h height;

W = width of the building;

x = independent variable showing distances in a cross-wise direction;

y = independent variable showing distances in a streamwise direction;

Z = height from ground surface;

Z_o = roughness length;

Z_g = gradient height;

α = velocity profile (power law exponent);

θ = angle of the airstream to the face of a building (degrees);

ψ_h = comfort parameter at height, h, 2 m or 10 m above ground (a dimensionless velocity ratio); and

ρ = air density.